Probing the neural mechanisms of adult-onset isolated focal dystonia

Trinity College Dublin
Coláiste na Tríonóide, Baile Átha Cliath
The University of Dublin

A dissertation submitted to the University of Dublin for the degree of

Doctor of Philosophy

by

Brendan Quinlivan

Supervisor: Prof. Richard Reilly

Neural Engineering Group, Trinity Centre for Bioengineering
Department of Electronic and Electrical Engineering
Trinity College Dublin

Declaration

I declare that this thesis has not been submitted as an exercise for a degree at this or any other University, and it is entirely my own work.

I agree to deposit this thesis in the University's open access institutional repository or allow the library to do so on my behalf, subject to Irish Copyright Legislation and Trinity College Library conditions of use and acknowledgment.

_____

Brendan Quinlivan

22th September 2018

Acknowledgments

Firstly, I would like to thank all the patients and families who have been so generous with their time and participated in the research that has been carried out here, none of this would have been possible without their generosity.

I thank Prof. Richard Reilly for the opportunity to be a part of the Neural Engineering Lab in Trinity College Dublin, I have learned a great deal under his supervision and the findings presented here have been strongly influenced by his guidance and support.

I thank Prof. Michael Hutchinson for his incredible support, his knowledge of AOIFD is astonishing and his advice has been essential to this research.

I am grateful to Prof. Rosalyn Moran for hosting me as part of her research team at Virgin Tech Carilion Research Institute. Her guidance was indispensable to much of the neuroimaging and to all the DCM work carried out here.

I would also like to thank Dr. John Butler, his knowledge of mathematics and statistics was instrumental to the research carried out here and he always made time to help, especially when I was finding my feet at the start.

I would like to thank Dr. Eavan McGovern, Ms. Struti Narasimhm and Dr. Ines Bieser for their help and collaboration on many of the studies presented here. I would also like to thank all members of the Neural Engineering Lab in Trinity College Dublin and all members of the Irish Dystonia Research Group for their continued support and collaboration.

Finally, I would like to thank my family and friends for their unconditional love and support over the years, especially Emma, for always standing by my side.

Table of contents

List of figures

List of tables

Glossary of terms

AOIFD	Adult Onset Isolated Focal Dystonia
CD	Cervical Dystonia
DBS	Deep Brain Stimulation
DLSC	Deep Layers of the Superior Colliculus
EMG	Electromyography
EOG	Electrooculography
ERP	Event Related Potential
GABA	Gamma-Aminobutyric Acid
GLM	General Linear Model
HMD	Head Mounted Display
JND	Just Noticeable Difference
MNI	Montreal Neurological Institute
MT	Movement Time
PSE	Point of Subjective Equality
SC	Superior Colliculus
SDT	Spatial Discrimination Threshold
SEM	Structural Evaluation Modelling
SLSC	Superficial Layers of the Superior Colliculus
SNpr	Substantia Nigra Pars Compacta
STD	Standard Deviation
TC	Target Cued
TDT	Temporal Discrimination
THM	Thalamus
TL	Target Learning
TTC	Time to Contact
VBM	Voxel-based Morphometry
VIIM	Vibration Induced Illusionary Movement

Publications arising from thesis

Peer reviewed journal papers

- **Quinlivan B**, Butler JS, Ridwan AR, Beiser I, Williams L, McGovern E, O'Riordan S, Hutchinson M, Reilly RB. Exploring the unknown: electrophysiological and behavioural measures of visuospatial learning. European Journal of Neuroscience, 43(9).

- **Quinlivan B**, Butler JS, Beiser I, Williams L, McGovern E, O'Riordan S, Hutchinson M, Reilly RB. Application of virtual reality head mounted display for investigation of movement: A novel effect of orientation of attention. Journal of Neural Engineering, 13(5).

- Butler JS, Molloy A, Williams L, Kimmich O, **Quinlivan B**, O'Riordan S, Hutchinson M, Reilly RB. Non-parametric bootstrapping method for measuring the temporal discrimination threshold for movement disorders. Journal of Neural Engineering, 12(4).

- Williams LJ, Butler JS, Molloy A, McGovern E, Beiser I, Kimmich O, **Quinlivan B**, O'Riordan S, Hutchinson M, Reilly RB. Young women do it better: Sexual dimorphism in temporal discrimination. Frontiers in Neurology, 6(160).

- Molloy A, Kimmich O, Williams L, **Quinlivan B**, Dabacan A, Fanning A, Butler JS, O'Riordan S, Reilly RB, Hutchinson M. A headset method for measuring the visual temporal discrimination threshold in cervical dystonia. Tremor and other Hyperkinetic Movements, 18(4).

- McGovern E, O'Connor E, Beiser I, Williams L, Butler JS, **Quinlivan B**, Narasiham S, Beck R, Reilly RB, O'Riordan S, Hutchinson M. Menstrual cycle and the temporal discrimination threshold. Physiological Measurements, 38(2).

- McGovern E, Butler JS, Beiser I, **Quinlivan B**, Narasiham S, Beck R, Reilly RB, O'Riordan S, Hutchinson M. A comparison of stimulus presentation methods in temporal discrimination testing. Physiological Measurements, 38(2).

Peer reviewed conference papers

- **Quinlivan B**, Butler JS, Ridwan AR, O'Riordan S, Hutchinson M, Reilly RB. Electrophysiological and behavioural measures of visuo-motor learning for application in movement disorders. Annual International Conference of the IEEE Engineering in Medicine and Biology Society. IEEE Engineering in Medicine and Biology Society. Chicago, USA.

Peer reviewed conference abstracts

- **Quinlivan B**, Butler JS, Ridwan AR, O'Riordan S, Hutchinson M, Reilly RB. Electrophysiological and behaviours study of movement learning in controls. 20th Annual Bioengineering in Ireland conference. Limerick, Ireland.

- **Quinlivan B**, Butler JS, Ridwan AR, Beiser I, Williams L, McGovern E, O'Riordan S, Hutchinson M, Reilly RB. Electrophysiological and behavioural measures of the dynamics of visuospatial learning: implications for probing learning in neurological conditions. 19th International Congress of Parkinson's Disease and Movement Disorders. San Diego, USA.

- **Quinlivan B**, Butler JS, Beiser I, Williams L, McGovern E, O'Riordan S, Hutchinson M, Reilly RB. Investigating head movements with virtual reality. Society for Neuroscience 45th Annual meeting. Chicago, UAS.

- Beiser I.M. **Quinlivan B**. Williams L.J. McGovern E.M. O'Riordan S. Butler J.S. Reilly R.B. Hutchinson M. Using the oculus rift for recording head turns. 19th International Congress of Parkinson's Disease and Movement Disorders. San Diego, USA.

- **Quinlivan B**, Moran R, McGovern E, Narasimham S, Beiser I, Williams L, Killian O, Beck R, O'Riordan S, Butler JS, Hutchinson M, Reilly RB. A dynamic causal model of the superior colliculus: Inhibitory activity increases with the temporal discrimination threshold. 20th International Congress of Parkinson's Disease and Movement Disorders. Berlin, Germany.

- Beiser I, **Quinlivan B**, McGovern E, Narasimham S, Williams L, Killian O, Beck R, O'Riordan S, Butler JS, Reilly RB, Hutchinson M. Investigation of head tremor in cervical dystonia: Novel application of virtual reality head mounted display, the oculus rift. 20th International Congress of Parkinson's Disease and Movement Disorders. Berlin, Germany.

- Beiser I, **Quinlivan B**, McGovern E, Narasimham S, Williams L, Killian O, Beck R, O'Riordan S, Butler JS, Reilly RB, Hutchinson M. Orientation of attention affects onset of head saccades: A novel representation of the Posner cueing effect. 20th International Congress of Parkinson's Disease and Movement Disorders. Berlin, Germany.

- Fearon C, Newman L, Butler JS, **Quinlivan B**, Reilly RB, Lynch T. Motor learning in Parkinson's disease using an action acquisition task. Neurological Association Meeting. Galway, Ireland.

- Fearon C, Newman L, **Quinlivan B**, Butler JS, Lynch T, Reilly RB. Investigation of motor learning in Parkinson's disease using an action acquisition task. Association of British Neurologists Meeting. Harrogate, UK.

Abstract

Adult onset isolated focal dystonia (AOIFD) is inherited in an autosomal dominant manner with a reduced penetrance of 12-15%; cervical dystonia (CD) is the most common phenotype in northern Europe. It is believed that the different phenotypes of AOIFD are cause by the same, currently unknown, genetic mutation(s). While the pathogenesis of AOIFD remains a mystery, recent animal and clinical studies have indicated its probable mechanisms. The temporal discrimination threshold (TDT) is the shortest interval at which two sequential stimuli appear to the observer to be asynchronous; a typically developing adult will have a TDT of 30 - 50 ms, although this varies with gender and age. It has been established that an abnormal TDT is a valid, sensitive and specific mediational endophenotype in several AOIFD phenotypes. The discovery of this mediational endophenotype has been instrumental in the formation of novel hypotheses regarding the pathogenesis of AOIFD. The hypothesis examined here states that both abnormal temporal discrimination and cervical dystonia are the result of a disorder of the midbrain network involved in covert orientation of attentional, caused by reduced gamma-aminobutyric acid (GABA) inhibition in the superficial layers of the superior colliculus, resulting from undetermined genetic mutations. Such disinhibition is manifested in two ways: (1) subclinically, by abnormal temporal discrimination due to prolonged duration firing of the visual sensory neurons in the superficial laminae of the superior colliculus, (2) clinically by AOIFD due to disinhibited burst activity of the cephalomotor neurons of the intermediate and deep laminae of the superior colliculus.

We tested this hypothesis by developing several experiments that involved the midbrain network for covert orientation of attention, specifically looking at various inputs and outputs from the superior colliculus in a principled and empirical manner. Three investigations were carried out to probe this hypothesis.

The first of these focused on the blood oxygen level-dependant (BOLD) response of the superior colliculus to looming, receding and random visual stimulus. In this investigation, responses of the superior colliculus and putamen during a visual looming task were examined in a cohort of unaffected first-degree relatives with (n = 18) and without (n = 18) abnormal temporal discrimination. General linear modelling (GLM) and dynamic causal modelling (DCM) approaches were employed to test the hypothesis that abnormalities previously observed in the putamen are an effect of inhibitory abnormalities in the superior colliculus. The GLM analysis revealed significantly reduced activity in the superior colliculus of those relatives with abnormal temporal discrimination during looming stimulus. The following DCM analysis supports the hypothesis that a link exists between this reduced superior colliculus activity and the previously observed putaminal abnormalities in AOIFD.

The second investigation involved the development of a novel system, designed for the presentation of visual stimulus and the acquisition of head kinematics and eye movements. This system was developed and validated in a group of healthy control subjects and was then employed for the characterisation of head and eye movements in cervical dystonia patients and age-matched controls. This system was developed around a virtual reality head mounted display (HMD) and synchronised to an external eye tracking system. We demonstrated the presence of a Posner effect in onset of head movement for the first time in man and then used this finding to show that covert attention abilities were abnormal in cervical dystonia patients. The presence of such an abnormality strongly supports the hypothesis of abnormal visual processing in the superior colliculus in cervical dystonia.

The final study investigated behavioural and electrophysiological objective measures during visuospatial learning in a cohort of healthy control subjects. The aim of this work was to develop and validate objective measures of visuospatial learning to facilitate future

13

research in a cohort of dystonic patients and unaffected relatives with and without abnormal temporal discrimination. The results presented in this chapter show that alpha power levels increase with automation of movement during visuospatial learning in healthy controls. This key insight can be used in future AOIFD research where automation of movement is expected to be abnormal under the current hypothesis.

The work than has been carried out here has expanded knowledge around the probably mechanism of cervical dystonia and has helped to validate the hypothesis that both abnormal temporal discrimination and cervical dystonia are the result of a disorder of the midbrain network involved in covert orientation of attentional, caused by reduced gamma-aminobutyric acid (GABA) inhibition in the superficial layers of the superior colliculus. BOLD signals, arising from the superior colliculus of AOIFD relatives, support the hypothesis by highlighting an important link between superior colliculus functional activity and temporal discrimination. A disproportionately large Posner effect in patients with cervical dystonia suggests an abnormality in covert attention processes. And finally, a novel paradigm and objective metrics of visuospatial learning will allow future researchers to search for additional abnormalities that may help to link AOIFD to a disordered midbrain network for covert attentional orienting.

1 Introduction

1.1 Classification of dystonia

Dystonia is a neurological movement disorder, recognised by sustained muscle contractions that cause twisting and repetitive movements or abnormal postures (Fahn, 1988, Fahn et al., 1998). The clinical features of dystonia were first introduced to the literature in detail in 1911 when Herman Oppenheim described 4 Jewish children affected by a syndrome that has since been considered to represent a familial case of DYT1 dystonia (Oppenheim, 1911). 64 years later, in 1975, the first international conference on dystonia was held in New York. At this time it was recognised that in addition to the generalised forms, the dystonia phenotype also included poorly progressive focal and segmental cases with onset in adulthood, such as blepharospasm and cervical dystonia (Marsden, 1976). It was in the following years that the true clinical complexity of dystonia began to be fully recognized.

Dystonia is amongst the most commonly misdiagnosed movement disorders (Fahn, 1984). As our understanding of dystonia evolves, so does our classification of the disorder. In general dystonia is classified based upon age of onset (young onset ($<$ 26 years) or adult onset ($>$ 26 years)), affected body region (focal, segmental or generalized) and aetiology (primary or secondary).

For the aetiology of a patient to be considered primary, they should present with dystonic features in the absence of other significant neurological abnormalities (excluding tremor or myoclonus). Where known, these patients can be classified by either genotype or else by phenotype (age of onset and affected body region). Secondary or "acquired" dystonia may be determined genetically or suspected in the presence of additional neurological or systemic abnormalities such as structural lesions, stroke, cerebral palsy or multiple sclerosis. Secondary dystonia can either be diagnosed as dystonia-plus, where dystonia is the primary feature or as heredodegenerative, where dystonia is an additional feature.
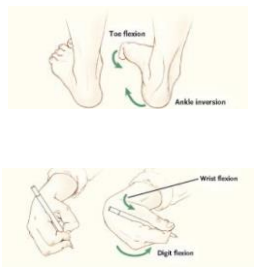
1.2 **Adult onset isolated focal dystonia**

Adult onset isolated focal dystonia (AOIFD) is the most common form of primary dystonia. AOIFD is generally classified as a focal dystonia although in some cases it may develop into a segmental dystonia over time, meaning that two or more contiguous parts of the body are affected (such as the eyes and mouth). AOIFD is comprised of several phenotypes including cervical dystonia, cranial dystonia and oromandibular dystonia,see Table 1.1 (Butler et al., 2004, Tarsy and Simon, 2006). Phenotypes of AOIFD are generally determined by the effected body region. Most cases of AOIFD appear to be sporadic but in up to 25% of cases patients are found to have an affected family member (Stojanovic et al., 1995, Leube et al., 1997). Familial AOIFD is inherited in an autosomal dominant fashion with a low penetrance of 12%-15% (Waddy et al., 1991). This low penetrance of the disorder means there are relatively few multiplex AOIFD families, making effective genetic studies of the disorder challenging. The prevalence of AOIFD has been investigated in several studies worldwide with large variations in estimations ranging from under 50 to over 7000 cases per million. Table 1.2 shows a summary of reported prevalence rates taken from European studies in AOIFD patients along with gender ratios and mean age of onset. This type of information can be very useful when investigating the impact of environmental factors on the onset of AOIFD (Molloy et al., 2014a).

Table 1-1

An overview of the common phenotypes of AOIFD. Illustrations and clinical features are given. As adapted from (Tarsy and Simon, 2006)

Phenotype	Illustration	Clinical Features
Cervical Dystonia (Spasmodic Torticollis) – most common focal dystonia.		Initially neck stiffness and restricted head mobility. Abnormal head posture follows, sometimes with irregular head tremor. Neck and shoulder pain is found in 75% of patients. Onset usually between 30 and 50 years of age.
Cranial Dystonia (including Blepharospasm)		May involve eyelids, jaw, vocal cords, face, tongue, platysma or pharynx. Blepharospasm is the most common form, manifesting with increased blinking, forced eye closure or difficulty opening eyes.
Oromandibular dystonia		Involuntary clenching, opening or deviation of the jaw. Muscles of the mount, tongue and neck are also frequently involved. Severe cases cause jaw pain and difficulty chewing.
Limb dystonia (including writers cramp)		Most commonly involves the legs. Involuntary twisting, flexion or extension postures of the arms, legs or digits. Occurs in association with skilled manual activities – occupation cramp disorders.

Table 1-2

Prevalence rates reported by European epidemiological studies in AOIFD patients are reported, along with reported gender ratio mean age at onset.

Study Location	No. of patients	Gender ratio (F:M)	Age at onset	Type	Prevalence (per million)
EDSE, 2000 Europe; 8 Countries	879	1:3	46.6	*Overall*	*117*
				Cervical	57
				Bleph	36
				Laryngeal	7
				Limb	14
Duffey et al, 1988 *Northern England*	372	1:2	42.4	*Overall*	*113*
				Cervical	61
				Bleph	30
				OMD	1
				Laryngeal	8
				Limb	12
Castelon Konkiewitz et al, 2002 *Germany*	188	1:5	50.4	*Overall*	*101*
				Cervical	54
				Bleph	31
				OMD	2
				Laryngeal	10
				Limb	4
Asgeirsson et al, 2005 *Iceland*	107	1:8	41.9	*Overall*	*312*
				Cervical	115
				Bleph	31
				OMD	28
				Laryngeal	59
				Limb	80
Duarte et al, 1999 *Spain*	48		48.4	*Overall*	*286*
				Cervical	75
				Bleph	102
				OMD	89
				Laryngeal	20
				Limb	
Le et al, 2003 *Norway*	129	2:1	46.3	*Overall*	*254*
				Cervical	130
				Bleph	47
				OMD	8
				Laryngeal	28
				Limb	
Pekmezovic et al, 2003 *Belgrade*	165	1:5	46.0	*Overall*	117
				Cervical	59
				Bleph	19
				OMD	3
				Laryngeal	11
Papantonio et al, 2009 *Italy*	69	1:4		*Overall*	*127*
				Cervical	44
				Bleph	68
				Other	15

1.3 Cervical dystonia

Cervical dystonia is characterized by sustained or intermittent neck muscle contractions which lead to abnormal and sometimes painful head movements, postures and dystonic tremor. Cervical dystonia is the most common form of AOIFD and will be the focus of much of the work reported here. There is huge variation when it comes to presentation of cervical dystonia and it can affect many combinations of the main cervical muscles, resulting in very distinct manifestations of the disorder. Broadly speaking, the presentation of dystonia will depend on whether the affected cervical muscles control posterior, lateral or anterior movement, and if those muscles impact movement of the head alone, or movement of both the head and the neck in relation to the trunk (see Figure 1.1) (Jost and Tatu, 2015).

Laterocollis:
ipsilateral
M. levator scapulae (M)
M. semispinalis cervicis (M)
M. scalenus medius (S)
M. longissimus cervicis (S)

Torticollis:
ipsilateral
M. semispinalis cervicis (M)
M. levator scapulae (M)
M. splenius cervicis (S)
M. longissimus cervicis (S)

Anterocollis:
bilateral
M. scalenus medius (M)
M. levator scapulae (M)
M. longus colli (S)

Retrocoliis:
bilateral
M. semispinalis cervicis (M)

Laterocollis   Torticollis   Antecollis   Retrocollis

Laterocaput   Torticaput   Antecaput   Retrocaput

Laterocaput:
ipsilateral
M. sternocleidomastoideus (M)
M. trapezius pars descendens (M)
M. splenius capitis (M)
M. semispinalis capitis (S)
M. longissimus capitis (S)
M. levator scapulae (S)

Torticaput:
contralateral
M. trapezius pars descendens (M)
M. sternocleidomastoideus (M)
M. semispinalis capitis pars med. (S)
ipsilateral
M. obliquus capitis inferior (M)
M. longissimus capitis (S)
M. splenius capitis (S)

Anterocaput:
bilateral
M. longus capitis (M)
M. levator scapulae (M)
M. sternocleidomastoideus (S)

Retrocaput:
bilateral
M. obliquus capitis inferior (M)
M. semispinalis capitis (M)
M. trapezius pars descendens (M)
M. splenius capitis (S)

Figure 1-1

Some of the primary subtypes of cervical dystonia and indicates which muscles are involved in generating the abnormal movement. Muscles can be considered as main contributors (M) or as secondary contributors (S). Adapted from (Jost and Tatu, 2015).

One of the most common and effective treatments for cervical dystonia is injection of botulinum neurotoxin into the dystonic muscles (Tsui et al., 1985). The effectiveness and safety of botulinum neurotoxin has been confirmed by a number of open and double-blind studies, with around 80% of participants having a positive responses to treatment (Truong and Jost, 2006). Treatment is generally provided every 3-6 months, depending on the patient's response. The effects of treatment take 5 to 10 days to manifest and can last anywhere from 10 weeks to 6 months. Incorrect use of botulinum can lead to complications

including difficulty swallowing and weakness of the cervical muscles; in a small number of cases patients have developed antibodies which can negate the positive effects of treatment. Ideally sonography and electromyography (EMG) would be employed to help ensure effectiveness of botulinum neurotoxin treatment in cervical dystonia, although equipment and training are not always available to clinicians. The ability to correctly and objectively characterise different forms of cervical dystonia could aid clinicians in muscle selection for botulinum treatment.

The use of deep brain stimulation (DBS) for treatment of cervical dystonia is becoming more common. It is generally recommended that patients exhaust all other treatment options before opting for DBS due to the inherent risks involved and the requirement for relatively frequent reviews to monitor and control settings. DBS is well established as a therapy in the management of movement disorders, most commonly in Parkinson's disease. In general, the target for deep brain stimulation in dystonia is the bilateral globus pallidus (Lettieri et al., 2015, Volkmann et al., 2012).

In addition to abnormal head and neck posture it has been reported than between 28% and 68% of patients present with abnormal head movements, often referred to as a tremor (Chan et al., 1991) (Pal et al., 2000, Jankovic et al., 1991, Dubinsky et al., 1993). Classification of tremor in cervical dystonia is ongoing but in general two different types of oscillatory movements have been reported in the literature. One of these movements is described as a regular sinusoidal oscillation with a frequency of 3 – 9Hz while the other is more irregular and jerky, with a frequency typically between 0.1 and 0.5 Hz (Shaikh et al., 2015b). These two distinct types of oscillation are depicted in Figure 1.2.
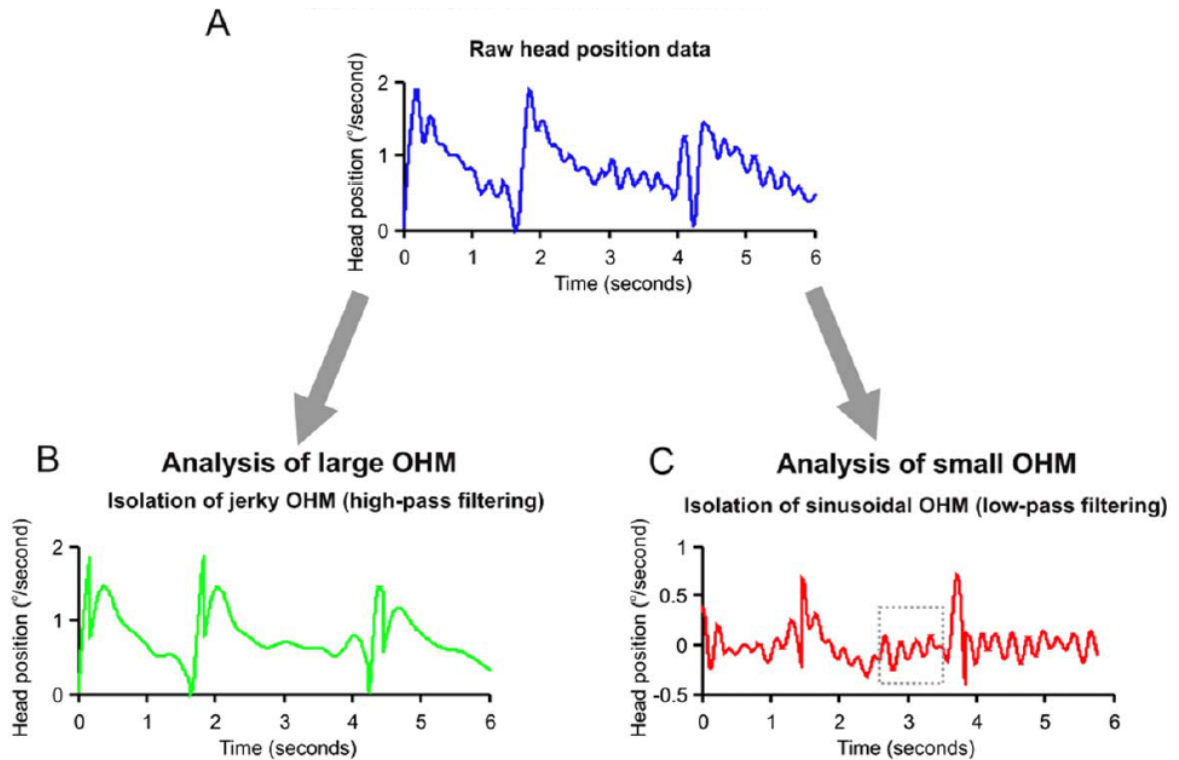
Figure 1-2

An example of oscillatory head movement collected using a magnetic search coil from a subject with cervical dystonia. Plot A show the raw movement data, collected from a patient who was instructed to hold their head steady. Plot B shows the isolated jerky oscillation which was obtained using a high-pass filter while plot C shows the isolated sinusoidal oscillation which was obtained using a low-pass filter. This data highlights how each of these distinct oscillations can be present in individual patients and indeed occur simultaneously. Adapted from (Shaikh et al., 2015b).

1.4   Mediational endophenotypes and temporal discrimination

An endophenotype is a subclinical quantitative marker of gene expression. Endophenotypes are useful for elucidating the genetic basis and the pathogenesis of disorders with low penetrance levels, such as cervical dystonia. For an endophenotype to be considered mediational, both the disorder and the endophenotype should be caused by the genetic disorder such that the pathway from the gene to disorder passes through the endophenotype, as shown in Figure 1.3. In other words, one cannot acquire the disease without first having the endophenotype. Only true mediational endophenotypes are useful

23

for understanding the genetic bases of disorders with low penetrance, and so, great care must be taken to ensure that any abnormalities that correlate with the disorder are true mediational endophenotypes and not a secondary or liability-index endophenotypes. There are two cases in which an endophenotype can be considered an epiphenomena, 1) if both the disorder and the endophenotype are caused by a genetic abnormality but lack any other relationship and 2) if the endophenotype results from the manifestation of the disorder, in which case we say the endophenotype is secondary. An example of a secondary endophenotype may be muscle atrophy in the effected region of a cervical dystonia patient; this atrophy is not caused by the genetic mutation but is instead a result of the manifestation of the disorder.
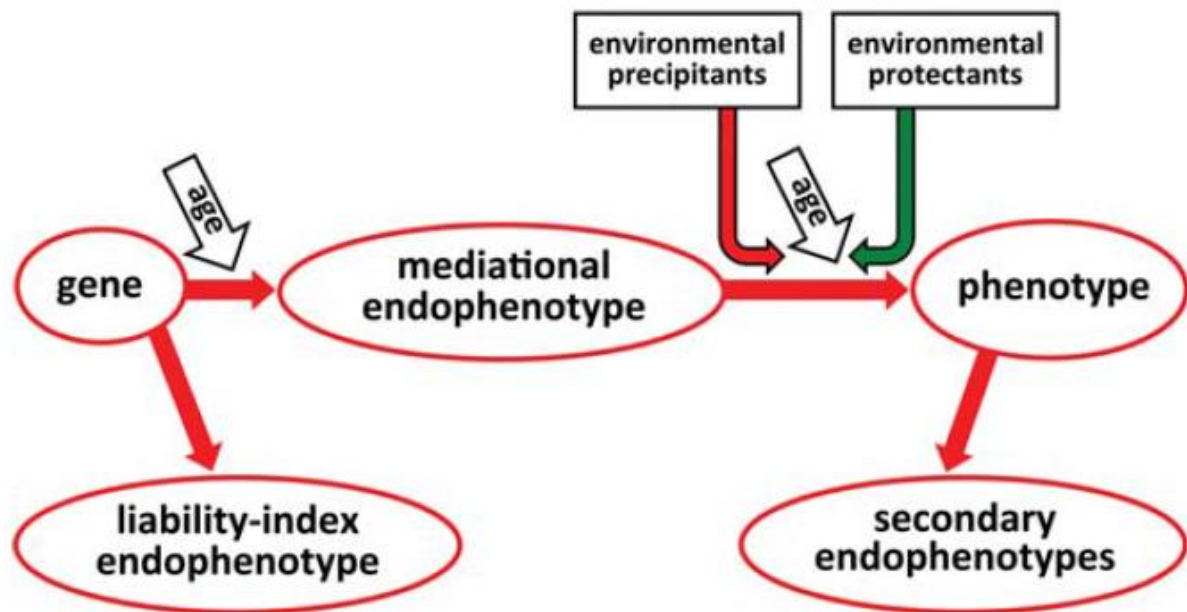
Figure 1-3

This figure highlights the interaction between the genotype, mediational endophenotype, other secondary endophenotypes and the phenotype. Mediational endophenotypes are closer to the genotype than that phenotype, such that one could not have the phenotype without first having the endophenotype. Secondary endophenotypes are products or symptoms of the disease and do not directly relate to the genotype. Distinguishing between mediational and secondary endophenotypes is critical as secondary endophenotypes are not useful for tracking the genetics of the disease. Adapted from (Hutchinson et al., 2013).

Significant sensory processing abnormalities have been found in patients with cervical dystonia. These abnormalities include deficits in both spatial and temporal discrimination thresholds (SDT & TDT) as well as vibration induced illusion of movement (VIIM) (Bradley et al., 2009, Bradley et al., 2010, Molloy et al., 2003, O'Dwyer et al., 2005, Frima et al., 2008, Fiorio et al., 2007). These sensory abnormalities may have utility as endophenotypes for cervical dystonia. In particular, abnormal TDT has shown promise as a robust mediational endophenotypes of cervical dystonia. Understanding the role of abnormal temporal discrimination in cervical dystonia will be a primary focus of this work.

The TDT is defined as the shortest time interval in which two stimuli may be determined as asynchronous, it is regarded as abnormal if it is more than 2.5 standard deviations above the control mean (Hutchinson et al., 2013). Abnormal TDTs show autosomal dominant transmission in both multiplex AOIFD families and in families of sporadic AOIFD patients (Kimmich et al., 2011, Bradley et al., 2009). Abnormal TDTs have been observed in 80% to 90% of patients with various AOIFD phenotypes and is highest in cervical dystonia at 97% (Bradley et al., 2012). There is an age related penetrance of an abnormal TDT in unaffected first-degree relatives. Full penetrance is observed in women by the age of 48 and 40% penetrance is seen in men (Kimmich et al., 2014).

There are two methods commonly employed to collect visual TDT. The original implementation of the paradigm employed table mounted stimulating lights positioned in the left and right peripheral vision and had to be carried out in a dimly lit room (Bradley et al., 2009). In order to obtain more accurate and repeatable measurements, a head mounted system was later developed which helped to ensure that the stimulus position remained consistent relative to head movements (Molloy et al., 2014b). This head mounted system was of particular importance for cervical dystonia, where patients reported difficulty in maintaining a neutral head position during the original implementation.
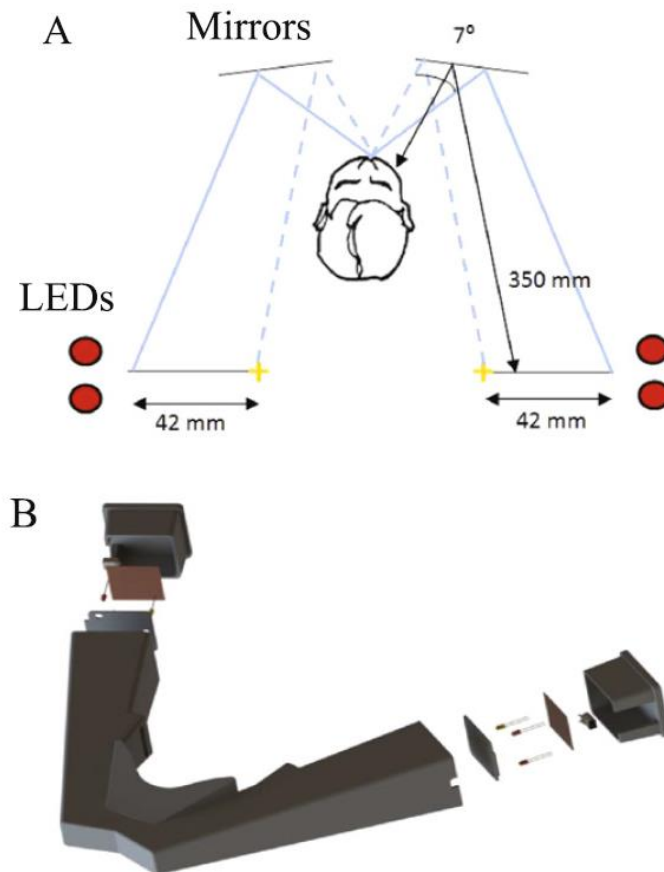
Figure 1-4

This figure shows; (A) a plan view schematic of the headset design. Light from the stimulating LEDs travels approximately 350mm to the eye of the participant via a reflecting mirror. (B) An exploded 3D model representation of the headset. Adapted from (Butler et al., 2015).

The head mounted system was designed using SolidWorks 3D CAD design software and was realised through the use of a ProJet^{TM} 6000 Professional 3D printer. The material selected for construction was a sintered nylon plastic called Strong and Flexible, supplied by Shapeways^{TM}. This material was selected for its low gloss level to help reduce unwanted internal reflections and for its low transparency to help reduce unwanted penetrance from external light sources. An Arduino Nano controls the LEDs and an LCD interface which is used by the clinician. The LCD interface allows the user to input participant information, select experimental parameters and to record the output responses of the participant.

The TDT test is carried out on each eye independently. The stimuli are initially synchronized with a difference in onset time of 0 ms, this difference is then increased in 5 ms increments after each presentation. Each stimulus presentation is separated by a 5 second interval, during this interval the participant is required to report whether the preceding stimuli appeared to be synchronous by stating "same" or asynchronous by stating "different". A single block is ended when a participant responds "different" on 3 consecutive occasions, the first of these is taken as the TDT score for that block. The task is preformed eight times, varying which LED leads and which eye is being tested in a randomized order such that each eye is tested for two "Top Lead" and two "Bottom Lead" blocks for a total of eight blocks per participant. The TDT for a participant is calculated by taking the median of the four runs for each side and then taking the mean value across left and right.

In addition to the single TDT score, a recent study highlighted the merits of looking at the data collected during TDT recordings in more depth. This method fits individual participant data with a cumulative Gaussian curve to extract the mean and standard deviation of the distribution of responses (Butler et al., 2015). The mean value is then taken as the point of subjective equality (PSE), the inter-stimulus interval at which a participant is equally likely to respond that two stimulus were synchronous as asynchronous. The standard deviation then represents the just noticeable difference (JND) which is a metric for how sensitive a participant is to changes around their own PSE. This data is then submitted to a non-parametric bootstrapping analysis to provide 95% confidence intervals for each participant's TDT, PSE and JND, Figure 1.5.
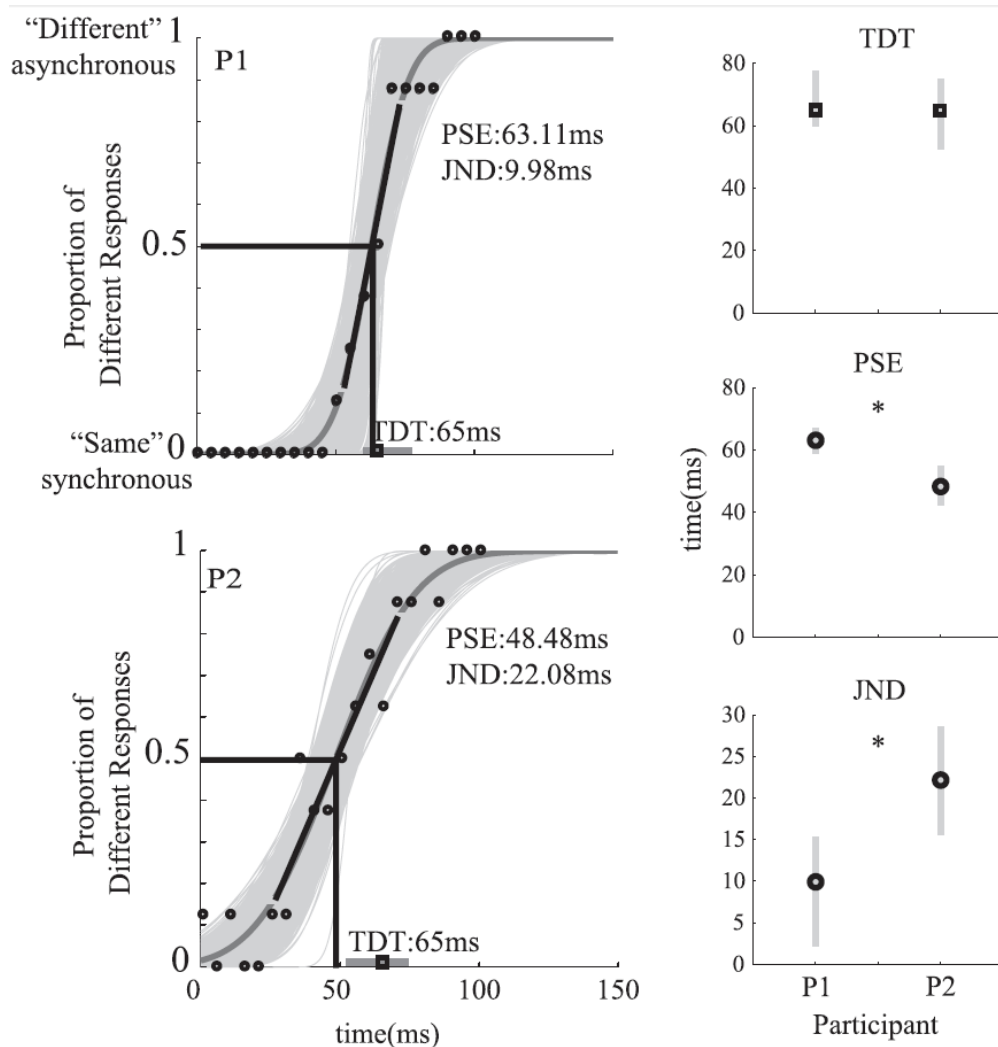
Figure 1-5

This figure shows TDT data collected from two cervical dystonia patients. Left: The black dots represent the proportion of "different" responses as a function of temporal asynchrony. The light grey curves show the 2000 Gaussian curves that are fitted during the bootstrap method. The vertical black line shows the participants point of subjective equality (PSE) while the slanted black line represents the participant's sensitivity or just noticeable difference (JND). The black square shows the participants TDT score. The plots to the right show the average and 95% confidence intervals for TDT, PSE and JND. This figure highlights how two participants can have statistically identical TDT scores with a different PSE and JND. Adapted from (Butler et al., 2015).

In that study it was found that both the PSE and the JND correlate with TDT while remaining independent of each other, suggesting that each metric represents a distinct aspect of a participant's TDT ability. It has been observed that both TDT and PSE are faster in women under the age of 40, but there is a sexual dimorphism such that the superiority is

reversed in the age group of 40 – 65. The JND was found to decrease equally in both sexes with age (Williams et al., 2015). This study highlights the point that the JND and the PSE represent different aspects of temporal discrimination and therefore allow researchers to ask more specific questions about temporal discrimination ability.

1.5   **The putamen and AOIFD**

In addition to the various phenotypes of dystonia, abnormal TDT abilities have been observed in Parkinson's disease (Artieda et al., 1992, Lee et al., 2005) and multiple system atrophy (Lyoo et al., 2007), suggesting a possible link between TDT ability and abnormal sensory integration in the basal ganglia. An fMRI study which employed a TDT task reported basal ganglia activation during the task and suggested that a disorder affecting the basal ganglia could therefore negatively impact temporal discrimination ability (Pastor et al., 2004). Another fMRI study employed an event-related experimental design to examine the time course of activation associated with different components of a TDT task and reported that activations in the basal ganglia occurred early and were uniquely associated with encoding time intervals, further supporting the idea that a disorder of the basal ganglia could affect temporal discriminability. A tactile TDT study employed electrical stimulus to the index finger of 84 normal participants and 51 patients with focal cerebral lesions (Lacruz et al., 1991). They found that lesions which did not produce any sensory impairment but still caused abnormal TDT scores were located in the posterior parietal cortex, the head of the caudate nucleus, the putamen, the medial thalamus and the lenticular nucleus. Furthermore they found that frontal, temporal and occipital cortex lesions did not produce any TDT abnormalities. Abnormal TDT scores were also observed on the affected side of patients with a lesion of the primary somatosensory cortex although this was likely caused by sensory impairment and would therefore represent a different mechanism to that involved in basal ganglia abnormalities.

The putamen is one of the structures that comprises the basal ganglia circuit, a group of nuclei in the brain that are connected with the cerebral cortex, the thalamus and the brain stem. It is a large round structure which together with the caudate nucleus forms the dorsal striatum. Abnormalities in the putamen in various forms of dystonia have been reported in the literature. An MRI study examined putamen size in 13 adults with either cranial or hand dystonia and compared them to 13 normal age and sex matched controls (Black et al., 1998). The volume of the putamen was measured using two independent methods, first by using the stereology method (Gundersen, 1992) and then by carrying out a manual tracing and using a direct voxel count. The study concluded that putamen volumes were 10% larger in patients than in controls and that this finding may reflect a response to the dystonia or may well relate to the genetic cause. The advent of voxel-based morphometry (VBM) has facilitated many new studies into putaminal volume in AOIFD. VBM studies have shown increased putaminal volume in patients with primary blepharospasm (Etgen et al., 2006) and in musicians with task-related dystonia (Draganski et al., 2009, Granert et al., 2011) further suggesting that the putamen may play an important role in the pathophysiology of these focal dystonias. Although these studies agree that putamen size is increased in these disorders, they were unable to address the questions of whether this enlargement represents a primary feature of AOIFD or a secondary feature which is caused in some way by the manifestation of the disorder, as was suggested by (Etgen et al., 2006).

In order to address this questions a VBM study employed visual TDT scores as a mediational endophenotype and examined putaminal volume of asymptomatic first degree relatives of cervical dystonia patients with and without abnormal TDT (Bradley et al., 2009). The study examined 13 unaffected relatives with abnormal TDT scores and 20 with normal TDT scores. It was observed that those relatives with abnormal TDT scores had a bilateral increase in putaminal grey matter volume, suggesting that the putaminal

enlargements observed in AOIFD are a primary phenomenon, stemming from the same, as yet unknown, genetic mutation that causes the disorder.
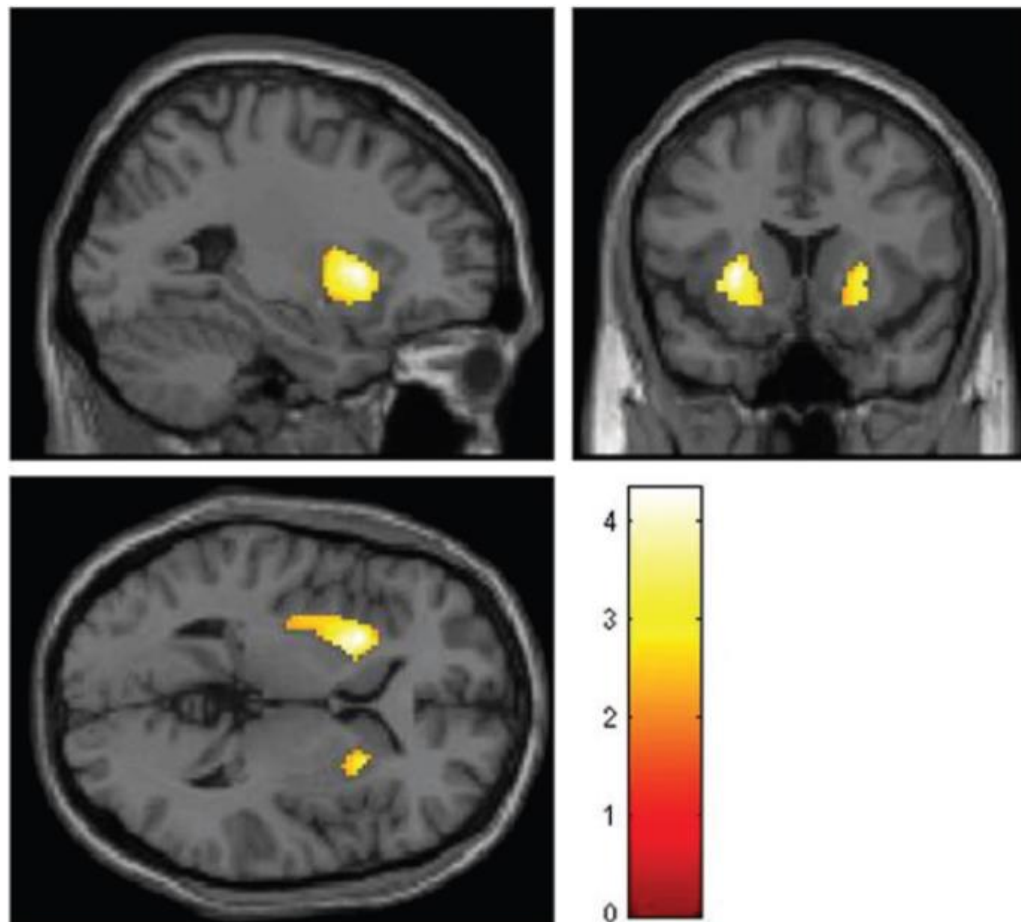
Figure 1-6

This figure shows results of the VBM analysis carried out by (Bradley et al., 2009). The figure shows increased volume in the anterior and posterior putamen on the left and right side in unaffected relatives with abnormal temporal discrimination compared to relatives with normal TDTs.

An fMRI study employing a temporal discrimination task found that unaffected relatives with abnormal temporal discrimination had less activation in the putamen and also in the middle frontal and precentral gyri (Kimmich et al., 2014). This study further supports the hypothesis that abnormal temporal discrimination is a robust mediational endophenotype of cervical dystonia involving a disordered basal ganglia network.

1.6 The role of the superior colliculus in AOIFD

The superior colliculus is a laminated deep brain structure. Its superficial layers (SLSC) responds solely to visual inputs from the retina via the retinotectal pathway while neurons in the deeper layers (DLSC) respond to multisensory, visual, auditory and tactile inputs (Redgrave et al., 2010). There is increasing evidence that the superior colliculus is central to the detection of unpredictable salient events that can trigger interruption of ongoing behaviour, contribute to higher-order decision making, initiate orienting responses of the head and cause saccades (Felsen and Mainen, 2012). This system, which alerts an individual to environmental changes, is known as the midbrain network for covert attention and the superior colliculus is a vital component of this network. The superior colliculus integrates multisensory information from visual, tactile and auditory sources and generates motor outputs for head, eye and upper limp movements as well as sending priority signals to substantia nigra pars compacta and the intralaminar nucleus of the thalamus (Redgrave et al., 2010).

The pathway through which salient environmental changes influence motor output involves a subcortical basal ganglia loop (Redgrave et al., 2010, Redgrave et al., 2011). The superior colliculus is the primary source of short latency visual inputs to the dopaminergic cells of the substantia nigra pars compacta (Dommett et al., 2005) and the intralaminar thalamic neurons (Coizet et al., 2007). The main output from the intralaminar thalamic nucleus is to the cholinergic interneurons of the striatum which respond to unexpected visual, auditory or somatosensory stimuli with brief short-latency firing (Matsumoto et al., 2001). Recent studies have shown that synchronous stimulation of cholinergic interneurons dramatically elevates the release of dopamine in the striatum (Threlfell et al., 2012). Elevation of dopamine release in the striatum was also observed with increase of glutaminergic input from the thalamus (Surmeier and Graybiel, 2012). Recent animal studies have shown that

thalamic stimulation causes a burst-and-pause response in the striatum, this burst of activity in the striatum causes a brief decrease in cortico-striatal transmission to medium spiny neurons in both the direct and indirect pathways. This is followed by a prolonged facilitation of transmission in the indirect ("no-go") pathway but not in the direct ("go") pathway (Thorn and Graybiel, 2010). This provides a mechanism by which one can stop an ongoing motor output in response to a salient environmental input and, if required, a redirection of that motor output. This collicular-thalamic-putaminal-pallidal-nigral loop is described in Figure 1.7 as a person responds to a looming stimulus with either a "go" or "no-go" decision.
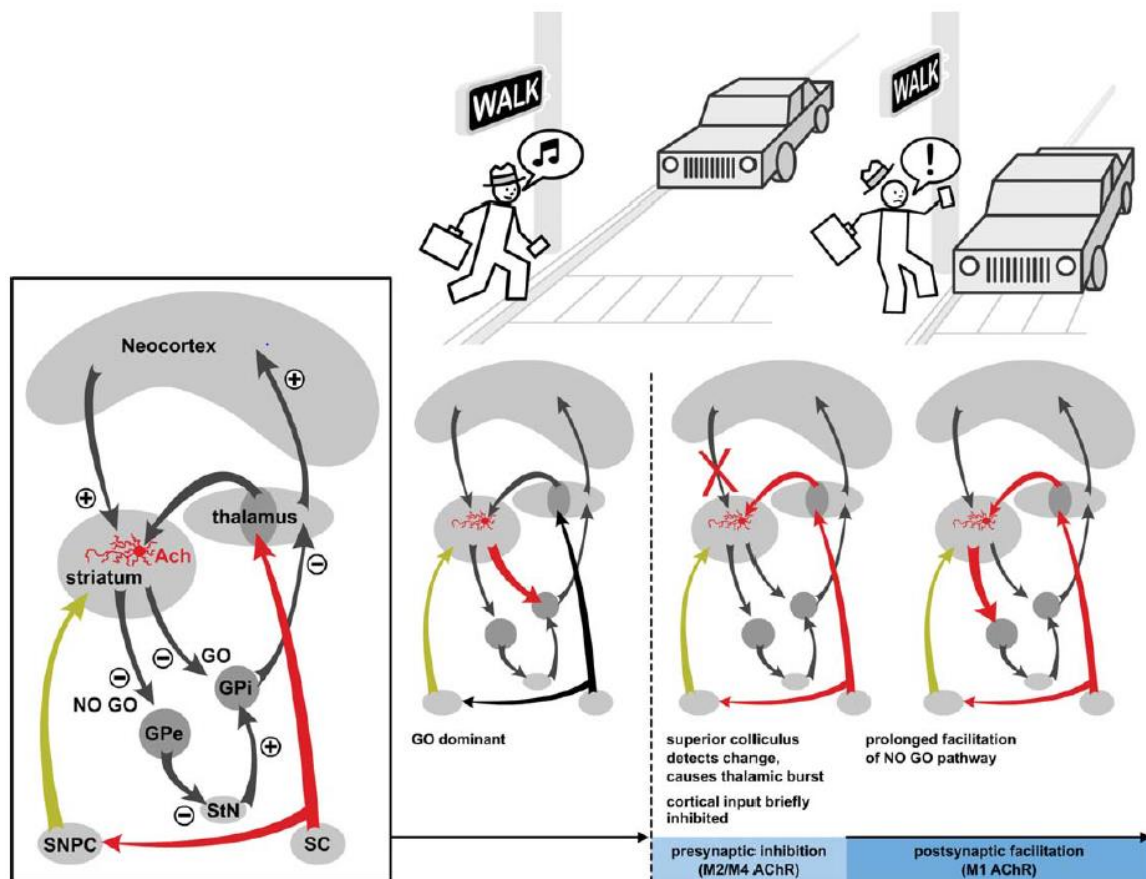
Figure 1-7

This figure shows the subcortical circuit employed for the detection of and response to unpredictable environmental changes. In response to a potentially hazardous looming visual input, a stimulus from the SC to the intralaminar thalamic neurons causes a burst of firing in thalamostriatal pathway to the cholinergic interneurons, resulting in a burst and pause response in the striatal cholinergic interneurons. The resulting burst of acetylcholine interrupts cortical inputs to the striatum for both the direct "GO" and indirect "NO-GO" pathway. This pause in the direct pathway allows for prolonged facilitation in the "NO-GO" pathway. This mechanism is activated by unexpected events in the environment and interrupts the ongoing activity in the "GO" pathway, allowing for an appropriate response. It has been postulated that this pathway is involved during the temporal discrimination task. Adapted from (Thorn and Graybiel, 2010)

Visual responses in the superior colliculus occur in the SLSC where the most predominant cell type is the wide field visual cell. Visual neurons in the SLSC respond to visual input with a transient "ON" response at a latency of less than 50ms (Kaneda and Isa, 2013). This is observed as a short burst of firing following a visual stimulus. If the visual stimulus is persistent in nature these neurons enter a "PAUSE" phase during which firing stops. When the visual stimulus is then ended another burst of activity is observed, known as the "OFF"

phase. This sequence is known as the "ON-PAUSE-OFF" sequence and is characteristic of the response in the SLSC to the switching on and off of visual stimulus such as that observed during the TDT testing described in section 2.4. In this way the superior colliculus acts as an edge detector, responding to changes in visual stimulus rather than persistent stimulus. A study in mice found that the application of a $GABA_B$ antagonist resulted in an increased "ON" firing duration. The application of a $GABA_A$ and a $GABA_B$ antagonist resulted in the prolonged firing duration of both the "ON" and the "OFF" phases of the sequence, resulting in the effective shortening of the "PAUSE" phase (Kaneda and Isa, 2013).
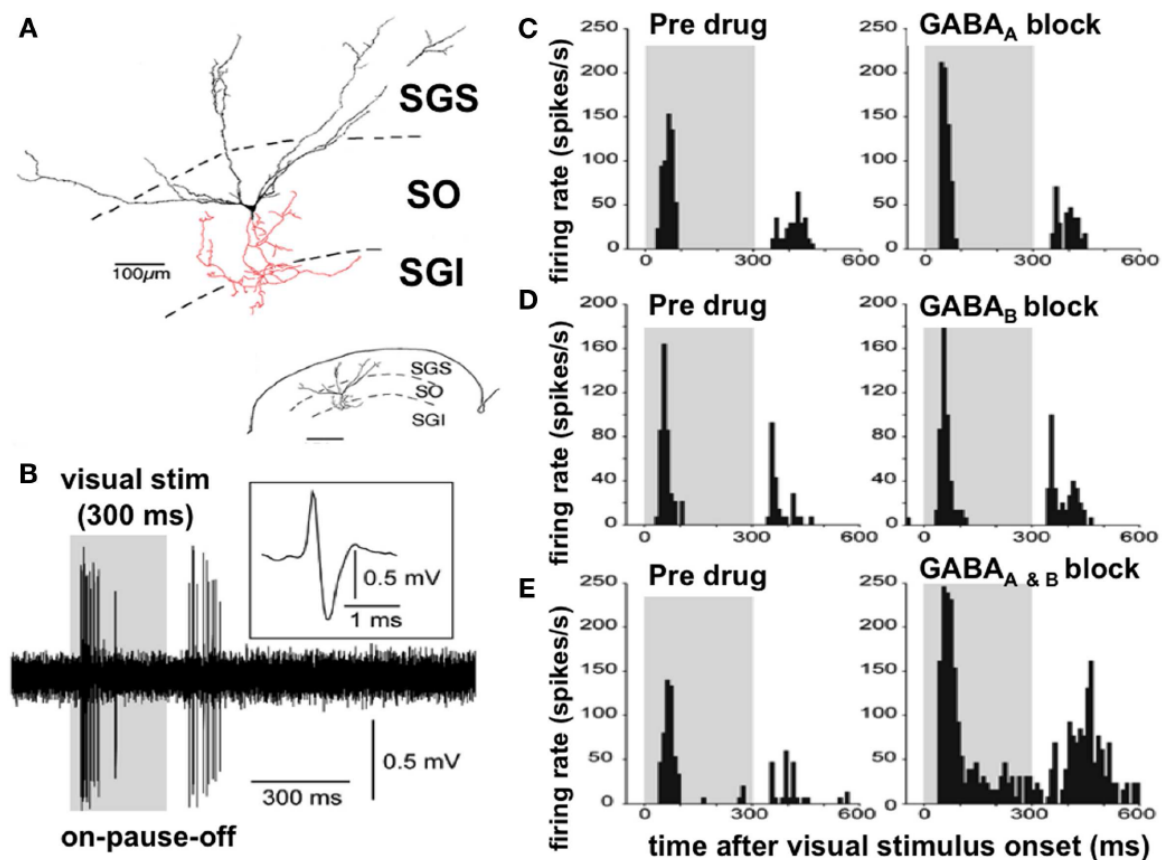
Figure 1-8

This figure shows the burst activity of WVF cells in the SLSC of mice. A: A typical WVF cell in the superficial layers of the superior colliculus. B: The "ON-PAUSE-OFF" burst sequence that is evoked in WVF cells in the SLSC during a persistent visual stimulus of 300ms. The grey shaded area shows the duration and location of the visual stimulus and the inset shows the morphology of a single spike. C: local application of the GABA$_A$ antagonist increases peak "ON" firing rate but does not significantly reduce decay rate. D: GABA$_B$ antagonist does not impact peak firing rates but significantly reduces the decay rate of "ON" burst activity resulting in increased "ON" duration and decreased "PAUSE" duration. E: Administration of both GABAA and GABAB antagonist results in both increased firing rates and reduces decay rates of both "ON" and "OFF" burst activity. Adapted from (Kaneda and Isa, 2013).

It is the role of GABAergic inter-neurons to activate GABA$_B$ receptors and turn off the "ON" and "OFF" burst activity that occurs following visual stimulus in the SLSC. This GABAergic inhibition prevents the prolonged burst activity and the resulting shortening of the "PAUSE" phase in the SLSC. It has been hypothesised that this mechanism allows the SLSC to detect the appearance or change of an object in the visual field while not being

impacting by persistent presentation of said stimulus, thus allowing the SLSC to function as a saliency detector (Endo et al., 2005).

It has been hypothesised that the temporal discrimination abnormalities that have been observed in AOIFD may relate to this "ON-PAUSE-OFF" sequence and the effect of reduced GABA (Hutchinson et al., 2014). As can be seen in Figure 1.8, inhibition of $GABA_A$ and $GABA_B$ results in a slower decay of firing for both the "ON" and "OFF" phases of the sequence resulting in a shortening of the "PAUSE" phase. During a TDT test a subject observes two LEDs as they turn on and off in close succession. The hypothesis is that the increased duration of both the "ON" and "OFF" firing caused by the GABAergic deficit would increase the required inter-stimulus interval between the LED onsets before two events could be detected to be asynchronous. The hypothesis is that impaired GABAergic activity in the SLSC result in an abnormally prolonged temporal discrimination threshold due to a decreased decay rate in the "ON" and "OFF" phases of the sequence. This hypothesis is graphically depicted in Figure 1.9.
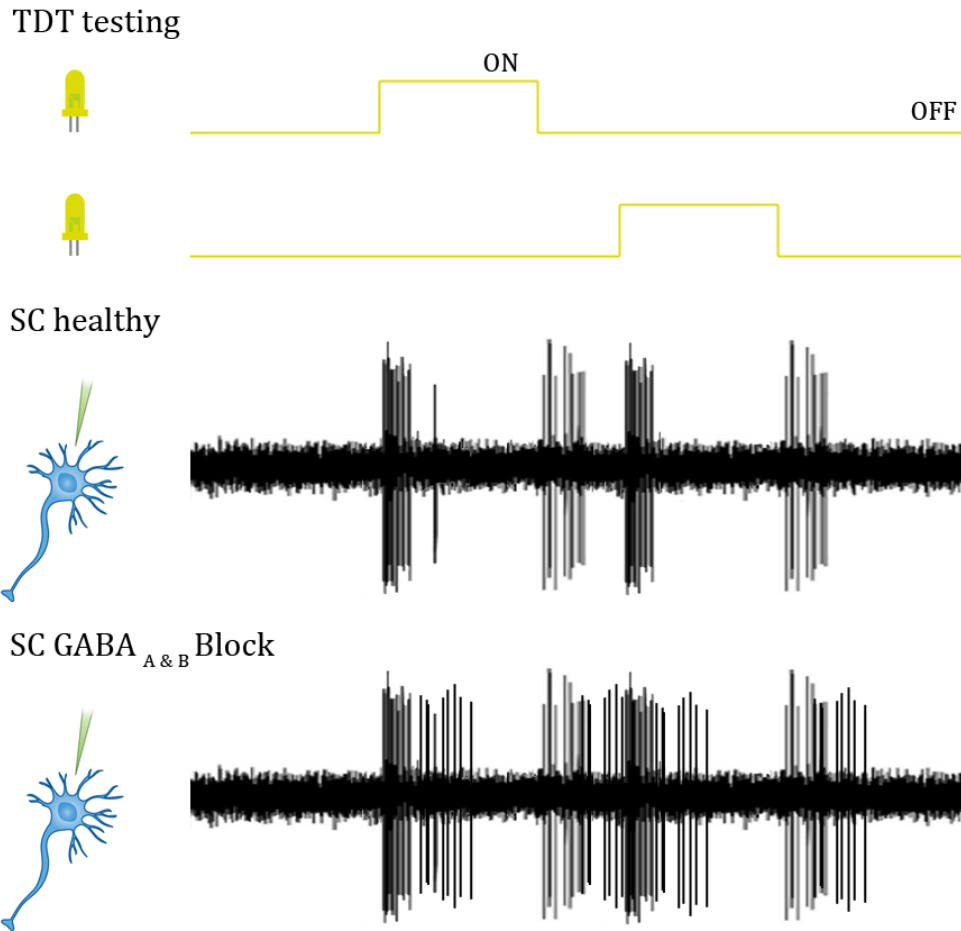
Figure 1-9

This figure depicts a graphical representation of the hypothesis that abnormal temporal discrimination abilities stem from a GABAergic abnormality in the superficial layers of the superior colliculus. Two LEDs are shown to turn on and off with a nominal inter stimulus interval while the burst activity of two WVF cells in the SCSC is shown below. This figure highlighted how this burst activity might overlap in the cell with the GABAergic deficit resulting in the two stimulus appearing to be synchronous while the healthy cell is able to delineate the timing of the two events.

The basal ganglia are essential for posture control, motor coordination, initiation of movement and motor learning. Substantia nigra pars reticulate (SNpr) and globus pallidus internal segment (GPi) are the two motor output nuclei of the basal ganglia and dysfunction of these nuclei can give rise to motor and postural abnormalities (Mink, 2003). Several studies have shown that a cervical dystonia-like disorder can be induced by inhibiting substantia nigra pars reticulate in the nonhuman primate. Unilateral SNpr lesions in

monkeys caused abnormal dystonia-like head turning and head tilting on the opposite side to the lesion (Lestienne and Thullier, 1998). The injection of a GABA agonist (muscimol) into the left SNpr resulted in a contralateral torticollis in 10 out of 12 monkeys (Burbaud et al., 1998). The injection of a muscimol into central and posterior sites of the SNpr resulted in contralateral torticollis in 3 out of 3 monkeys (Dybdal et al., 2013). Inhibition of GPi, the second output of the basal ganglia, has never been shown to cause cervical dystonia, suggesting that a target of SNpr projections may have an important role in cervical dystonia. The only projection of SNpr not shared by GPi is the superior colliculus, SNpr has a GABAergic projection to the DLSC. A recent study pretreated the DLSC of four macaques with muscimol to test the hypothesis that this key target of nigral projection is required for the emergence of experimental cervical dystonia (Holmes et al., 2012). The study found that this treatment prevented experimental cervical dystonia, implicating the superior colliculus as an important node in future cervical dystonia research.

Given the importance of the superior colliculus as a node in the covert attentional network and the evidence of abnormal temporal discrimination in cervical dystonia, a hypothesis that intrinsic sensory processing in the superior colliculus is disrupted in individuals with abnormal TDTs has been established. To fully explore this hypothesis a series of experiments were proposed to test superior colliculus function in different experimental cohorts. These studies were designed to examine different processes involving the superior colliculus and employed behavioural, electrophysiological and neuroimaging methods to develop objective measures of superior colliculus disruption.

2 Research Questions

AOIFD is a neurological movement disorder believed to stem from GABAergic abnormalities in the subcortical basal ganglia networks involved in covert attention, specifically affecting the superficial layers of the superior colliculus. A detailed review of the current literature, as outlined in Chapter 1, has uncovered several key findings that help to outline the research questions that this work will aim to address. These findings include behavioural abnormalities in terms of reduced temporal and spatial discrimination and physiological abnormalities in terms of putaminal size and activation in dystonic patients and their relatives with abnormal temporal discrimination.

The common question at the heart of this thesis is: What is the role of the superior colliculus in the pathogenesis of AOIFD?

2.1   Looming responses in the superior colliculus

- Are superior colliculus abnormalities detectable with the current generation of 3T fMRI scanners? Recent fMRI work has demonstrated the capability of a 3T scanner to detect functional differences in superior colliculus activation between looming and random motion in a group of healthy controls (Billington et al., 2011). The current hypothesis suggests that abnormal processing may exists in the superior colliculus, but it is unclear if such an abnormality would result in a detectable difference in BOLD signal.

- Can a GLM analysis be employed to detect visual processing abnormalities in the superior colliculus? Previous fMRI work investigating the superior colliculus has focused on a region of interest analysis and did not report on any 2nd level (group level) GLM results. It is likely that the small size of the structure coupled with inter-subject differences made such an approach unsuccessful, although this was not reported in the literature. The work carried out here will attempt to employ such a GLM analysis although the small size of the superior colliculus may represent a significant challenge.

- How will reduced GABA in the superior colliculus be manifested the BOLD signal? A reduction in GABA could be manifested in several ways. In general, one would expect an increase in activity, and therefore BOLD signal, in a region with reduced GABA. This is because GABA is an inhibitory interneuron and so acts to retard firing. However, given that the superior colliculus is primarily populated by GABAergic neurons, it is also plausible that a reduction in GABA would manifest with a reduced BOLD signal in the superior colliculus.

- Is the proposed GABAergic abnormality limited to the superior colliculus? Under the current hypothesis it is unclear whether the proposed GABAergic deficit is a global phenomenon or if it specifically effects the superior colliculus or basal ganglia loop. If the mood disorders that have been associated with AOIFD (Hentschel et al., 2017) are also a result of the proposed GABAergic deficit then it is likely that it is a global issue.

- Does the superior colliculus respond solely to looming stimulus? This study work will employ looming, receding and random visual stimulus. Although the literature suggests that the superior colliculus will respond primarily to the looming stimulus it is unclear if a response will also be generated by the receding stimulus given this condition still represents a form of structured movement. It is not expected that random dot motion should elicit any response, although this will need to be confirmed.

- Are the putaminal abnormalities associated with AOIFD linked to the proposed superior colliculus abnormality? The putamen has been observed to be physically enlarged and less active in dystonic patients and unaffected first-degree relatives with temporal discrimination abnormalities. Under the current hypothesis these changes must also be explained by the proposed GABAergic abnormality in the superior colliculus. The proposed DCM work will aim to test if these putaminal abnormalities are a downstream effect of abnormal GABAergic activity in the superior colliculus.

- Is the superior colliculus an acceptable target for a DCM analysis approach? It is unclear if DCM of fMRI can be successfully employed to investigate superior colliculus connectivity given its size and location. For such an approach to be successful it will be important to identify the most relevant circuits for modelling. Connections between the superior colliculus and putamen exist via the frontal eye field and are commonly investigated in the saccade literature. Perhaps of higher significance are the connections from the superior colliculus to the putamen via the thalamus and SNpc within the sub-cortical network for covert attention. It is likely this circuit, or some simplification of this circuit, that is most suitable to address the current hypothesis using a DCM approach.

2.2 Head kinematics, eye movements and orientation of attention

The superior colliculus is a key node of the sub-cortical network involved in the orientation of covert attention and the Posner paradigm is a common tool employed for investigating the functionality of this network. The Posner paradigm uses valid and invalid cues to elicit button press or saccadic responses. In healthy subjects a delay in onset is observed for invalid cues, this delay is known as a Posner cueing effect. The current study will aim to develop a modified Posner task that will be designed to employ head movements rather than eye-movement or button press responses.

- Does the Posner effect exist for onset of head movement in man? It is currently unclear if the Posner effect, which has been demonstrated in onset of eye-movement and button press response is present in the ecologically valid onset of head movement. This study will first aim to address this question by collecting head-kinematic data during a novel iteration of the Posner paradigm in healthy control subjects. This study will employ a virtual reality head-mounted display (HMD) to accomplish this task.

- Do AOIFD patients have abnormal Posner effect during onset of head movement? Rapid head and eye movements in response to external visual and auditory stimulus are generated in the superior colliculus. Under the current hypothesis it could therefore be expected that responses to a peripheral target may be abnormal in AOIFD patients and first-degree relatives with abnormal temporal discrimination. This question would be best answered by investigating head movements of normal and abnormal relatives in a Posner style paradigm. However, given the nature of the Posner effect, as a self-normalized measurement, it may be possible to address this question using a control-patient comparison. If an abnormal Posner effect is present in cervical dystonia, it will be unclear if the abnormality stems from a disordered network for orientation of covert attention or is a result of the manifestation of a movement disorder effecting the muscles of the neck. It is possible that this question can be addressed by carrying out a segmented analysis of patients. Such an analysis would test if the disordered side produced a larger abnormality than the unaffected side. If this were the case it would suggest than any abnormality is in fact a result of the disorder.

2.3 **Visuospatial learning and electrophysiological correlates**

Visuospatial learning uses the same subcortical basal ganglia networks thought to be abnormal in AOIFD. Therefore, visuospatial learning may be negatively affected in AOIFD patients and in unaffected abnormal relatives. This study will develop a paradigm and objective measures of visuospatial learning which will have future applications in the investigation of superior colliculus function in AOIFD.

- Is there a valid relationship between visuospatial learning and P3b amplitude? The task employed in this study will be adapted from a recent publication (Bednark et al., 2013). That study investigated how the amplitude of the P3b EEG component changed during

learning and suggested a link between this metric and visuospatial learning. This analysis was carried out at a very coarse level, comparing only the first and second half of each block. The proposed study will investigate this relationship at a higher resolution and test if a relationship exists between P3b amplitude and visuospatial learning in the current task.

- Can EEG data be incorporated in the current task to provide additional, meaningful information? Movement times will be employed as a behavioural measure of visuospatial learning. This is the most straightforward measure of learning for the current task and does not involve the inclusion of cumbersome EEG recording equipment. This study will include EEG on a pilot basis and will only recommend its inclusion for further research if additional information is to be gained. A correlation between P3b amplitude and movement times does not grant any additional information over the use of movement times alone.

- Can alpha power be employed as a measure of automation of movement during visuospatial learning? This study will investigate novel components of the EEG signal to uncover new metrics that may be informative for the investigation of visuospatial learning in AOIFD. Alpha power will be investigated, as the current literature would suggest that it may be informative about automation of response during the proposed task.

- Can visuospatial learning be employed as a tool to investigate superior colliculus function in AOIFD? If this study is successful in developing a robust paradigm and objective metrics of visuospatial learning and automation of response in a control population, then future work will be able to investigate if these metrics are abnormal in AOIFD patients and their unaffected relatives with reduced temporal discrimination. This would help to support the hypothesis that AOIFD and reduced temporal

discrimination stem from an abnormality of the covert attention circuit including the superior colliculus.

3 Looming responses in the superior colliculus

3.1 Introduction

AOIFD is a common neurological movement disorder recognised by sustained muscle contractions that cause twisting and repetitive movements or abnormal postures (Fahn, 1988, Fahn et al., 1998). The pathogenesis and the genetic basis of AOIFD remain poorly understood. In recent years research into this disorder has revealed some interesting mediational endophenotypes and neurological abnormalities, these include abnormal temporal discrimination of visual and tactile stimuli as well as abnormalities in size and BOLD activation of the putamen.

Significant sensory processing abnormalities have been found in patients with AOIFD. These abnormalities include deficits in both spatial and temporal discrimination thresholds (SDT & TDT) (Bradley et al., 2009, Bradley et al., 2010, Molloy et al., 2003, O'Dwyer et al., 2005, Frima et al., 2008). In particular, abnormal TDT has shown promise as a robust mediational endophenotypes of AOIFD. The TDT is defined as the shortest time interval in which two stimuli may be determined as asynchronous; it is regarded as abnormal if it is more than 2.5 SD above the control mean (Hutchinson et al., 2013). Abnormal TDTs show autosomal dominant transmission in both multiplex AOIFD families and in families of sporadic AOIFD patients (Kimmich et al., 2011, Bradley et al., 2009). Abnormal TDTs have been observed in as much as 97% of cervical dystonia patients (Bradley et al., 2012). There is an age related penetrance of abnormal TDT in unaffected first-degree relatives. Full penetrance is observed in women by the age of 48 and 40% penetrance is seen in men (Kimmich et al., 2014). Unaffected relatives with abnormal TDTs have also been seen to have larger putaminal volumes by voxel-based morphometry than relatives with normal TDTs (Bradley et al., 2009). This putaminal enlargement is also observed in patients with AOIFD and in musicians with task-related dystonia (Draganski et al., 2009, Granert et al., 2011).

It has been hypothesized that the endophenotype, putaminal abnormalities and the disorder are an effect of reduced inhibitory activity in the superior colliculus, the current work aims to address this hypothesis. This study will attempt to probe this question by employing a dynamic causal modelling (DCM) approach to fMRI data collected during a looming paradigm in normal and abnormal first-degree relatives of AOIFD patients. This DCM analysis will focus on the superior colliculus and the putamen and will aim to test the hypothesis that the endophenotype, putaminal abnormalities and the disorder are an effect of reduced inhibitory activity in the superior colliculus.

DCMs can be applied to both fMRI and EEG data sets and are primarily useful in understanding neural connectivity. When employing a DCM approach, one must make simplifying assumptions about the neural circuits under investigation. In the case of a clinical application, such as dystonia, these assumptions must be informed by pre-existing knowledge of the pathophysiological mechanisms of that disorder. DCM is a hypothesis driven approach and requires detailed models of neuronal circuitry to be proposed a priori. For this approach to be successful it is important that the correct structures are identified and incorporated into the proposed models.

In a recent fMRI study, activation of the superior colliculus was associated with a looming stimuli but not with receding or random stimuli, suggesting superior colliculus sensitivity to looming objects (Billington et al., 2011). The paradigm employed by Billington will be utilized here as it has been shown to produce activity in the superior colliculus during recordings with a scanner of a similar specification to that available to the current study.

3.2 **Dynamic causal modelling overview**

Functional specialization of different neural areas depends largely on experimental context. This idea can be explained in terms of functional integration, which is mediated by context-dependant interactions among spatially segregated areas (McIntosh, 2000). In other words, the function of an area in the brain may be altered by its connectivity, which in turn can be altered by experimental context. In this vein, the functional role of a neural structure is largely defined by its connections and interactions with other neural structures (Passingham et al., 2002).

Three types of qualitatively different connections are commonly talked about in neural literature: 1) structural connectivity, 2) functional connectivity and 3) effective connectivity. Structural connectivity describes the anatomical layout of axons and synaptic connections. It determines which neural units have explicit interactions and can be studied using techniques such as MRI and blunt dissection of major fibre systems. The distinction between functional and effective connectivity is more subtle but extremely relevant, especially in the context of DCM. This topic was explored by Karl J. Friston is great detail in his review of functional and effective connectivity (Friston, 2011). Functional connectivity is usually inferred on the basis of correlations among measurements of neuronal activity, it is defined as statistical dependencies among remote neurological events. However, correlations can arise in a variety of ways that are not necessarily indicative of biological interactions. For example, in EEG recordings, correlations can occur in stimulus-locked transients evoked by a common input or can reflect stimulus-locked oscillations mediated by synaptic connections (Gerstein and Perkel, 1969). Interaction within a distributed system (i.e. the brain) can be better explained in terms of effective connectivity. Effective connectivity refers explicitly to the influence that one neural system exerts over another, either at a synaptic or population level. Two of the most

important points in relation to effective connectivity are: 1) effective connectivity is dynamic (activity-dependant) and 2) it depends on a model of interactions or coupling.

DCM is a novel approach for testing effective connectivity, first introduced for fMRI in a seminal paper by Friston et al (Friston et al., 2003). The concept of causal modelling in neuroimaging had been explored earlier than this but inputs to those models were treated as unknown or stochastic signals and had limited applications in research (Jansen et al., 1993, Dujardin et al., 1995). It was the use of designed deterministic inputs that made the work of Friston meaningful. The aim of DCM is to estimate, and make inference about, the effective connectivity among brain areas and to determine how this connectivity is influenced by changes in experimental context (Friston et al., 2003).

The DCM framework is made up of two primary components, a biophysical model and a probabilistic statistical method of data analysis. A realistic neurobiological model is required to relate experimental manipulations (e.g. visual or tactile input, task demand) to the dynamics of the observed data. However, highly context-dependant variables of these models cannot be known a priori, therefore, statistical techniques are required for inference of these context-dependant effects, which are the experimental questions of interest. Simply put, the two primary components of DCM are, 1) a modelling component and, 2) a statistical evaluation component. Here, a brief description of each component is presented.

All forms of DCM aim to describe how observed data was generated based on knowledge of the experimental inputs and previous knowledge of neural connectivity. The foundation of DCM is the generative model, a quantitative description of the mechanisms by which the observed data were generated. In general, it is assumed that both electromagnetic (EEG/MEG) and hemodynamic (fMRI) signals arise from a network of brain regions or neuronal populations that are functionally segregated, rather than arising from a single node

or multiple independent nodes. This network can be thought of as a directed graph where the sources correspond to nodes and the conditional dependencies among the hidden states are mediated by effective connectivity.

DCMs describe how experimental manipulations (input, u) influence the dynamics of hidden neuronal states of the system x, using ordinary differential equations. These differential equations are sometimes referred to as evolution equations in the DCM literature.

$$\dot{x} = f(x, u, \theta)$$

(1)

Where $\dot{x}$ is the rate of change of the systems state x, f represents the biophysical mechanisms underlying the temporal evolution of x and θ is a set of unknown evolution parameters. The structure of the evolution function f determines the presence or absence of edges in the graph and determines how these edges influence the dynamics of the systems states Figure 3.1.
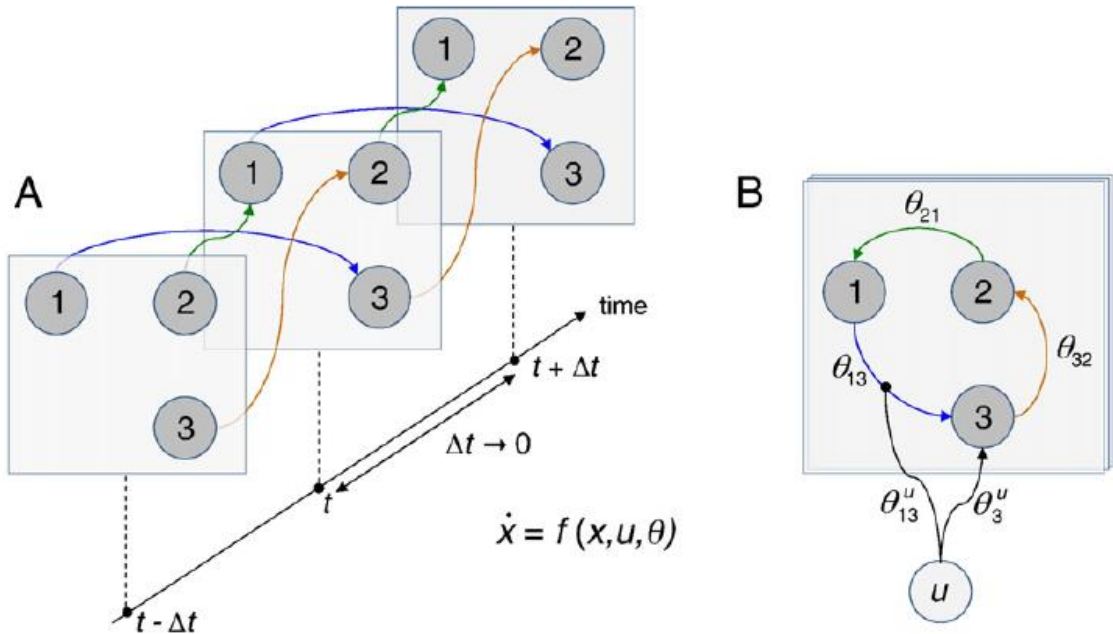
Figure 3.3-1

This figure depicts two equivalent representations of an exemplar DCM structure. A: This figure shows a time-dependant acyclic graph (DAG), which depicts the condition dependencies between hidden states. Edges are shown as directional arrows, highlighting how different regions impact on one another, e.g. region 3 is determined by the state of region 1 from the previous sample (-Δt). B: An equivalent time-invariant effective connectivity graph. Here state-state connectivity is indicated using the parameter (θ_{21}, θ_{32}, θ_{13}). The input to this system is also shown as the node u, which has connections to node 3 as well as the connectivity parameter θ_{13}. In all variant of DCM, these coupling parameters and modulatory effects are modelled as unknown parameters. Adapted from (Daunizeau et al., 2011)

DCMs map the system's hidden state (x) to experimental measures (observed data, y). This can be expressed using the following static observation equation:

$$y = g(x, \varphi)$$

(2)

Where g represents the instantaneous mapping from system sates to the observed data and φ is a set of unknown observation parameters.

These equations form a hierarchical chain, which can be described by the flow chart below. The input (u, experimental manipulation) maps to our hidden state (x) though the evolution

equation f. The observed data (y) can then be explained from the hidden state through the static observation equation g.

| u (input) | f | x (hidden state) | g | y (observed data) |
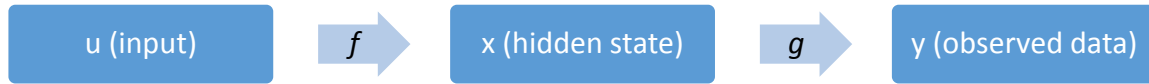
This chain of causality is critical in the DCM framework for the process of model inversion, as it accounts for potential spurious covaritations of measured time series that are due to the observation process g. For example, spatial mixing of sources at the macro level of the EEG/MEG sensors. Model inversion describes the process of estimating the unknown parameters, θ and φ, based on the observed data y. This means that the biophysical model validity for both the evolution and observation functions is important for correctly identifying the presence of effective connectivity in the data.

The need for neurobiological plausibility in DCM models can sometimes make the DCM analysis quite complex, at least when compared to other regression-based models of effective connectivity, such as structural evaluation modelling (SEM) (Friston et al., 1997), or autoregressive models (Harrison et al., 2003). This level of complexity, with potential non-identifiable problems, requires a sophisticated model inversion technique which is usually cast within a Bayesian framework. Below is an outline of the theoretical steps involved in this statistical analysis.

Using statistical assumptions about the residual errors in the observation process, Equations 1 and 2 are compiled to derive a likelihood function p (y|ϑ, m). This function specifies how likely it is to observe a particular set of observations y, given the parameters $\vartheta \equiv (\Theta, \phi)$ of the model m.

The priors p (ϑ, m) are defined on the model parameters ϑ which reflect given knowledge about a likely range of values. Such priors can be (i) principled (e.g., certain parameters cannot have a negative value), (ii) conservative (e.g., shrinkage priors express the assumption that the coupling parameters are zero) or (iii) empirical (based on previous experimental measurements).

By combining the priors and the likelihood function, the marginal likelihood of the model can be derived via Bayes' Theorem. In DCM, the marginal likelihood of the model is usually referred to as the model evidence.

$$p(y|m) = \int p(y|\vartheta, m)p(\vartheta|m)d\vartheta$$

(3)

Combination of priors and the likelihood function also allows an estimator $\vartheta\text{^}$ of model parameters ϑ to be estimated through the posterior probability density function p (ϑ|y, m) over ϑ:

$$\vartheta = \int \vartheta \, p(\vartheta|y, m)d\vartheta$$

$$where \quad p(\vartheta|y, m) = \frac{p(y|\vartheta, m)p(\mu|m)}{p(y|m)}$$

(4)

Where the estimator $\vartheta\text{^}$ is the first order moment of the posterior density, the expected value of ϑ given the observed data y. The role of the estimator is to minimise the expected sum of squared error, $E[(\vartheta-\vartheta\text{^})^2|y]$.

The model evidence that is calculated using Equation 3 is then used for model comparison, selecting which model (described in the different evolution functions f) best fits the

observed data y. The posterior density equation is used to make inference about different model parameters such as context-dependant modulation of effective connectivity.

3.3 Materials and methods

3.3.1 Participants and Ethics

Thirty-six subjects were scanned during the current study, 18 unaffected first-degree relatives of cervical dystonia patients with normal temporal discrimination (9 female, age = 51.7 +- 7.1) and 18 unaffected first-degree relatives of cervical dystonia patients with abnormal temporal discrimination (9 female, age = 54 +- 8.7). In accordance with the Declaration of Helsinki, all participants gave their written informed consent to the study, which was approved by the Faculty Ethics Committee of the Faculty of Health Sciences at Trinity College Dublin.

Table 3-1

Subject details

	Normal	Abnormal
n	18	18
Age: mean (std)	51.7 (7.1) years	54 (8.7) years
TDT-score: mean (std)	0.26 (0.82)	4.48 (1.65)
Male	9	9
Female	9	9

3.3.2 Experimental protocol

MRI acquisition was carried out on a Philips Achieva 3T scanner located in the MRI lab in the Trinity College Institute of Neuroscience, Dublin. A SENSE 32 channel head array coil was employed during image acquisition. During functional scans, 40 slices were acquired across the whole brain with a slice thickness of 3mm and an interstice distance of 0mm,

resulting in a voxel resolution of 3x3x3 mm. A gradient-echo planar image sequence was employed with a repetition time of 2 seconds, an echo time of 25 ms and a flip angle of 90°. Slices were oriented such that they were parallel to the brainstem at the level of the pons to ensure inclusion of the superior colliculus.

The task employed in the current study is an adaptation of the loom recede paradigm presented by Billington et al. (Billington et al., 2011). This paradigm was selected as it was shown by Billington to be very effective in generating activation of the superior colliculus in a cohort of healthy control subjects. All stimuli were presented monocularly to the left eye; a patch covered the right eye for the duration of the experiment. Monocular stimulus presentation was employed to increase the perceived effect of 3-dimentional movements for the participant and increase the likelihood of superior colliculus activation. Forty repetitions of three conditions were presented over the course of four blocks in a randomized order. The inter stimulus interval was varied between 7.5 and 9 s to facilitate an event-related fMRI design and to prevent habituation of response. An overview of this experimental paradigm is shown in Figure 3.2. An event related design was selected to facilitate region of interest and dynamic causal modelling analysis approaches, neither of which can be applied to the more conventional block experimental design.

Stimuli were generated and presented using Neurobehavioral Systems' Presentation software to meet the specifications as outlined by Billington. In each condition a spherical structure was generated by placing light points at 500 vertices on the shell of an invisible sphere. The spacing of these points expanding during looming flight and contracting during receding flight to produce an impression of a structured object moving in space. To further the impression of three-dimensional movement, a rotation of 45^0 s^{-1} was added to spheres in flight, randomized across the 3 axes of rotation, yaw, pitch and roll. The motivation to use light points on the shell of a sphere rather than a solid object was that the light point

method allows the luminance and chrominance levels to remain constant over the entire movement. Basic visual changes such as increasing or decreasing luminance would add unwanted variance to the BOLD signal and would make it more difficult to observe variance related to looming alone.

In all conditions, two pairs of vertical lines were also presented. The colour of these lines (green, yellow or blue) corresponded to one of the three experimental conditions, which was explained to participants prior to the experiment. These lines were also employed in the loom and recede condition as the targets for the time to contact (TTC) task. At the beginning of each trial the sphere faded into the start position over 1.5 s before undergoing motion for 1 s and then disappearing some time before a TTC button response was required.
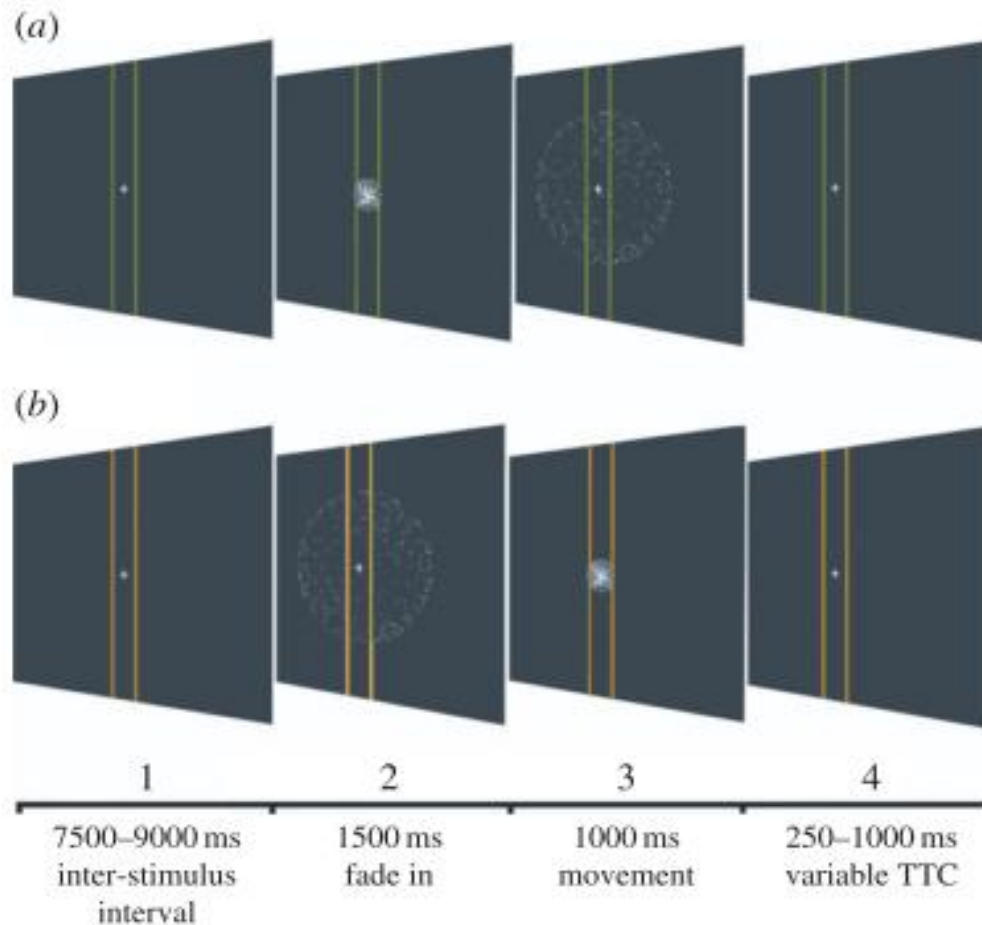
Figure 3-2

The figure gives an overview of the sequence of events during a looming (a) and receding (b) trial. The colour of the vertical lines indicates the trial type, loom, recede or random. Timings are shown by the time scale at the bottom of the figure. Figure adapted from (Billington et al., 2011)

Loom: During the looming condition a sphere faded into view with an optical diameter of 8^0 over the initial 1.5 s. It then underwent linear and rotational movement towards the participant for 1 s and disappeared approximately 0.25s before contacting the outer set of vertical lines, at this point the sphere had a visual diameter of 18^0. Participants were instructed to press a button when they judged the diameter of the sphere would match the width of the outer vertical lines.

Recede: During receding trials the sphere started with an optical diameter of 18^0 and moved away from the participant until it had an optical diameter of 8^0. Fade-in and movement timings were matched to the loom condition. In this condition participants were directed to press a button when they estimated that the diameter of the sphere would match the width of the inner vertical lines. This condition was included to control for visual movement in space and the requirement to make a TTC judgement.

Random: During the random condition a sphere faded-in with an optical diameter of 18^0. In this condition the dots did not undergo any linear or rotational movement but instead underwent random motion at a speed equivalent to the mean rate of dot motion from the other two conditions. This persisted for 1 s and the participant was directed to press the button when a blue square appeared approximately 0.25s after the sphere disappeared. This condition was included to act as a low level visual control.

Velocities and starting positions were randomized with a jitter of +-10% across trials to minimize habituation of the TTC motor response.

3.3.3   fMRI data analysis

Pre-processing and data analysis were carried out using MATLAB 2014a and the statistical parametric mapping toolbox (SPM12; http:/www.fil.ion.ucl.ac.uk/spm). The first 4 images from each session were discarded to allow for equilibrium magnetization. EPI blood oxygen level-dependant (BOLD) images were first realigned and re-sliced using a six-parameter spatial transformation with the first non-discarded image as a reference. Estimated motion parameters calculated during the realignment step were saved for later use as nuisance regressors in the first level general linear model (GLM). The structural T1 weighed image was co-registered to the mean of the resliced and realigned images. The unified segmentation routine was employed to perform the segmentation bias correction

and the spatial normalization. All images were normalized to MNI space using the standard ICBM template. Two sets of smoothed images were then generated using a kernel with 4mm and 8mm full-width at half maximum. The images smoothed using an 8mm kernel were employed for the group level 2nd level GLM work; the larger kernel was selected to account for inter-subject variability as well as individual movement. Images were smoothed using the 4mm kernel were employed for DCM work which is carried out at the individual level where there is no concern about inter subject variability. The four blocks collected from each subject were treated as a different session during the pre-processing stage.

A single GLM was created for each subject, concatenating scans from all four blocks and including 4 nuisance regressors to account for discontinuity between recordings. Onset of movement for loom, recede and random trials were included as three separate regressors of interest. The duration of each event was set to one second to correspond to the duration of stimuli movement. The time between offset of stimuli and the TTC response was excluded from the duration time to avoid directly modelling early motor preparatory responses. The 6 movement parameters that were estimated during the realignment procedure were also concatenated across blocks and included as nuisance regressors to account for unwanted movement. All regressors were then convolved with the canonical hemodynamic response function before being entered into the GLM analysis.

For each subject a set of contrast images was generated for further testing at the group level. These contrast images were divided into two groups, basic 1-sample t-tests which tested for activation against a 0 baseline (condition $>/<$ 0) and contrast 2-sample t-tests which looked for differences in activation between different condition and different sets of conditions (condition A $>/<$ condition B). Each of these contrasts is outlined below.

- Basic 1-sample t-test

- Loom (loom >/< 0)

- Recede (recede >/< 0)

- Structured movement (loom & recede >/< 0)

- Random (random >/< 0)

- Basic visual (loom & recede & random >/< 0)

- Contrast 2-sample t-test

  - Loom vs. recede (loom >/< recede)

  - Loom vs. random (loom >/< random)

  - Recede vs. random (recede >/< random)

  - Structured movement vs. random (loom & recede >/< random)

The above contrast images were generated at the first level and then submitted to a second level analysis. Three second level GLMs were generated for the current data set. In the first of these models all participants were included in a single GLM to provide an overview of activity under the current paradigm. In this model a significance level of 0.05 was selected with a family wise error correction applied.

Then the 36 participants were separated into two groups based on TDT score and a GLM was generated for each group. The groups were made up of first degree relatives with normal temporal discrimination and first-degree relatives with abnormal temporal discrimination. For simplicity, these groups will be referred to as normal relatives and abnormal relatives. An uncorrected significance level of 0.001 was selected for this group level analysis to account for the smaller number of subjects in each group.

3.3.4 Superior colliculus boundary definition

It was important to specify an objective superior colliculus boundary prior to examining any results arising for the 2nd level GLM analysis. In order to accomplish this, T1

anatomical scans were imported into Mango and the superior colliculus was localised by a trained neurologist, a neuropathologist and a neuroradiologist. An image representing this boundary definition is shown in Figure 3.3, this boundary was employed for all superior colliculus GLM analysis and during the eigenvariate extraction procedure which is carried out for each subject during the DCM analysis.
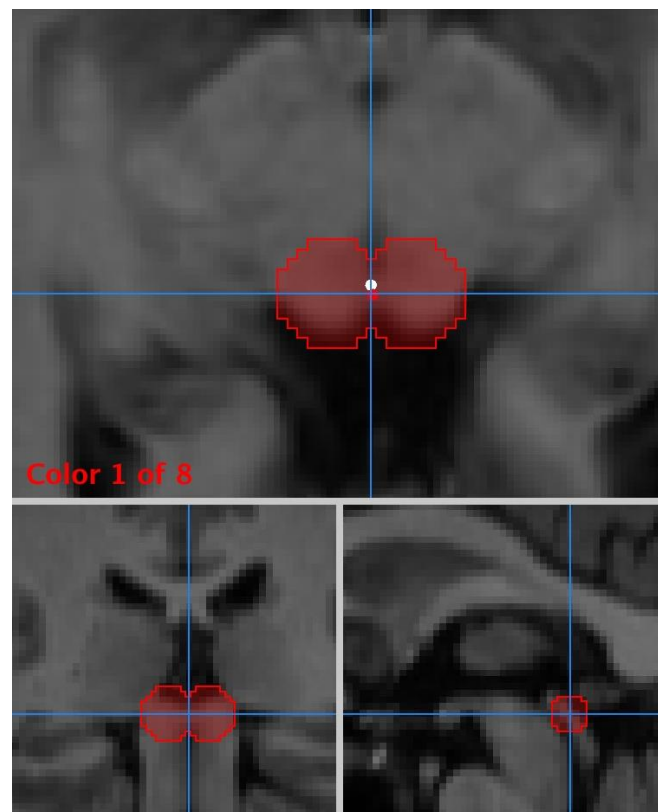
Figure 3-3

Superior colliculus boundary employed during GLM and DCM analysis steps.

3.3.5   *Region of Interest Analysis*

Event-rated time course data was extracted for each subject from within the superior colliculus boundary for the looming, receding and random motion conditions. Percentage signal change following stimulus was calculated for each individual as an estimate of BOLD signal change within the region. Peak percentage signal change was selected to represent the magnitude of an individual's functional activation to each stimulus type. The

peak percentage signal change was then compared between groups using an independent Student's t-test for the three main conditions. Following from this, a Pearson's correlation analysis was carried out to compare TDT scores and peak percentage signal change for the three main conditions.

3.3.6 Dynamic causal modelling

The results revealed by the 2nd level GLM analysis at the segmented group level suggest that differences exist in superior colliculus activation between the normal relative group and the abnormal relative group. Broadly speaking, it was observed that activation of the superior colliculus was lower in abnormal relatives, see Results section of this chapter for further details surrounding this statement. Previous work has suggested that GABA abnormalities in the superior colliculus may be related to abnormal temporal discrimination, which has been observed in dystonic patients and some first-degree relatives (Hutchinson et al., 2013, Bradley et al., 2012).

Previous work in this area has shown that unaffected relatives of cervical dystonia patients with abnormal temporal discrimination show less putaminal activation during temporal discrimination tasks (Kimmich et al., 2014). Voxel based morphometry studies have also shown that the putamen is physically larger in these abnormal relatives (Bradley et al., 2009). These studies suggest a link between abnormal temporal discrimination in dystonia and the putamen. Given that the superior colliculus has inputs to the putamen via the thalamus and substantia nigra pars compacta (SNPC) it is possible that an abnormality in the superior colliculus would lead to the putaminal abnormalities that have been observed to date. The aim of this DCM analysis was to test this hypothesis.

A DCM model was created to investigate the hypothesis that the differences being observed at the putamen are in fact a downstream effect of erroneous visual processing in the superior

colliculus, caused by a GABAergic deficit in dystonic patients and their first-degree relatives with abnormal temporal discrimination. This model was based upon the subcortical circuit which is employed for detecting and responding to unpredictable environmental change and looming objects. This circuit is covered in more detail in chapter 2 of this thesis and is shown in Figure 3.4.

1: Anatomic Loom Circuit
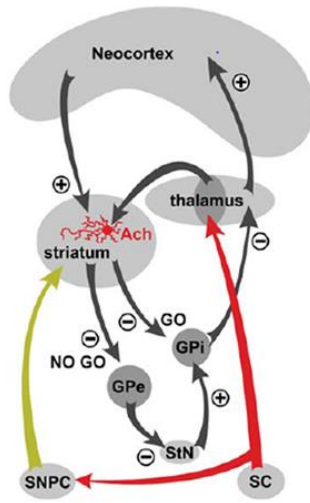
2: Extensive uni-lateral DCM model for Loom
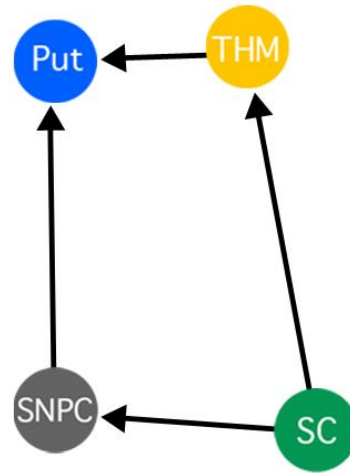
3: Condensed uni-lateral DCM model

4: Final bi-lateral DCM model
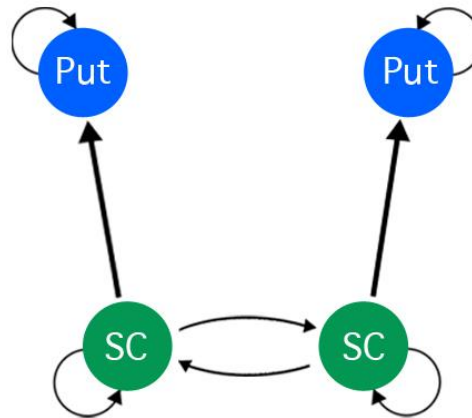
Figure 3-4

This figure was designed to demonstrate development of the DCM model that has been employed in this study. The model is based upon the anatomical loom circuit as outlined in Chapter 2. From this circuit the extensive unilateral model was create which includes both paths from the superior colliculus (SC) to the putamen (Put) via the thalamus (THM) and SNPC. This model was then condensed so that the effect of superior colliculus activity on the putamen could be examined, regardless of its path. Finally, this model was expanded to create the final bi-lateral DCM model which represents the basic fixed connections common to all models under the current DCM analysis.

Due to the limitations of DCM it is not possible to model the entirety of the anatomical looming circuit. This model would be too complex, contain too many nodes and be likely to run into problems during model estimation. Furthermore, each of these nodes would need to be active for all participants and so it is likely that many would be rejected from the analysis. To avoid these issues when using DCM, it is advisable to select a subsection of a given circuit that will have the most relevance to a given hypothesis. In the case of the current study and the proposed looming circuit, the most relevant subset of nodes and connections would include the superior colliculus, the putamen, SNPC and the thalamus. This model is depicted in the second image in Figure 3.4 and would represent the most complex DCM model that might be investigated under the current study. This model was rejected for two reasons. Firstly, this model in its bi-lateral form would consist of eight nodes and 20 fixed connections which would still be too large a model to investigate and would still lead to many participants being rejected during the analysis. Secondly, the current hypothesis is not concerned with activity in SNPC or the thalamus, they are only included in this model as they act as an intermediary connection to the putamen. By ignoring these nodes and summing their inputs towards the putamen we arrive at the 3rd model in this progression. This unilateral model is designed to capture how activity in the superior colliculus effects activity in the putamen, regardless of which path is involved. This simplistic model captures the essence of the looming circuit while also meeting the requirements for a valid DCM analysis. The 4th image in this figure shows the final bi-lateral version of this model. In this model the superior colliculus has connections bi-laterally to its counterpart and excitatory connections toward the putamen. Each node in the model also has an inhibitory self-connection as is required under the DCM framework.

Having identified regions of interest at the group level, BOLD time series data was extracted from each participant individually for each of the nodes in the model. Time series

was extracting from all regions using a t-contrast for loom, recede and random and a p-value threshold of p < 0.1 uncorrected (note: This p-value is used to locate clusters for principal eigenvariate extraction and does not have any bearing in the final DCM statistic). For each participant voxels of interest were selected around the group peak co-ordinates for the superior colliculus and the putamen. Principal eigenvariates were extracted for a 5mm sphere, correcting for effects of interest of the three regressors of interest, loom, recede and random motion.

Five models were proposed to test the potential interactions that could best explain the time series data for each subject. The fixed connections and inputs remained consistent across these models and the modulatory effects were varied. As it was not practical to test all possible combinations of different modulatory effects, a subset of five models was constructed to probe the entire model space in a principled manner. A null model with no modulatory effects was also tested. Each of these models are depicted in Figure 3.5. All models were estimated, and the winning model was found using a random-effects comparison for all participants. Fixed and modulatory connections strengths were then extracted from the winning model and tested for correlation with TDT scores. Given the hypothesis that abnormal temporal discrimination stems from an inhibitory abnormality in the superior colliculus, self-connections of the superior colliculus were the focus of this analysis.

Due to the high computational demands of stochastic DCM model estimation and the high number of participants in the current study it was necessary to employ parallel cluster-based computing during this step of the analysis. The Lonsdale server, based in the Trinity Centre for High Performance Computing was employed for this task and an individual core was dedicated to each participant.
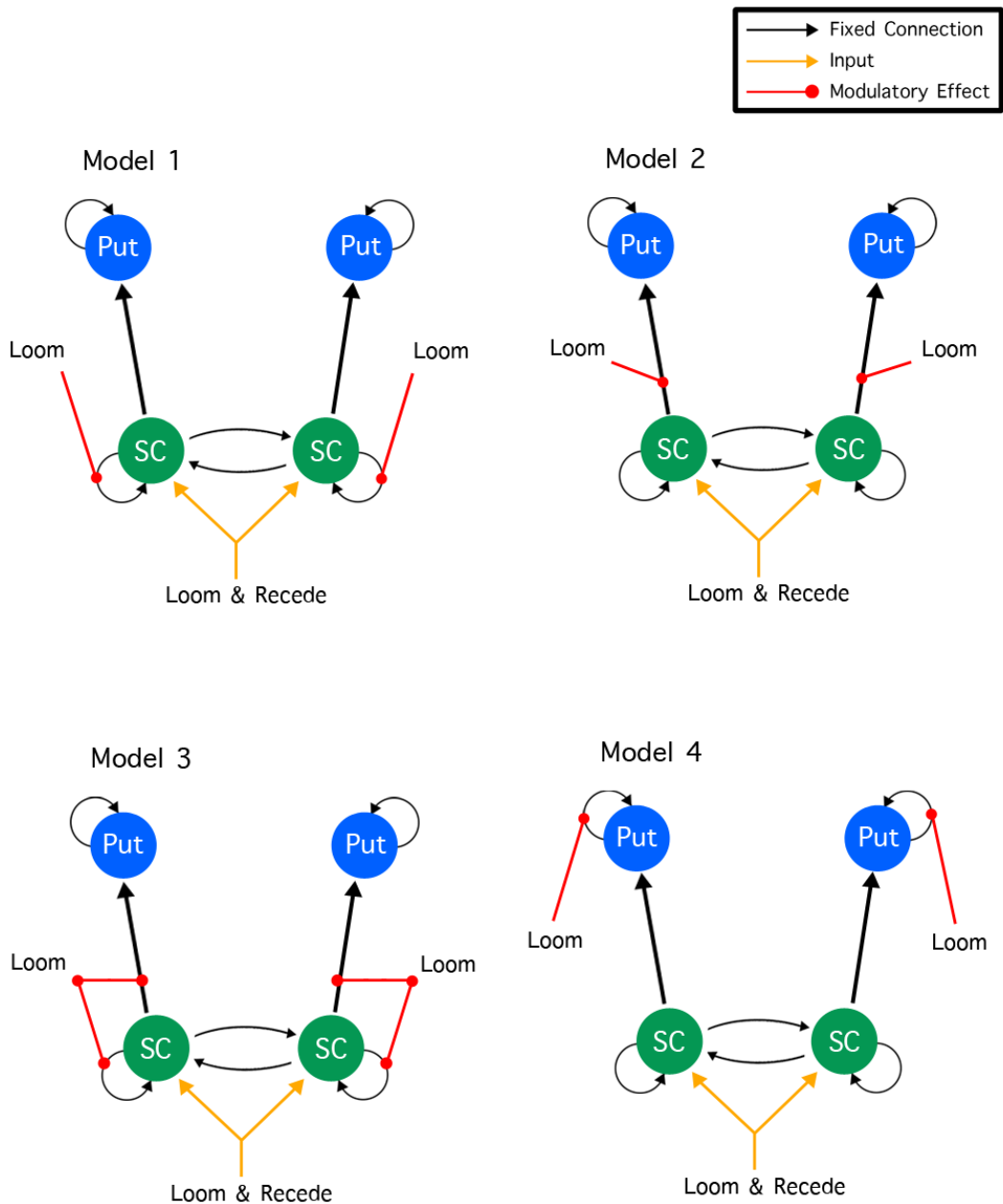
Figure 3-5

This figure shows four of the five models that have been employed in the current DCM analysis. The null model (model 0), which does not include any modulatory connections is not displayed here. Black arrows represent fixed connections which are constant across all models. Orange arrows represent experimental input to the model, based on the results of the 2nd level GLM analysis and the literature review in chapter 2, all structured movement (loom & recede) were selected as inputs to the model. The red dots represent modulatory connects, different modulatory connections distinguish these models from one another.

3.4 Results

3.4.1 Second level GLM: All participants, superior colliculus

This section will focus on the 2nd level GLM analysis that was carried out to include all subjects. The results of the whole group 2nd level GLM analysis are displayed in Figure 3.6. A threshold of significance of 0.05 with a family wise error correction was selected for this larger data set. The results of the basic contrasts analysis shown in Figure 3.6 seem to support the findings reported by Bednark et. al in their original publication of this paradigm (Bednark et al., 2013). The results for the loom condition show a significant activation of the bi-lateral superior colliculus. This activation pattern is highly consistent with the superior colliculus boundary as outlined in the methods section of this chapter. This result supports the existing literature which tells us that the superior colliculus responds primarily to looming visual stimulus which is projected directly from the retina via the retinotectal pathway to the intermediate layers of the superior colliculus.

The contrast images for both the recede and random conditions (recede >/< 0 & random >/< 0) failed to reach statistical significance within the pre-defined superior colliculus boundary. This result would suggest that activation during receding and random dot motion is lower than during looming motion.

The structured movement contrast (loom & recede >/< 0) also showed a significant activation pattern, the centre of which appears to overlap with the superior colliculus boundaries outlined above. This result would suggest that the superior colliculus responds to both looming and receding motion but that the activation is stronger in the case of looming stimulus as receding motion alone did not reach significance.
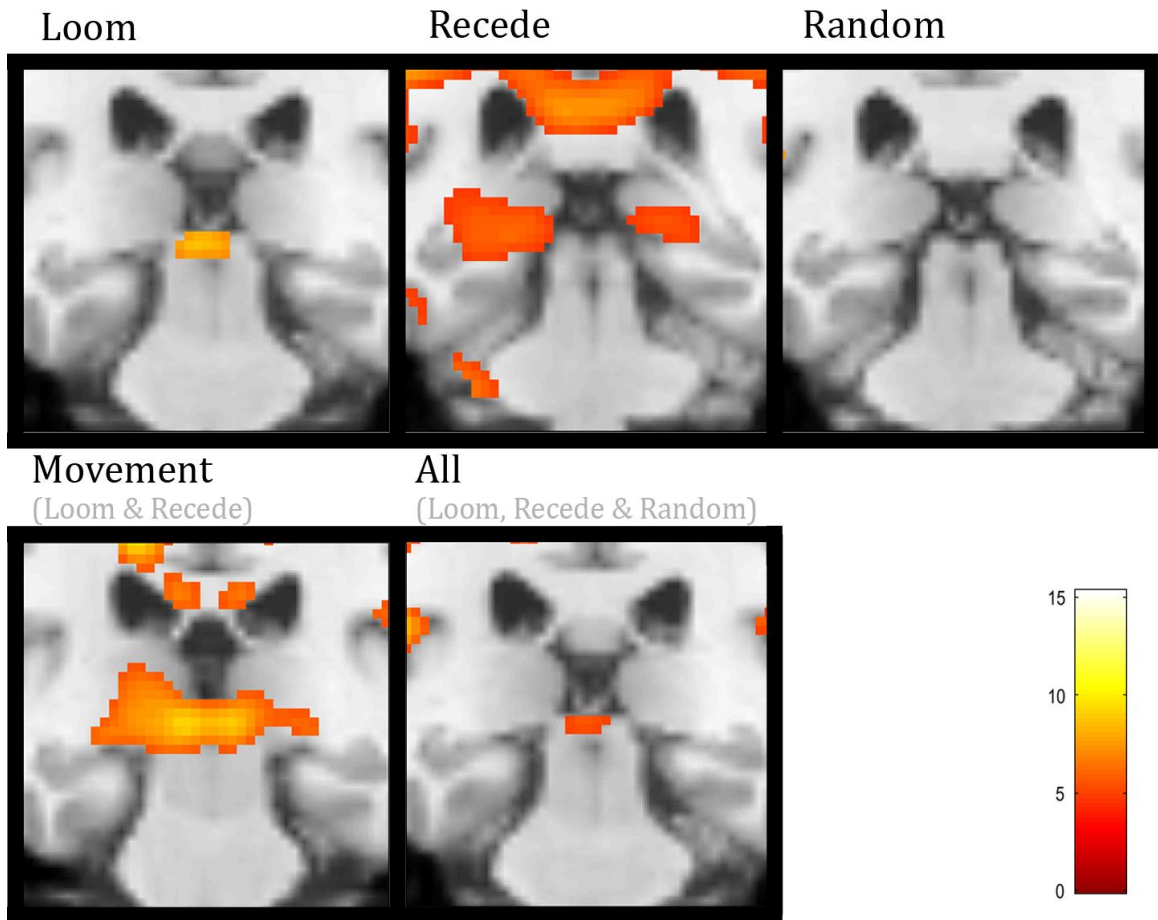
Figure 3-6

This figure shows an overview of the full group 2nd level GLM analysis. Each of the basic contrasts are shown in this figure: loom, recede, random, structured movement (loom & recede) and all visual (loom, recede & random). 80 x 80 mm frontal slices are shown. Slices were selected to best highlight peak superior colliculus activity.

The results for all visual input (loom, recede and random $>/< 0$) show a similar but smaller activation pattern to that observed to purely looming stimuli. This reduction in activation with the inclusion of the random condition would suggest that the superior colliculus is less active during the random condition when compared to either the looming or receding condition. This would therefore suggest that the superior colliculus is activated more by structured movement than by random dot motion which is highly consistent with much of the literature as outlined in section 2.6 of this thesis.

71

Given the results of this basic contrast 1-sample t-test analysis it can be concluded that superior colliculus activation is largest during the looming condition and smallest during the random dot motion condition. Furthermore, it appears highly likely that there is some activation during receding condition, but the size of this effect is not large enough to reach statistical significance here. If this was not true, then we would not expect to see the increased activation visible in the structured movement condition (loom & recede $>/<0$) compared to the loom condition (loom $>/<0$). The importance of this result is two-fold; firstly, it confirms that this paradigm can produce robust and repeatable activation of the superior colliculus which can be observed at the whole group 2nd level GLM analysis. This represents a significant extension of the findings of Bednark et al. who were successful in showing superior colliculus activation at the individual subject level using a region of interest approach. Secondly, from the standpoint of the DCM analysis, this result confirms that both looming and receding stimulus should act as the experimental input or perturbation to the superior colliculus in the model and that the random condition can be excluded without any risk of reducing the model's ability to explain variance in the underlying BOLD signal.

Figure 3.7 gives an overview of the superior colliculus activation observed during the various 2-sample t-test contrast analyses at the whole group level. This analysis is carried out to test for differences in activation levels between different experimental conditions. These results seem to agree with the observations and interpretations of the basic 1-sample analysis as well as agreeing with the previously published work of Bednark et. al. and the general literature surrounding visual activation in the superior colliculus.
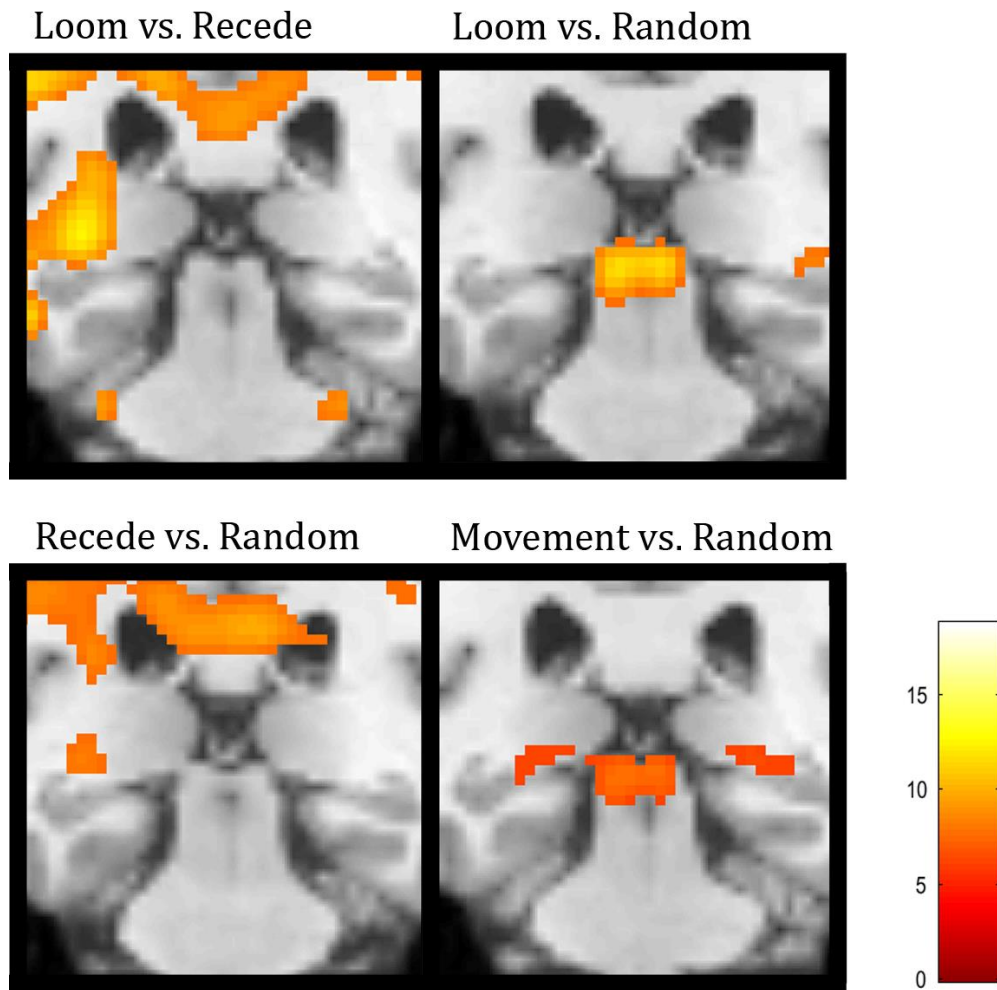
Figure 3-7

This figure shows an overview of the full group 2nd level GLM analysis. Each of the 2-sample contrasts are shown in this figure: loom vs. recede, loom vs. random, recede vs. random and structured movement (loom & recede) vs. random. 80 x 80 mm frontal slices are shown. Slices were selected to best highlight peak superior colliculus activity.

No statistically significant clusters are observed in the loom vs. recede contrast which again would suggest that the superior colliculus is active in both experimental conditions. The results of the 1-sample contrast analysis above did suggest that activation was stronger in the loom condition and so one may have expected to see activation in the loom vs. recede analysis. This result implies that the difference in activation between these conditions is not large enough to overcome noise and inter-subject variabilities to reach the statistically

73

significant level of 0.05 after family wise error correction. An increase in the number of participants or in the number of stimulus presentations to each participant may overcome this limitation by increasing the signal to noise ratio of the data. This limitation should be considered in any future work, although the inclusion of the random condition should be sufficient for the current study.

In the loom vs. random condition a statistically significant cluster is present in the bilateral superior colliculus, this activation falls within the superior colliculus boundary as outlined in the methods section. This result confirms the interpretation of the 1-sample contrast analysis and supports the findings reported by Bednark. From this result, we can conclude that activation of the superior colliculus is statistically significantly larger during looming stimulus than during random dot motion in the current paradigm. This result supports the argument that this paradigm is particularly well suited to study of the superior colliculus.

In the recede vs. random analysis no statistically significant clusters are observed within the superior colliculus boundary. This result suggests that any difference between these conditions is not large enough to overcome noise and inter-subject variability in the current data set. As with the loom vs. recede result, it is expected that significance would be achieved with an increase in participant numbers or with longer recording sessions as the results of the 1-sample contrast analysis and the literature do suggest that activation should be lowest in the random condition.

The results of the structured movement vs. random condition are highly consistent with the previous results reported at this whole group level. A statistically significant cluster is present in the bilateral superior colliculus, falling within the superior colliculus boundary as outlined. This analysis would suggest that activation of the superior colliculus during looming and receding motion is larger than during random dot-motion.

The results obtained from this whole group 2nd level GLM analysis are extremely promising and confirm that this paradigm may be useful for addressing the hypothesis that abnormal visual processing in the superior colliculus may be present in cervical dystonia patients and in first degree relatives with abnormal temporal discrimination abilities.

3.4.2   Second level GLM: Group segmentation superior colliculus

To test for group differences in superior colliculus activation the 36 participants were divided into two groups; first degree relatives with normal temporal discrimination (n = 18) and first-degree relatives with abnormal temporal discrimination (n = 18). Separate 2nd level GLMs were calculated for each of these groups and the same contrasts that were examined in the whole group analysis were examined for each sub-group. To account for the smaller number of participants within each group a significance level of $p = 0.001$ uncorrected was selected. This significance level is less strict than the $p = 0.05$ family wise error corrected level employed at the group level and thus care must be taken when interpreting the results.

Figures 4.8 shows an overview of the superior colliculus activation observed during the segmented group analysis for the 1-sample t-test contrast as outlined in the methods section of this chapter. These results seem to support the observations made during the whole group analysis while this additional segmentation reveals some significant trends which are of interest to the research questions at the heart of this thesis.

In the looming condition (loom $>/< 0$) a statistically significant cluster which occupies the bilateral superior colliculi is observed in the normal relative group, no such activation is observed in the abnormal group. This result would suggest that activation of the superior colliculus in unaffected first-degree relatives of cervical dystonia patients with abnormal temporal discrimination is reduced when compared to age-matched unaffected relatives with normal temporal discrimination abilities. This result strongly supports the hypothesis

75

that abnormal temporal discrimination stems from a disorder of the superior colliculus and the DCM and region of interest analysis to follow should help to highlight the nature of this abnormality.

No activation is observed in the superior colliculus across either of the groups for the receding motion or random dot motion experimental conditions. These results are highly consistent with those reported at the whole group level where no activations were observed for these contrasts. It is always important to note that failing to reach statistical significance in fMRI does not imply that no activity occurred during the condition in question, it only suggests that any activation during that condition was not large enough or consistent across participants to the point where it could pass the noise floor and reach significance.

The result of the structured movement contrast (loom & recede $>/<$ 0) show activation of the superior colliculus in both groups. Activation is strongest in the normal relative group while in the abnormal relative group the cluster only includes the left superior colliculus and is weaker than that of the normal group.
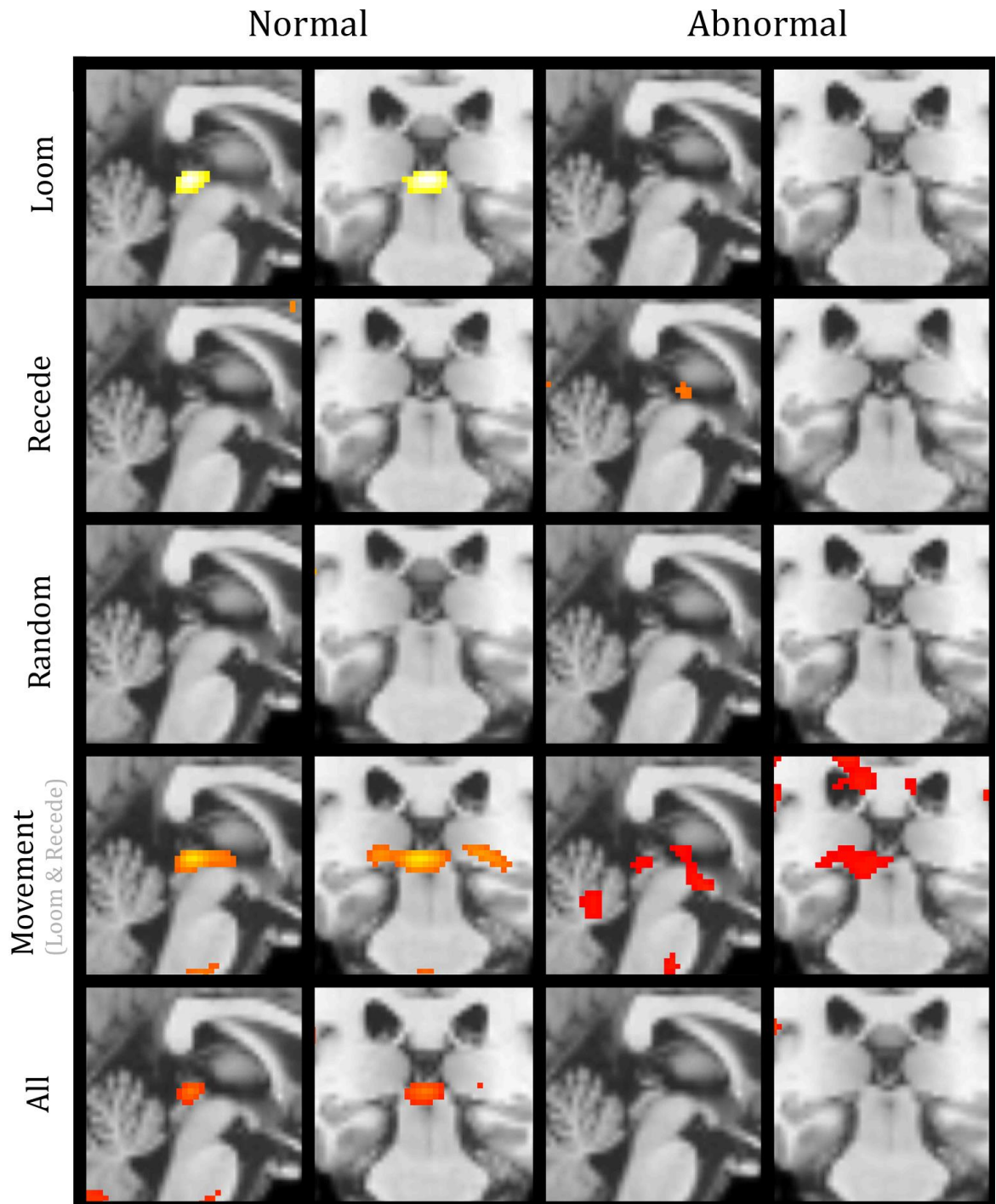
Figure 3-8

This figure shows an overview of the segmented group 2nd level GLM analysis. Each of the basic contrasts are shown in this figure: loom, recede, random, structured movement (loom & recede) and all visual (loom, recede & random). 80 x 80 mm slices are shown. Slices were selected to best highlight peak superior colliculus activity.

In both groups, it can be observed that the level of activation in the structured movement contrast is greater than of the loom contrast alone. Activation is relatively weak in the abnormal group and only reaches significance for the left superior colliculus. This is expected given than the loom contrast failed to reach significance in this group. This supports the interpretation that the superior colliculus is active in both the loom and recede conditions but that the activation is likely larger in the loom condition which allows the loom contrast to reach significance in the case of the normal relative group.

The contrast images for all visual stimulus (loom & recede & random >/< 0) reveal a statistically significant activation in the bi-lateral superior colliculus for the normal relative group. The activation appears to be weaker than what is observed in either the structured movement contrast or even in the loom contrasts. This suggests that the inclusion of the random condition has reduced the ability of this contrast to reach significance which supports the overall view that activation is lowest during this random condition. This result supports the suitability of the random dot motion as a control condition in this paradigm. In the case of the abnormal relative group it can be observed that no significant activation occurs with the inclusion of the random condition in the all visual contrast. This result suggests that the activation observed in the structured movement condition was not robust enough to reach significance with the inclusion of the random condition.

Figures 4.9 shows an overview of the segmented group 2-sample t-test contrast analysis. The images for loom vs. recede indicate that no activation occurs within the superior colliculus boundaries for either the normal or the abnormal relative group. This result is consistent with the whole group GLM analysis discussed previously. Also, in the recede vs. random condition there is no activation in the superior colliculus for either of these relative groups which is again consistent with the whole group analysis.
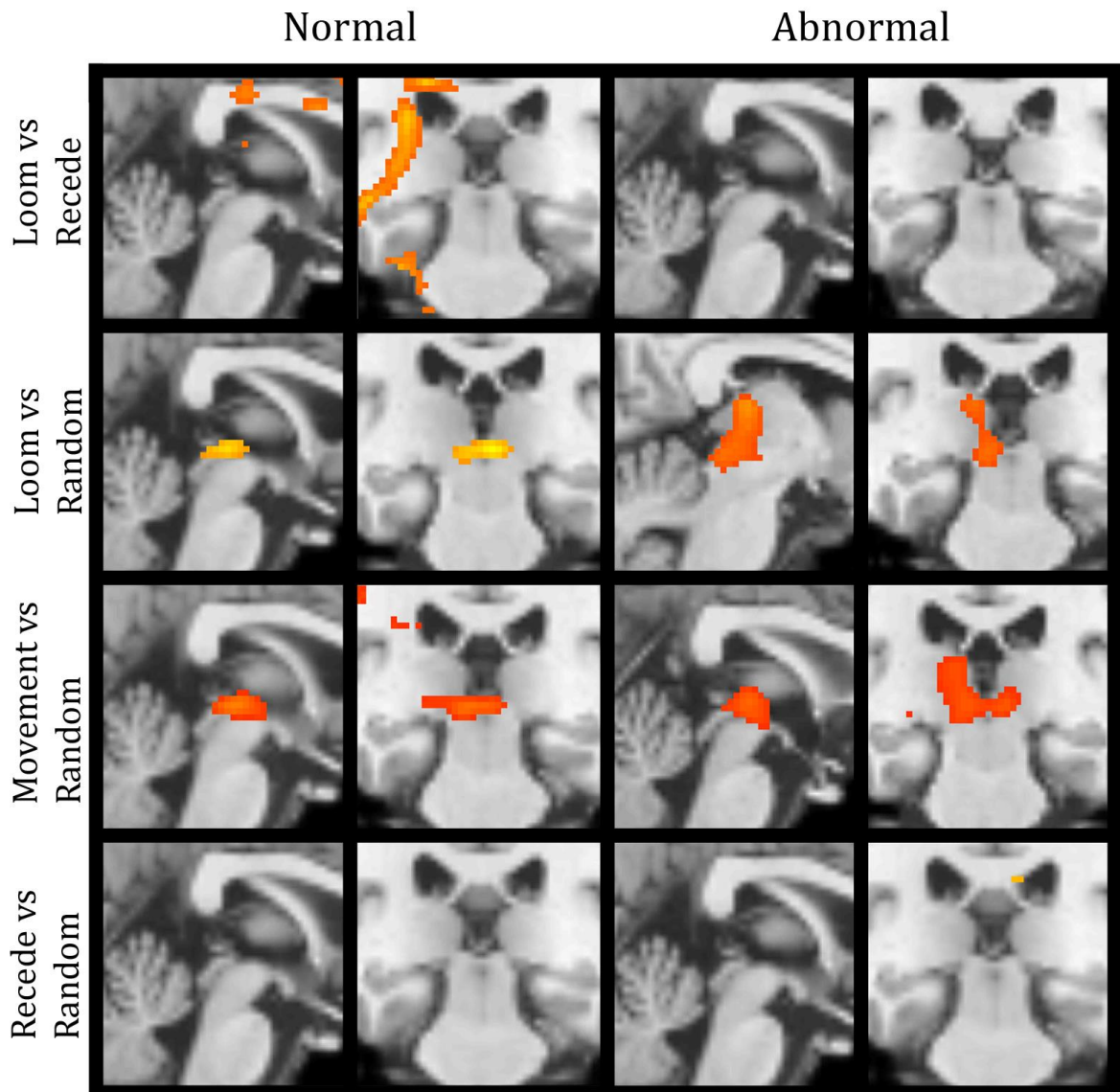
Figure 3-9

This figure shows an overview of the segmented group 2nd level GLM analysis. Each of the 2-sample contrasts are shown in this figure: loom vs. recede, loom vs. random, recede vs. random and structured movement (loom & recede) vs. random. 80 x 80 mm frontal slices are shown. Slices were selected to best highlight peak superior colliculus activity.

The contrast images for loom vs. random show a very focal activation within the boundaries of the bi-lateral superior colliculi for both the normal and abnormal relative groups, with the strength of this activation being slightly larger in the normal relative group. In the case of the abnormal group it can be observed that this activation is limited to the left superior colliculus as was observed in the structured movement contrast image for the same group.

79

This result is very informative about a question which was raised during the segmented 1-sample t-test analysis. From that analysis, it could be determined that looming motion produced a stronger activation than receding motion in the normal relative group, however, the same could not be concluded for the abnormal relative group as no activation was seen for either the loom or recede condition. This result confirms that looming produces a stronger activation than receding stimulus even in the abnormal relative group with the distinction being that the activation for looming and receding motion must both be reduced with abnormal temporal discrimination abilities.

The structured movement vs. random motion contrast shows the same superior colliculus activation pattern that was observed at the group level for both normal and abnormal relatives. This activation is less focal that what is seen in the loom vs. random condition but again the centre of this activation seems to occupy the superior colliculus boundary. This result confirms that structured movement leads to a greater activity in the superior colliculus when contrasted against random dot motion. This result seems intuitive given the 1-sample t-tests carried out above where it was observed that structured motion resulted in significant superior colliculus activation, but random dot motion did not.

3.4.3 Region of Interest Results

The results of the region of interest analysis support the whole brain results reported above. The independent Student's t-test revealed a trending difference between normal (M = 0.59, SD = 0.24) and abnormal relatives (M = 0.44, SD = 0.21) in peak percentage signal change in the SC following looming visual stimulus; $t(17) = 1.87$, $p = 0.06$. This result would suggest that activation to looming stimulus is reduced in people with reduced abnormal temporal discrimination abilities. No significant difference was observed for either the random or receding condition, Figure 3.10, Table 3.2.

A correlation analysis was carried out to compare the effect of TDT-score on peak percentage signal change for looming, receding and random motion. This analysis revealed a significant negative correlation between TDT-score and peak percentage signal change following looming visual stimulus, $r = -0.69$, $n = 36$, $p = 0.0025$. This result further supports the statement that activation to looming stimulus is reduced in people with abnormal temporal discrimination. No significant correlation was observed for receding or random motion, Figure 3.10, Table 3.2.
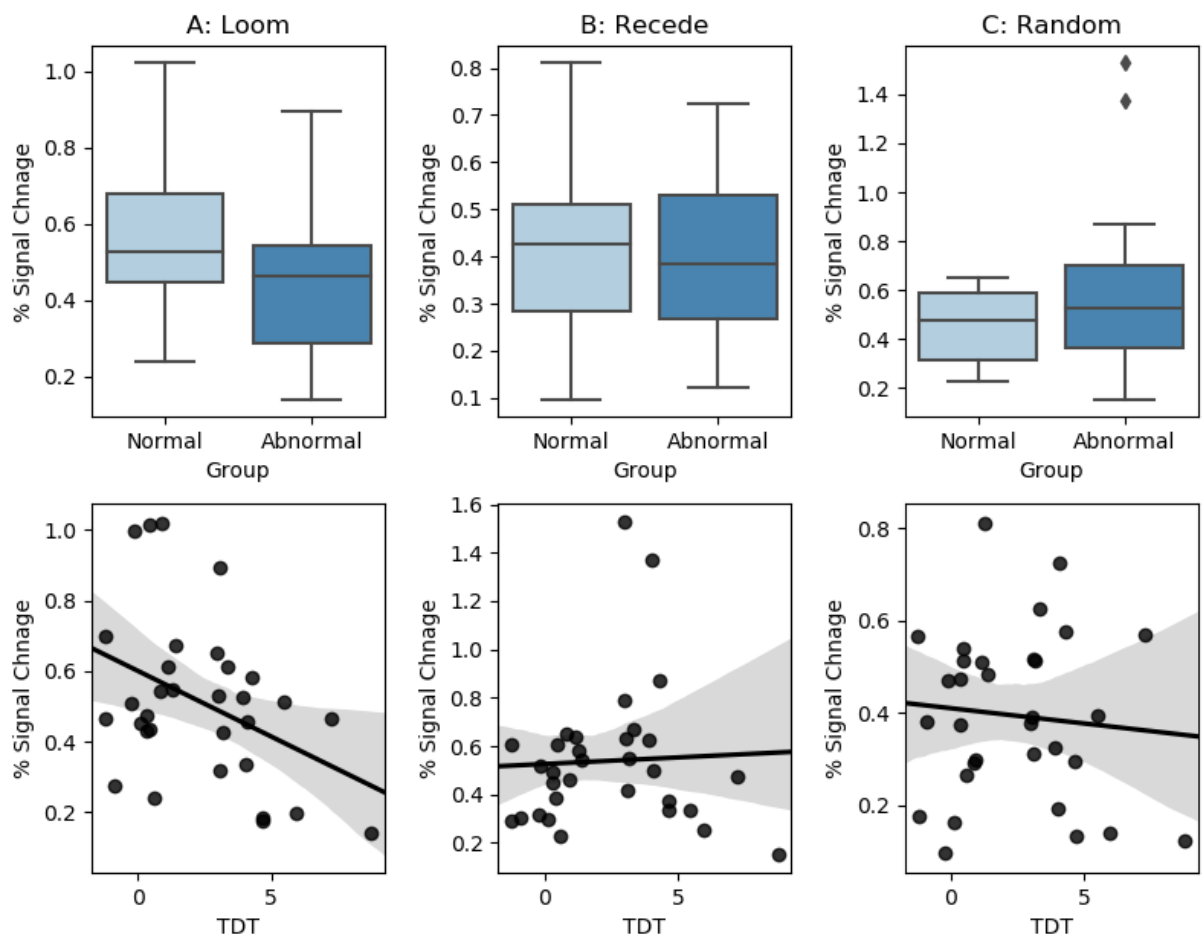
Figure 3-10

This figure shows the results of the region of interest analysis. The top row contains box plots of the data that was used during the independent Student's t-test. These box plots represent the median, 25th and 95th percentiles of the peak percentage signal change data for loom, recede and random conditions. The bottom row depicts the correlation analysis that was carried out between peak percentage signal change and TDT-score. The black dots represent individual subjects, the black line is the least squares fit to the data and the grey region is the 95% confidence interval for this fit.

Table 3-2

This table summarized the results of the between groups region of interest analysis, t statistics and p-values are reported for the independent t-test. R-values and p-values are reported for the Pearson's correlation that was carried out between TDT-score and peak percentage signal change.

	Loom	Recede	Random
Ind. t-test (df = 17)			
t statistic	1.87	0.19	-1.56
p-value	0.06	0.84	0.128
Correlation (n = 36)			
R-value	-0.69	0.08	0.03
p-value	0.0025	0.76	0.907

3.4.4   Dynamic causal modelling results

The results of the second level analysis revealed significant abnormalities in superior colliculus activation in the abnormal relative group. These results support the hypothesis that abnormal temporal discrimination and dystonia stem from a GABAergic abnormality in the superior colliculus. Previous work has also shown putaminal abnormalities in abnormal relatives in the form of increased sized by VBM and reduced activation during a temporal discrimination task. The aim of this DCM analysis was to probe the hypothesis that putaminal abnormalities may be a downstream effect of this GABAergic deficit in the superior colliculus.

Figure 3.11 shows an overview of the node locations for each subject, this plot shows that node locations were consistent across subjects and is an important plot to produce during any group level DCM analysis.
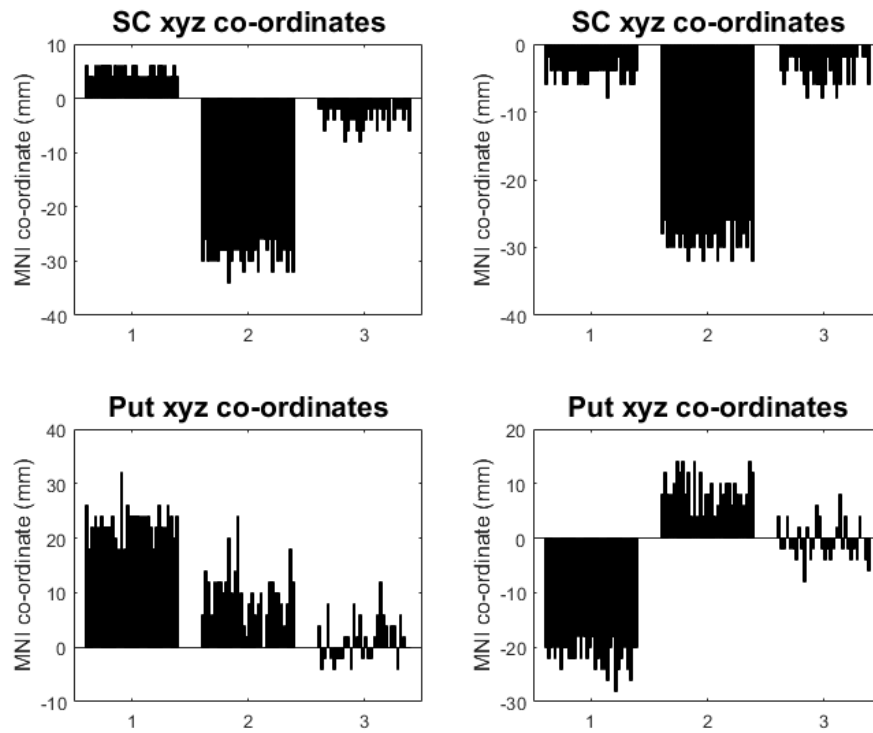
Figure 3-11

This figure depicts the X (1), Y (2) and Z (3) MNI co-ordinates of all four nodes of interest for each of the subjects in the DCM analysis. This figure shows that node selection was consistent across subject but that there was more variation in the larger putamen than in the superior colliculus.
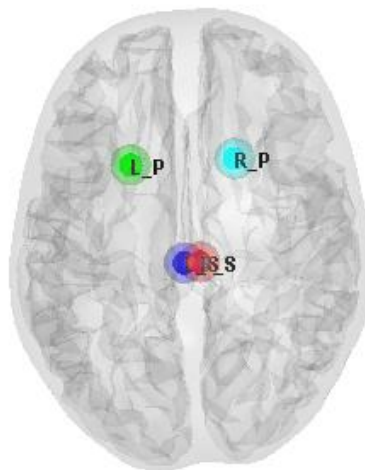
Figure 3-12

Physical node locations for an exemplar subject. This figure highlights the adjacent nature of the bi-lateral superior colliculi and motivation to include bi-lateral connections between these nodes.

In DCM, model selection is employed to assess which of several models best describes the data of a single person or a group of people. When assessing groups of people random effects model selection should be used, the random nature of this selection process accounts for inter-subject variabilities. When assessing individuals, a fixed effects model selection procedure can be employed.

Several model selection procedures were carried out during this analysis. First a whole group analysis was carried out to determine which of the 5 proposed models would best explain the observed data for all subjects. It is clear from the plots shown in Figure 3.13 that the model which includes modulation of superior colliculus to superior colliculus and modulation of superior colliculus to putamen preformed best in terms of explaining the variance in the data for the whole group.
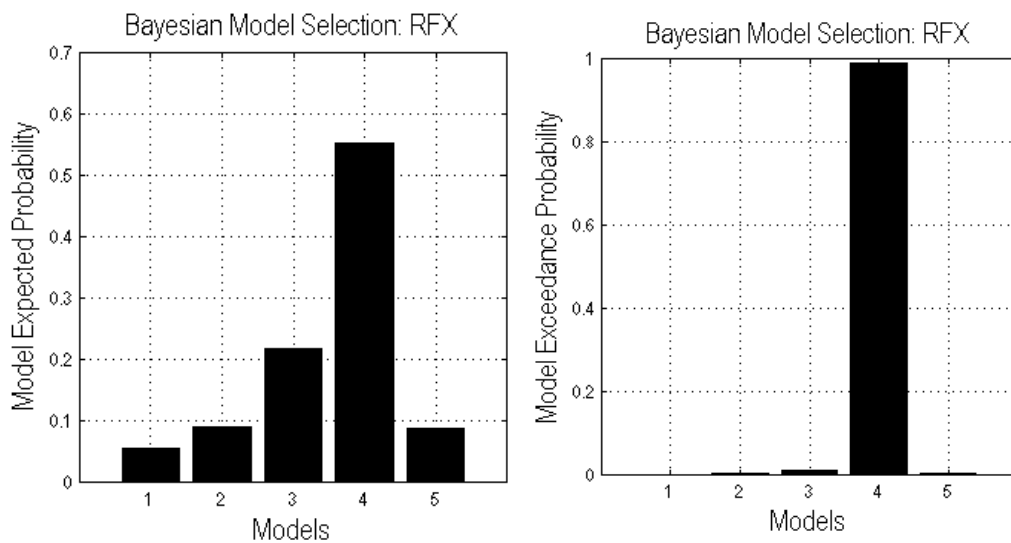
Figure 3-13

Plots of the model exceedance probability and model expected probability. It is clear from these metrics that model four performed better in terms of explained variance.

Next the whole group was divided into subsets of normal relatives and abnormal relatives to explore whether data from each group would be best explained by the same model. A random effects selection procedure was employed and plots of model exceedance and model expected probabilities were produces for each group. The results of this analysis are given in Figure 3.14. These plots clearly suggest that the data from each of the groups is best explained by the same model, model 4, which is consistent with the model selection from the whole group analysis.
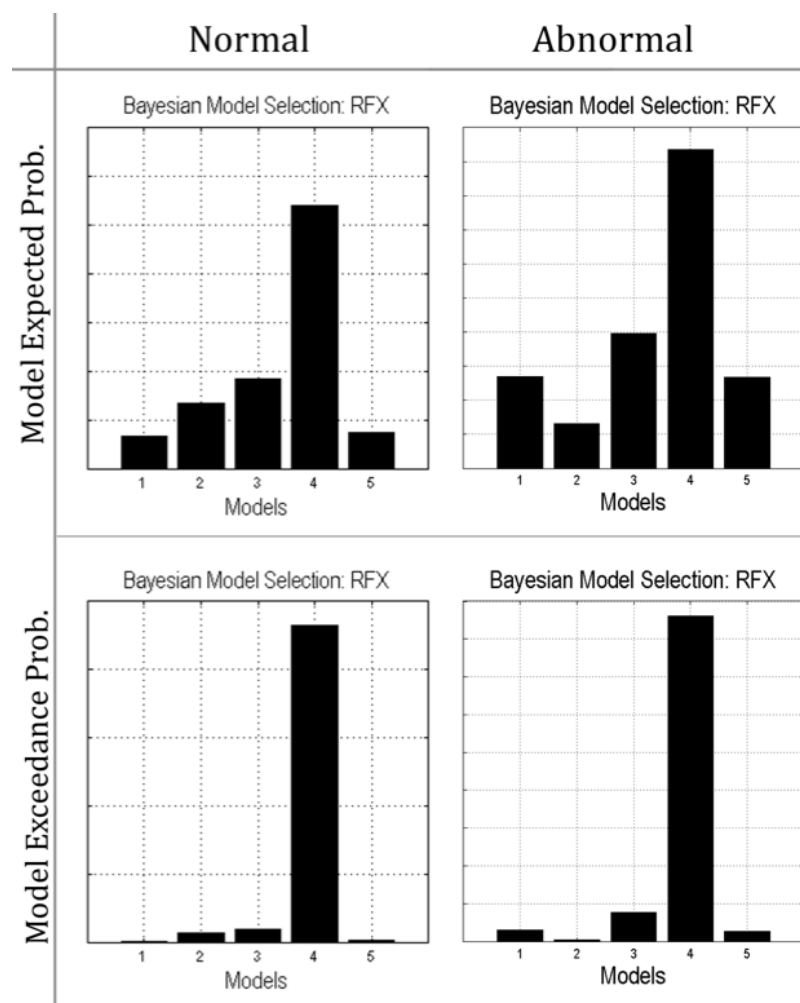
Figure 3-14

Plots of the model exceedance probability and model expected probability for each of the sub groups, abnormal relatives and normal relatives. These plots indicate that each of group's model selection is consistent with that observed at the whole group level.

The results of the model selection analysis, both at the whole and segmented group levels, suggest that model 4 best describes the connectivity between the superior colliculus and at the putamen during looming and receding visual stimulus. Model 4 allows the connection strength from the superior colliculus to the putamen and the self-connection of the superior colliculus to be modulated by looming and receding stimulus, Figure 3.15. Given that significant differences in activation were seen at the superior colliculus during the group level GLM analysis, these modulatory connections were examined and a correlational analysis was carried out to determine any relationship existed between the modulation of these connections and the temporal discrimination abilities of the participants, Figure 3.16.
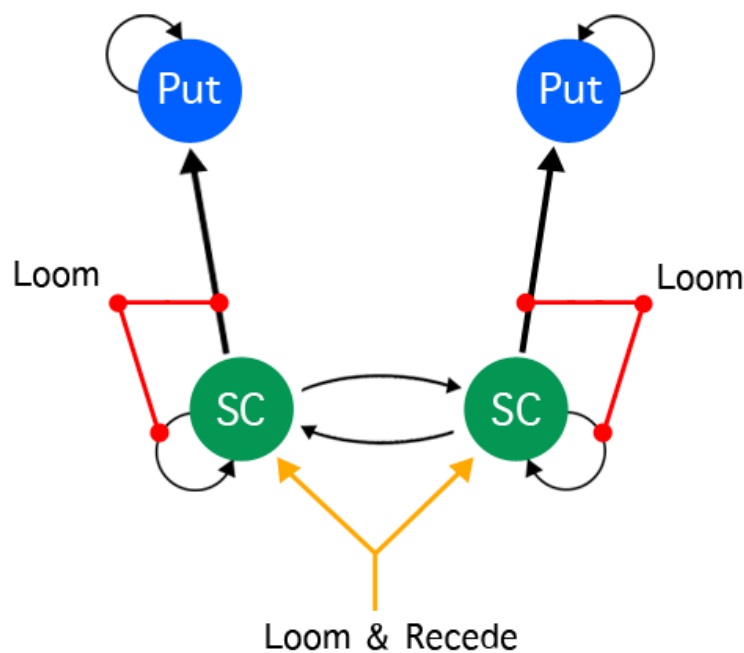
Figure 3-15

This figure shows the winning model from the whole group and segmented group model selection analysis. This model has the same driving inputs and fixed connections as the others models tested but uniquely allows modulation of the inhibitory self-connection of the superior colliculus and excitatory connections from the superior colliculus to the putamen.
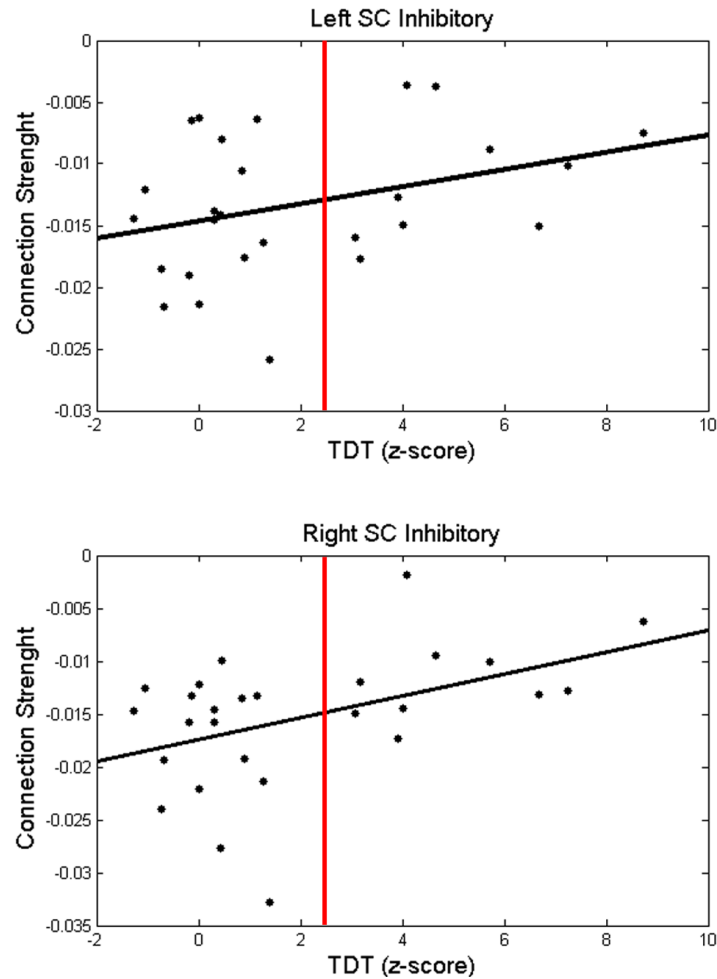
Figure 3-16

Plots of the modelled inhibitory superior colliculus self-connections, extracted from the winning model, model 4, for each participant and plotted against temporal discrimination thresholds (TDT). The vertical red line on each plot represents the upper limit of normal temporal discriminations. Normal relatives and controls lie to the left of this line while abnormal relatives lie to the left.

A Pearson's correlation test was employed to test for a relationship between temporal discrimination thresholds and modelled connection strength of the left and right superior colliculus nodes separately. Given that these self-connections are bounded to be inhibitory under the DCM framework they may be viewed as a proxy for local GABA at a given node in the model.

At the right superior colliculus node, a statistically significant correlation between temporal discrimination thresholds and self-connection strength of the superior colliculus was

87

observed, (r = 0.445, p = 0.02). This results suggests that inhibition in the right superior colliculus is larger in healthy controls and normal relatives and decreases in relatives with abnormal temporal discrimination abilities. Given that this self-connection represents a GABAergic proxy under the DCM framework this result could suggest that first-degree relatives of dystonic patients with abnormal temporal discrimination have a deficit of GABAergic inhibitory interneurons in the right hand superior colliculus, Figure 3.16.

This relationship is also visible in the left superior colliculus although in this case the correlations fails to reach statistical significance, (r = 0.335, p = 0.08). Given that the stimulus was presented monocularly to the left eye it is not surprising that the largest effect is observed on the right-hand side of the circuit. An increase in participant numbers, specifically of abnormal relatives, would likely allow this result to reach statistical significance.

3.5   Discussion

This study sought to investigate the functionality of the subcortical circuit employed during the detection of and reaction to looming stimuli in relatives of cervical dystonia patients with abnormal temporal discrimination. Specifically, this work aimed to test the hypothesis that reduced temporal discrimination, putaminal abnormalities and cervical dystonia are an effect of reduced inhibitory activity in the superior colliculus. To address this hypothesis two groups of participants were enrolled in an fMRI-based looming paradigm which has previously been successful in producing activation of the superior colliculus in healthy adult humans. The two groups in this study were made up of first-degree relatives with normal temporal discrimination and first-degree relatives with abnormal temporal discrimination. Given that cervical dystonia is a movement disorder of the neck and given the sensitivity of fMRI techniques to head movement, especially when investigating a

structure as small as the superior colliculus, a patient group was not included in this analysis.

The lack of a patient group should not negatively impact the ability of this study to draw conclusions about the nature of cervical dystonia. This is because abnormal temporal discrimination, the factor separating the normal and abnormal relative groups, has been shown to represent a true mediational endophenotype, meaning that cervical dystonia and reduced temporal discrimination stem from the same underlying genetic mutation(s). Therefore, any comparison made between the normal and abnormal relative groups should be equivalent to comparing the normal relative group with a patient group if movement in the scanner were not an issue. This rational has been applied in previous fMRI work but remains a significant limitation which should not be overlooked.

The analysis carried out during this study focused on 2nd level GLM analysis at both the whole group and segmented groups levels with a follow-on DCM analysis which was motivated and guided by the 2nd level GLM results as well as by the existing literature surrounding cervical dystonia.

3.5.1 Second level GLM

The whole group GLM analysis included all 38 recordings across both groups and was motivated by the opportunity to reduce signal to noise ratio and gain a deeper understanding of general superior colliculus activations under the current paradigm. A limitation of this analysis is that abnormal relatives are being grouped with normal relatives and so any functional differences could in fact reduce statistical power when compared to a group of 38 healthy controls, this limitation is especially relevant for smaller structures like the superior colliculus.

The basic 1-sample contrast images suggest that activation in the superior colliculus is largest during structured movement and smallest during random dot-motion, furthermore it may be deduced that activation is larger during looming stimulus than during receding stimulus. This interpretation is supported by the 2-sample contrast images which show a significant difference in activation between looming and random motion but not between looming and receding or between receding and random motion. These results support and extend the work presented by Bednark et al. and confirm the utility of this paradigm for the investigation of superior colliculus abnormalities in cervical dystonia.

The 1-sample contrast image for looming stimulus also suggested that activation of the left superior colliculus is larger than that of the right. Stimulus was presented centrally but only to the left eye. For the left eye, the nasal hemisphere represents the right visual field and is projected to the left superior colliculus while the temporal hemisphere represents the left visual field and is projected to the right superior colliculus, Figure 3.16. If the participant maintains focus at the central point of the sphere the visual stimulus should have been evenly divided between the left and right visual hemispheres. However, the superior colliculus has been shown to be more sensitive to visual stimulus arising in the temporal visual field which in the case of the left eye is made up of the left visual field and is therefore projected to the right superior colliculus (Sylvester et al., 2007, Johannesson et al., 2012). This mechanism developed because predatory attacks will often arise from the side and so occur in the temporal visual fields. This would lead one to expect a larger activation in the right superior colliculus which is not observed here. The contradictory nature of this result suggests that the laterality of the activation may not represent a valid result but may instead be caused by noise in the data or inter-subject variability. Head movement is always an issue with fMRI analysis and given the size of the superior colliculus and the fact that the left and right colliculus are centrally located and thus very close to each other it may not be

advisable to draw conclusions about laterality of response. This argument would also support the notion of examining the left and right superior colliculi as a single structure and is something that should be explored in future work in this area.
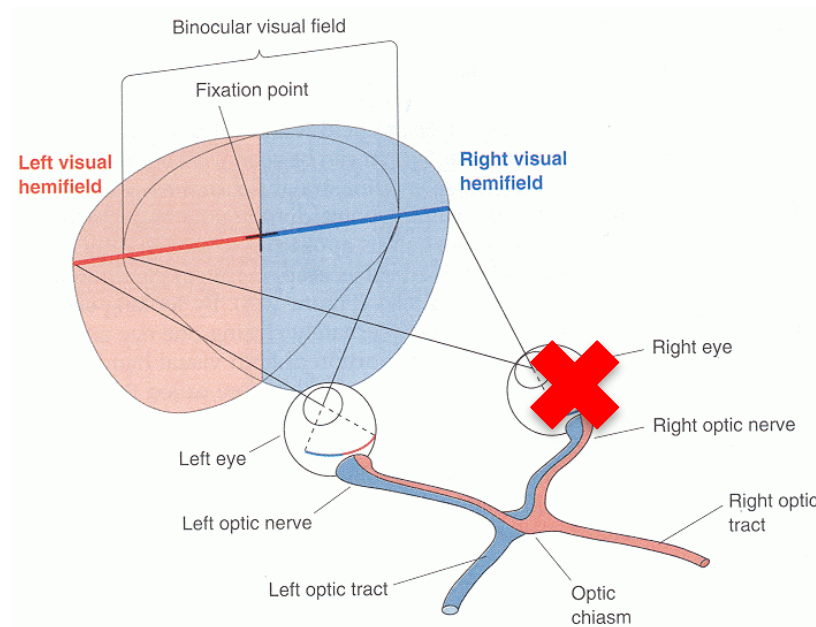
Figure 3-17

An illustration of the left and right visual hemispheres and their projections in the human brain. Under the current paradigm visual stimulus was presented only to the left eye, the right eye was covered using a patch.

The whole group analysis gives great insights into superior colliculus activity under the current paradigm but does not allow comparison of superior colliculus activity between groups. To address this aspect of the hypothesis the 2nd level analysis was carried out separately for each of the groups, this segmentation of the data allows for functional differences between groups to be assessed. The results of this segmented analysis largely support the results of the whole group analysis while also revealing important functional differences in abnormal relatives.

The most striking of these results was observed in the 1-sample contrast images presented in the results section. Specifically, the contrast for looming stimulus (loom $>/< 0$) shows

focal activation of the bi-lateral superior colliculus in normal relatives, however, no activation was observed for abnormal relatives under this contrast. A reduced activation in the superior colliculus in abnormal relatives supports the hypothesis that the superior colliculus is implicated in abnormal temporal discrimination but is contradictory to the more specific hypothesis that this abnormality is a GABAergic deficit. GABA is an inhibitory interneuron and so a deficit of GABA in the superior colliculus should in fact lead to greater levels of activation in abnormal relatives and in patients. It is, after all, this excess of activity that is believed to manifest as cervical dystonia. The reduced activation observed in unaffected relatives may suggest that alterative compensatory circuits are being exploited to deal with the detection of and reaction to unpredictable and looming stimuli and the superior colliculus is therefore not being activated as much during these tasks. Although this result does not address the full hypothesis it certainly supports the idea that the superior colliculus is involved in abnormal temporal discrimination and therefore also likely involved in cervical dystonia.

The 2-sample contrast analysis showed very similar results for the normal and abnormal relatives. The fact that similar results are observed for normal and abnormal relatives would suggest that superior colliculus activity is reduced for all conditions so that the difference in activation remains significant. This idea would support the hypothesis that this network is less active in abnormal relatives and that they may be employing compensatory cortical circuits during these tasks.

3.5.2   Region of Interest

The results of the region of interest analysis support those of the whole brain analysis. The between groups interdependent t-test shows a trending decrease in activation to looming stimulus in the abnormal group while no difference was observed for either random dot motion or receding motion. Furthermore, the correlation analysis shows a significant

inverse relationship between TDT-scores and peak SC activation to looming stimulus. No such relationship was observed for receding motion or random dot motion. These result support the view that abnormal temporal discrimination is related to abnormalities in the SC.

3.5.3   DCM

The results of the model selection procedure during the DCM analysis at both the whole and segmented group levels revealed a consistent selection. Model 4, which allows modulation of the inhibitory self-connection of the bi-lateral superior colliculus in addition to modulation of the excitatory connection towards to putamen produced the best fit to the data in all cases of the models tested in this analysis. This result implies that the effective connectivity of the superior colliculus is significantly altered by looming stimulus and is consistent with the results observed during the GLM analysis and with much of the literature surrounding the superior colliculus.

A follow-on analysis investigated how this modulatory self-connectivity of the superior colliculus was related to temporal discrimination in the current population. Self-connections are always inhibitory under DCM and for a structure like the superior colliculus which relies on GABAergic inhibition this connection variable in the model can be viewed as a proxy for GABA. The current hypothesis states that abnormal temporal discrimination stems from reduced GABA in the superficial and intermediate layers of the superior colliculus and so to test this hypothesis a correlation analysis between this inhibitory self-connection and TDT scores was carried out. The results revealed a statistically significant relationship for the right superior colliculus and a trending relationship for the left. This result strongly supports the hypothesis that abnormal temporal discrimination is linked to a GABAergic deficit in the superior colliculus. Following on from this statement, if abnormal temporal discrimination is indeed a true

mediation endophenotype of cervical dystonia then this result would suggest that this abnormality in the superior colliculus may also be related to the abnormal movements and postures associated with cervical dystonia, although further research will be required to fully address this statement.

4   Head kinematics, eye movements and orientation of attention

4.1 Introduction

It is well documented that the appearance of novel visual targets outside our central field of view results in a deflection of gaze towards the appearing stimulus (Collewijn, 1977). Furthermore, it has been established that these shifts in gaze are generated through a combination of distinct head, and eye movements (Volle and Guitton, 1993, Bizzi et al., 1971, Chen et al., 2012) for smaller displacements and head, eye and upper trunk movements for larger ones. The command to shift one's gaze in response to a salient stimulus is generated in the superior colliculus and separated downstream into these distinct head and eye commands (Freedman and Sparks, 1997, Corneil and Munoz, 2014). While saccades have been well characterized through electrooculography (EOG) and retinal eye tracking studies (Huang et al., 2014, Watanabe et al., 2014, Hollingworth et al., 2013), the role of head movement in gaze displacement has been less widely investigated (Shaikh et al., 2013). This may be due, in part, to the relative difficultly involved in recording head movements in an accurate and objective manner.

Early research into head kinematics relied on subjective observational studies or objective studies that recorded induced voltage in a sensor coil inside two perpendicular horizontal magnetic fields (Shaikh et al., 2015a, Bremen et al., 2010, Friston et al., 1997). The introduction of motion capture technology has found utility across a wide range of kinematics research, including investigations of the contribution of directed head and body movements into larger displacements in gaze in control (Hollands et al., 2004, Anastasopoulos et al., 2009) and clinical (Anastasopoulos et al., 2011, Anastasopoulos et al., 2013) cohorts. These studies employ eccentrically located LEDs as peripheral visual targets and recorded saccade activity with EOG for comparison with head and body movements during deflections in gaze. While these studies have produced robust and accurate objective measures of head movement, paradigms built around motion capture

systems come with many unavoidable drawbacks. Motion capture systems require large open spaces, lack portability, are prohibitively expensive and are limited by the choice of stimulus and mode of stimulus presentation. We posit that virtual reality head mounted displays (HMD) may represent an alternative to motion capture for such studies while also addressing many of the limitations of motion capture systems.

Here the capabilities of a virtual reality HMD (Oculus Rift DK 2) are utilized to examine the effects of orientation of attention on onset of head movement in a Posner-style paradigm. The HMD presents an immersive 3D task that is updated at a rate of 75Hz to reflect the movements of the user. The device is employed to collect head turn trajectories in 3 axes (yaw, pitch and roll) at up to ~1000Hz for offline analysis. To allow for comparisons of head movements and saccade activity, simultaneous EOG was also collected for a subset of participants.

The Posner cueing paradigm (Posner, 1980) is a neurological test often employed to assess an individual's ability to perform covert attentional shifts under different experimental conditions. The task has been applied to investigate manual (button-press) (Feldmann-Wustefeld and Schubo, 2013, Rieth and Huber, 2013, Johnson et al., 2012) and automatic (saccade) (Dawel et al., 2015, Yokoyama et al., 2012, Chaminade and Okka, 2013) reaction times to target stimuli with the aim of investigating the effects of covert orienting of attention in response to different cue conditions. Variations of the Posner cueing task have been applied in many areas of research and have proven useful in assessing the effects of focal damage or disorders of attention (Ethier et al., 2015, Reuter et al., 2011, Lopez et al., 2011) as well as increasing the understanding of spatial attention in healthy populations (Wang et al., 2015, Fan et al., 2009). Here it is hypothesised that the Posner effect, which has been widely demonstrated in automatic saccade responses, would also be present in the ecologically valid onset of head movement, given the well-established link between head

movement and saccade activity during displacement of gaze (Bizzi et al., 1971, Hollands et al., 2004, Daye and Roberts, 2015, Scharli et al., 2013).

The Posner effect is of particular interest to the research questions present in this work given its utility as a metric for assessing a participant's ability to make covert shifts of attention. The hypothesis at the core of this work states that a GABAergic abnormality in the superior colliculus is responsible for cervical dystonia, abnormal temporal discrimination and putaminal abnormalities. Given that the superior colliculus acts as an important input to the network responsible for orientation of covert attention, it is hypothesised that abnormalities in covert attention should be present in cervical dystonia patients. Furthermore, a Posner style paradigm should be a sensitive to such abnormalities. Another important advantage of the Posner task is that it looks at the difference between two onset conditions at the single subject level. This will allow us to make group level comparisons by looking at percentage change in onset timing rather than looking at un-normalized onset timings alone. This fact should help to validate patient-control comparisons employed here, although this is still a limitation of the current study. Future work should aim to compare unaffected relatives with and without abnormal temporal discrimination as this would be more informative to the current hypothesis.

The work presented in the first half of this chapter will aim to highlight how newly emerging technologies can be employed to record head kinematics and answer important oculomotor research questions in a general sense. This section will focus on data collected from control subjects and show how theis protocol can be employed to collect many different head and eye movement parameters, which could be useful across a number of research questions. The second half of this chapter will then apply these protocols to collect head movement data from a cohort of cervical dystonia patients and healthy age-matched controls. This section will focus of the Posner effect as a measure of covert attention to

address the hypothesis that cervical dystonia is caused by a GABAergic abnormality in the superior colliculus.

4.2 Materials and methods

4.2.1 Participants and ethics

Forty healthy adults (21 male) (mean age ±SD: 26.7 ± 2.9 years) participated in the control study. In the follow-on study data was collected from a further 38 controls (20 male) (mean age ±SD: 45.8 ± 9.5 years) and 28 patients with cervical dystonia (16 male) (mean age ±SD: 53.8 ± 8.1 years). All participants had normal or corrected to normal vision. In accordance with the Declaration of Helsinki, all participants gave their written informed consent to the study, which was approved by the Faculty Ethics Committee of the Faculty of Health Sciences at Trinity College Dublin.

Table 4-1

Subject details, patient study.

	Control	Patient
n	38	28
Age: mean (std)	45.8 (9.5) years	53.8 (8.1) years
Male	20	16
Female	18	12

4.2.2 The task

The task employed in the current study is a modified Posner task (Posner, 1980). All recordings were carried out in a quiet room; participants were seated in a ridged, upright chair. The straps of the HMD were adjusted for each participant to ensure the unit was secure and comfortable. Before each test, the HMD was calibrated to ensure correct

alignment between the virtual world and the participant's chair. At the beginning of each trial, a small focal sphere appeared at eye level at the 0° position (Figure 4.1, a). The sphere's colour was black when the yaw of the HDM was greater than ±5° and green when the yaw was less than ±5°. To elicited a cue and begin a trial, participants were required to maintain a yaw of less than ±5° for 1 second continuously. The cue (left or right pointing arrow) then appeared in place of the green sphere for 0.2 seconds. The cue was then removed and a larger target sphere appeared in one of six possible locations (eye level; ±30°, ±45° or ±60°) (Figure 4.1, b). All target spheres were equidistant from the participant at 6 meters and had a diameter of 60 centimetres. Target spheres were coloured red when the yaw of the HMD was outside ±5° of the target's location and changed to blue inside this range. To end a trial, participants were required to maintain a yaw within ±5° of the target for 1.5 seconds continuously. At this point, the target sphere was removed and replaced with the smaller focal sphere at the 0° location, marking the end of a trial. Valid cues were shown in 80% of trials, invalid cues were shown in the remaining 20%. Participants were asked to complete a total of 6 blocks; each block consisted of 20 trials (120 trials). Trials were presented in a pseudo-random order across all blocks such that 16 valid and 4 invalid trials were presented for each of the 6 target locations. Participants were also asked to complete a shorter 15 trial practise block to help eliminate unwanted learning effects during the initial blocks. Participants were instructed to complete each trial in the shortest possible time. Targets at ±30° and ±45° appeared within the field of vision of participants at a neutral 0±5° positions, targets at ±60° were not visible from this neutral position. It is important to note that this task represents a deviation from the traditional Posner paradigm in that targets do not appear in central vision.

a Experimental design: Stimuli presentation order

Valid Trial   Invalid Trial

Focal Sphere *(Yaw > ±5⁰)*

Focal Sphere *(Yaw < ±5⁰)*
1 second

Cue
0.2 seconds

Target Sphere *(Yaw > ±5⁰)*

Target Sphere *(Yaw < ±5⁰)*
1.5 seconds
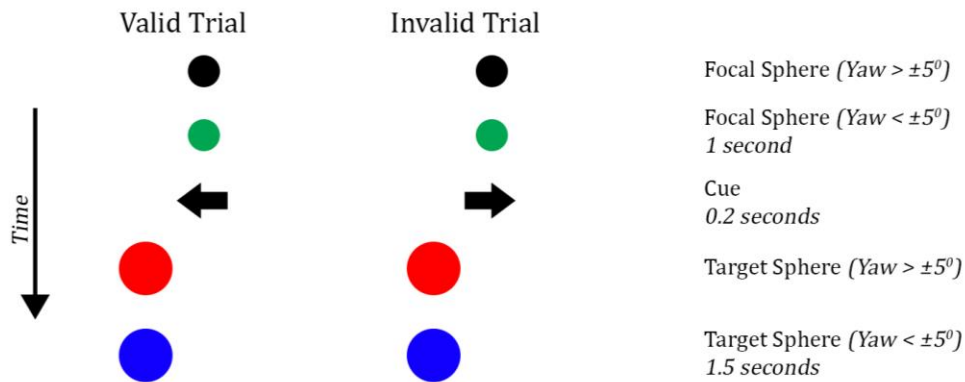
b Experimental design: Stimuli positions

Focus/Cue

-30⁰   +30⁰
-45⁰   +45⁰
-60⁰   +60⁰

Target Sphere
Focal Sphere
Target Angle ± 5
Neutral ±5
FOV from Neutral
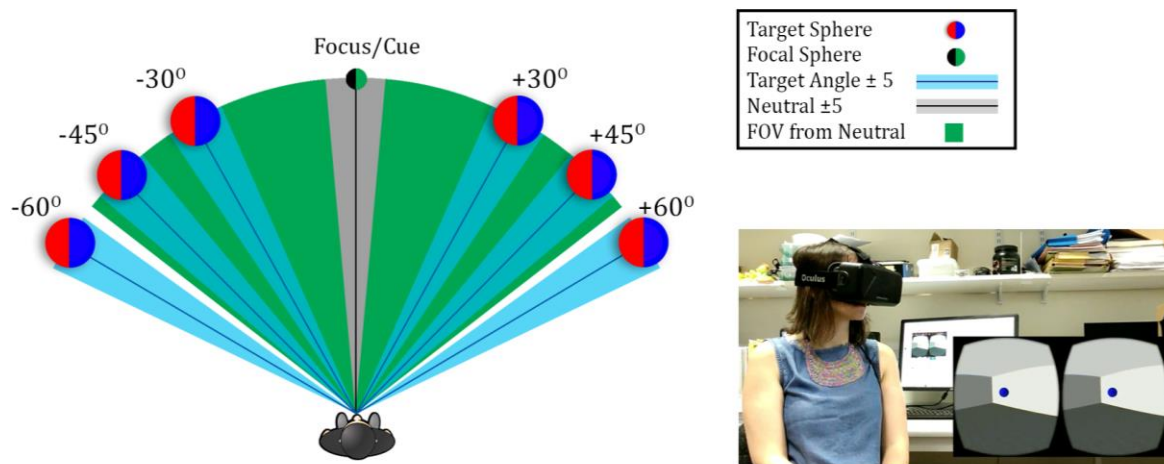
Figure 4-1

This figure shows an overview of the experimental design employed in the current study. Panel a contains an illustration of a valid and an invalid trial. This illustration depicts the order and timing of stimuli presentation during valid and invalid trials. Panel b contains a schematic plan view of the experimental architecture. The green segment represents a participant's approximate field of view (FOV) at the 0° position. Target locations and target angle ranges are also indicated. All stimuli

4.2.3   Data acquisition

Yaw, pitch and roll of the HMD were recorded for all 40 participants at a sample rate of up to 1000Hz. In 18 of these participants, EOG was also recorded. EOG data, sampled at 512Hz, was collected from two active electrodes using a BioSemi high impedance recording system. Electrodes were placed inferiorly and laterally of the left eye. CMS and DRL electrodes were placed on the mastoids. Stimulus was generated and presented using custom software developed with Unity Pro 4.1 and the Oculus Rift software development

100

kit for Unity. Triggers were generated at the beginning of each trial (cue onset) by the Unity software and were sent to the BioSemi system for synchronisation of EOG data via a custom micro-controller USB interface.

4.2.4   Data analysis

The sample rate of the raw HMD data was dictated by the frame rate of the custom software. Due to changes in processing demand, this frame rate was variable between $600 - 1000$ Hz. To account for this, data were first resampled to 500Hz using a cubic spline data interpolation. Given the high signal to noise ratio of this data, no further pre-processing steps were required. The data were epoched for each trial from 0.4 seconds pre-cue to trial completion ($2.5 - 3.5$ seconds post cue). For each trial, the following metrics were calculated; movement onset (ms), outbound movement duration (ms), max outbound velocity (°/s), return movement duration (ms), max return velocity (°/s) and turning point (ms). All metrics were calculated using yaw data. Both displacement and velocity were employed for detection the dependent metrics (Figure 4.2). Velocity was calculated using the forward Euler differentiation method. Some attempts were made to employ acceleration and jerk as additional inputs for the onset detection algorithm as they would help to narrow the temporal window even further. Unfortunately, the data was not clean enough for this and the additional differentiations were not useful for the detection algorithm.

a HMD displacement and velocity profile: Representative trial
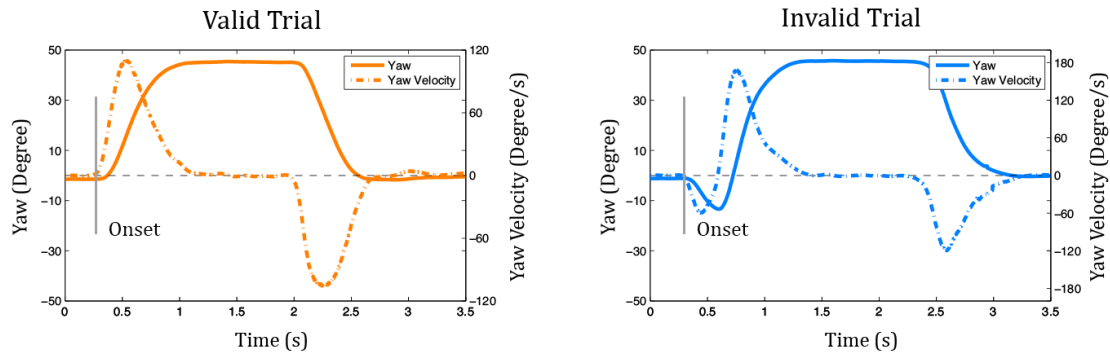
b HMD and EOG displacement profile: Representative trial
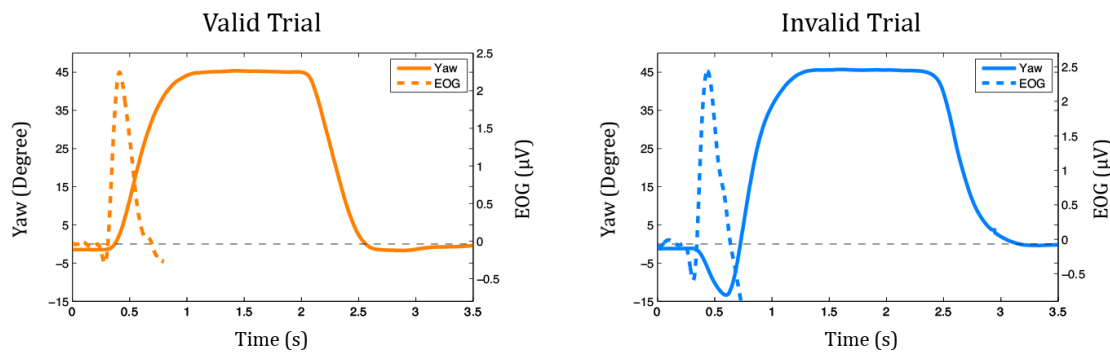
Figure 4-2

HMD and EOG data from a representative single valid and invalid +45° trial. Panel a contains yaw and yaw velocity profiles which are exploited for the movement parameter extraction algorithms described here. The solid line represents the resampled yaw data and the dot-dashed line represents the rate of change (velocity) of this data. The point of movement onset is represented as a vertical grey line. Panel b contains representative head yaw and EOG data from the same trial as panel a. The solid line represents yaw data from the HMD sensors and is referenced to the left axis (degrees). The broken line represents EOG data and is referenced to the right axis (µV).

To find the point of movement onset, the maximum velocity and maximum displacement in the direction of the target were found. From the point of maximum velocity, the algorithm stepped back through the epoch until the velocity fell to < 20% of its maximum value and displacement fell to within < 30% of its maximum value continuously for 50 samples (100 ms). Onset of movement was defined as the latest of these samples. To find the outbound duration, the offset of the outbound movement was found and the time difference from onset to offset was calculated. Offset of outbound movement was defined at the first point the displacement reached 10% of its maximum displacement and its

velocity dropped below 2°/s. Max outbound velocity was defined as the maximum velocity during the outbound movement. To determine the return movement duration, the onset of return movement and offset of return movement were calculated. This onset was defined as the first time the displacement dropped 10% from its maximum and velocity exceeded its 2°/s threshold. The offset was defined as the first point the displacement dropped below 90% of its maximum and the velocity dropped below 2°/s. The max return velocity was defined as the maximum velocity during the return movement. Turning point refers to invalid cues were participants initiate movement in the direction of the invalid cue and then need to change direction towards the actual location of the target. The turning point is defined as the point of max displacement in the invalid direction. This parameter is only informative in invalid cues and will return a value of ≈ 0 on valid trials.

EOG data were analysed using custom MATLAB R2013b scripts and EEGLAB (Delorme and Makeig, 2004). First, data were de-trended by removing the line of best fit from each channel to correct for signal drift. The data were then filtered using a 4th order band-pass Butterworth filter with a pass band of 0.1 − 10 Hz. Next, EOG data from each trial were epoched with respect to cue onset, 1 second of data was used for each trial (399ms pre- to 600ms post-stimulus). Artefact rejection was carried out separately for each channel of EOG. If both channels were rejected, the trial was removed from further analysis. In all other cases, the mean of the remaining channels was employed for further analysis. Channels were marked as artefacts if they contained an absolute value of greater than 10uV or if they were uncorrelated with the other channel of EOG (p > 0.001).

Onset of EOG was detected for comparison with onset of head movement. The head movement outbound onset detection algorithm, as described above, was also employed for EOG data; letting the EOG data correspond to displacement and its first derivative therefore correspond to velocity. Other parameters, as calculated for the HMD data, were not reliably

obtainable using EOG, as such, onset of saccade was the only parameter extracted in this case.

4.2.5 Statistical analysis

Analysis of Variance (ANOVA). Each of the 6 behavioural measures extracted from the HMD data, as described in the previous section, were submitted to same analysis of variance (N = 40). Onset of saccade, as extracted from EOG data, was also submitted to this analysis of variance (N = 18). This analysis was designed to explore the effects of target angle, target side and cue validity on participant performance. Each parameter was submitted to a 3-way ANOVA. The independent variables used for this analysis were cue validity (level = 2; valid and invalid), target side (level = 2; left and right) and target angle (level = 3; 30°, 45° and 60°).

Head movement onsets and saccade onsets were also submitted to an analysis of variance for the subset of participants for whom EOG was collected (N = 18). This analysis was carried out to probe the relationship between head and eye movement onset during eccentric deflections in gaze. A 4-way ANOVA was employed with the independent variables data type (level = 2, HMD and EOG), cue validity (level = 2; valid and invalid), target side (level = 2; left and right) and target angle (level = 3; 30°, 45° and 60°).

Regression Analysis. To further explore the relationship between head movement onset and saccade onsets, two linear regression models were created using valid and invalid trials. The dependant variable of these models was saccade onset and the predictor variable was head movement onset. Each model was created using onset data from all possible target locations. In cases where trials had been rejected from the EOG data due to artefact detection, the corresponding trials were also rejected from the HMD data for use in the

regression model. In the valid model 1303 out of a possible 1728 (75.41%) trials were maintained, in the invalid model 380 out of a possible 432 trials (87.96%) were maintained.

To test the utility of the current task as an investigative tool, some follow up single participant statistical analysis was carried out. The primary aim of this analysis was to show that the Posner effect, which was observed at group level, was reproducible at a single participant level, i.e. invalid cues should result in a slower onset of head movement when the target sphere is visible at the neutral position. In line with this definition, only targets from ±30° and ±45° were employed for this analysis, as targets at ±60° were not initially visible and therefore do not represent a Posner task per se. For each participant, all valid trials from ±30° and ±45° were grouped, as were all invalid trials for the same angles. These two groups were then submitted to a 2-sample unpaired t-test to determine if statistically significant differences existed due to trial validity, which would represent a Posner effect.

Next the regression analysis, as detailed above, was repeated at a single participant level to show that the relationship between head movement onset and saccade onset was also reproducible at the single participant level. Due to the limited amount of invalid data, this analysis was only carried out for valid trials, although results of the group level regression analysis suggest that this relationship should exist for both valid and invalid trials.

4.3   Results: Control study

4.3.1   Head turn results

The task employed in the current study represents a modified Posner cueing task. In this context, onset of head movement is employed rather than the typical button press or saccade response usually used for Posner tasks. The results presented here indicate that onset of head movement is delayed when the cue presented to participants is invalid (Figure 4.3, a). This delay in movement onset during invalid trials represents a Posner cueing effect; the 3-

way ANOVA analysis revealed a highly significant effect of cue validity ($F_{(1, 39)} = 144.9$, $p < 0.001$). There was also a significant main effect of target angle ($F_{(2, 78)} = 3.2$, $p < 0.05$) suggesting that the position of the target in the participant's field of view had some impact on movement onset. An interaction effect of cue validity and target angle was also observed ($F_{(2, 78)} = 12.8$, $p < 0.001$) suggesting that the variation due to target angle was not consistent across valid and invalid trials. This is explained by the absence of a Posner effect at the $\pm 60°$ target angles. As the target sphere is not initially visible, the contradiction between cue and target that cause the Posner effect is also absent. No other factors in this analysis were significant, a full summary of these results are displayed below, Table 4.2.

During invalid trials, when participants initiate movement in the invalid direction, a point of correction or a turning point is recorded. The results of the ANOVA analysis demonstrate a significant main effect of cue validity ($F_{(1, 39)} = 219$, $p < 0.001$), a significant main effect of target angle ($F_{(2, 78)} = 196.6$, $p < 0.001$) and a significant interaction effect of cue validly and target angle ($F_{(2, 78)} = 150.2$, $p < 0.001$). Both the main effect of cue validity and the interaction effect of cue validity and target angle relate to the absence of a turning point in valid trials; a value of ≈ 0 is returned in such cases. The significant effect of angle is more informative and is driven by the variance in invalid trials across target angles. Turning points for $\pm 30°$ and $\pm 45°$ are largely equivalent but turning points for $\pm 60°$ tend to be significantly slower (Figure 4.3, b). This is because the target is visible from the start position during these $\pm 30°$ and $\pm 45°$ trials and so the participant will quickly realise the cue was invalid and correct their movement. During trials where the target is at $\pm 60°$ the turning point is much later as participants need to partially complete an invalid movement to discover that the cue was invalid. This difference causes the significant effect of angle that has been observed here.

Head movement parameters
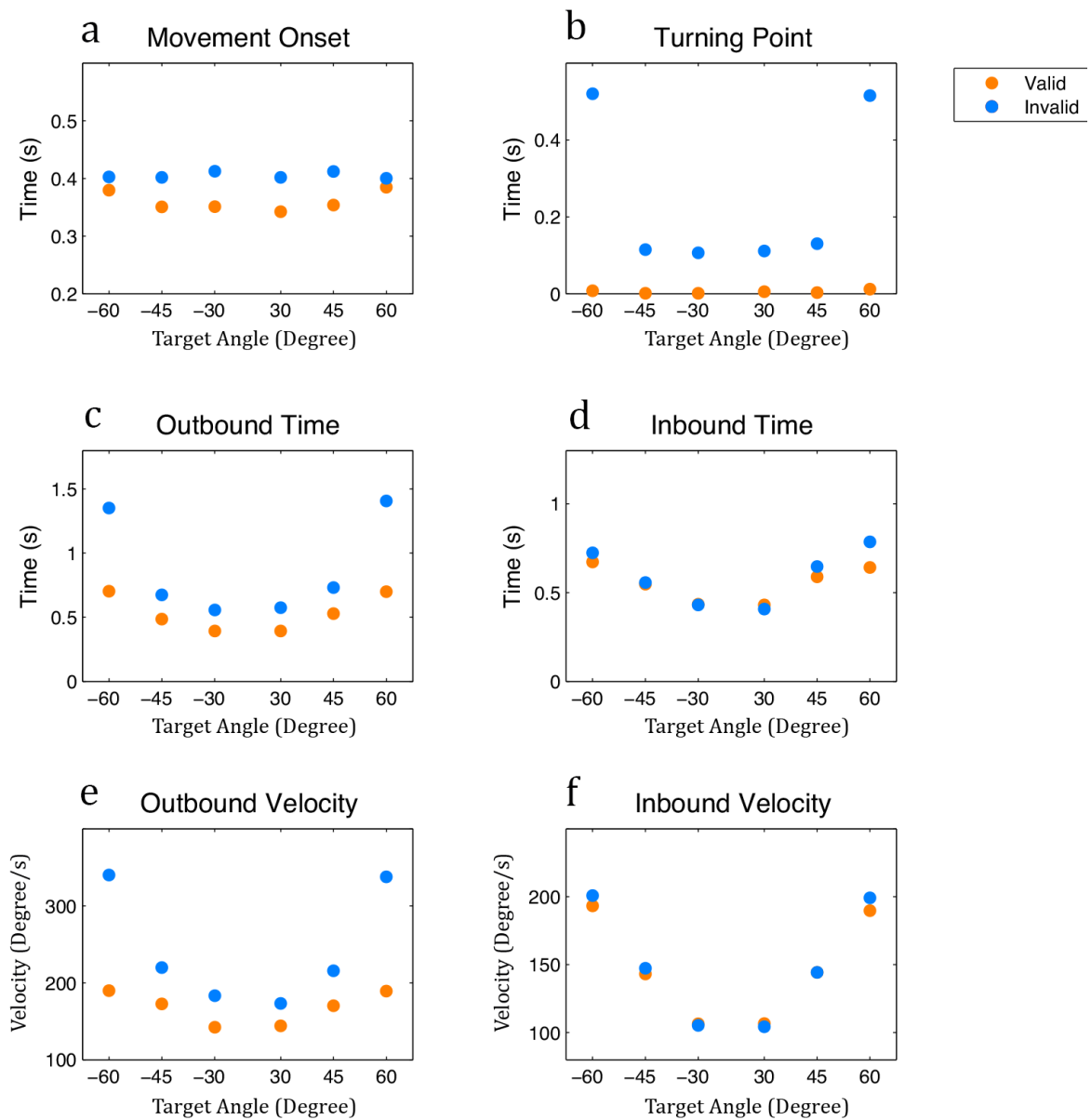
Figure 4-3

The 6 movement parameters as extracted from the head movement data. These plots represent group average data. All target angles (x-axis) are displayed for each parameter as well as cue validity (valid: orange, invalid: blue). Panel a shows movement onset times, Panel b shows turning point times, Panel c and d show outbound and inbound duration respectively and panel e and f show outbound and inbound maximum velocity respectively.

Table 4-2

A summary of the 3-way repeated measure analysis of variance (ANOVA) results for the 6 movement parameters as depicted in Figure 3. This table represents the group level data only. Degrees of freedom (df), F- and p-values are reported for all tests. The 3 factors of interest in this analysis are cue validity (Valid), target side (Side) and target angle (Angle).

Onset	df	F	p	**Turning Point**	df	F	p
Valid	(1, 39)	144.9	<0.001	*Valid*	(1, 39)	219	<0.001
Side	(1, 39)	0.9	0.33	*Side*	(1, 39)	0.1	0.78
Angle	(2, 78)	3.2	<0.05	*Angle*	(2, 78)	196.6	<0.001
*Valid*Side*	(1, 39)	0.1	0.78	*Valid*Side*	(1, 39)	1.1	0.32
*Valid*Angle*	(2, 78)	12.8	<0.001	*Valid*Angle*	(2, 78)	150.2	<0.001
*Side*Angle*	(2, 78)	2.1	0.13	*Side*Angle*	(2, 78)	0.1	0.92
*Valid*Side*Angle*	(2, 78)	1.5	0.23	*Valid*Side*Angle*	(2, 78)	0.3	0.74

Outbound Time	df	F	p	**Return Time**	df	F	p
Valid	(1, 39)	177.8	<0.001	*Valid*	(1, 39)	4.1	0.06
Side	(1, 39)	0.3	0.58	*Side*	(1, 39)	0.1	0.98
Angle	(2, 78)	13.4	<0.001	*Angle*	(2, 78)	67.3	<0.001
*Valid*Side*	(1, 39)	0.1	0.99	*Valid*Side*	(1, 39)	0.4	0.5
*Valid*Angle*	(2, 78)	92.6	<0.001	*Valid*Angle*	(2, 78)	2.1	0.12
*Side*Angle*	(2, 78)	0.4	0.68	*Side*Angle*	(2, 78)	2.4	0.1
*Valid*Side*Angle*	(2, 78)	0.4	0.65	*Valid*Side*Angle*	(2, 78)	0.3	0.74

Outbound Velocity	df	F	p	**Return Velocity**	df	F	p
Valid	(1, 39)	80.4	<0.001	*Valid*	(1, 39)	2.4	0.13
Side	(1, 39)	0.3	0.58	*Side*	(1, 39)	1.1	0.31
Angle	(2, 78)	170.8	<0.001	*Angle*	(2, 78)	194.1	<0.001
*Valid*Side*	(1, 39)	0.1	0.83	*Valid*Side*	(1, 39)	0.1	0.76
*Valid*Angle*	(2, 78)	87.6	<0.001	*Valid*Angle*	(2, 78)	3.1	0.067
*Side*Angle*	(2, 78)	0.1	0.87	*Side*Angle*	(2, 78)	1.5	0.22
*Valid*Side*Angle*	(2, 78)	0.6	0.55	*Valid*Side*Angle*	(2, 78)	0.8	0.46

Outbound time is a measurement of the time taken for a participant to complete a movement towards the target location. Again, the results show a delay in the invalid trials. This delay corresponds to the delayed onset (Posner effect) and the fact that some movements are initiated in the invalid direction. Outbound time shows a statistically significant effect of

cue validity (F(1, 39) = 177.8, p < 0.001), target angle (F(2, 78) = 13.4, p < 0.001) and an interaction effect of cue validity and target angle (F(2, 78) = 92.6, p < 0.001). No other effects were significant in outbound time, Table 4.2.

Return time refers to the time taken for a participant to complete the return movement to the neutral position after trial completion. As expected, the results show that larger movements take longer to complete. The results of the ANOVA analysis support this, showing a significant effect of target angle (F(1, 39) = 67.3, p < 0.001). No other main or interactions effects were significant, Table 4.2.

Outbound velocity is a measure of the maximum velocity of yaw during the outbound movement. The results suggest that larger movements tend to result in larger peak amplitude, as might be expected. During valid trials is observed as a linear increase with target angle. Invalid trials tend to have a larger peak velocity as subjects often move in the invalid direction initially before correcting back to the valid direction. This is most noticeable in the ±60° condition where the target is outside the field of view at cue presentation. In such cases the participant could be completing a movement of up to 120°, resulting in the larger peak velocity seen. The results of the 3-way ANOVA show a statistically significant effect of cue validity (F(1, 39) = 80.4, p < 0.001), target angle (F(2, 78) = 170.8, p < 0.001) and an interaction effect of cue validity and target angle (F(2, 78) = 87.6, p < 0.001). No other factors or interaction were statistically significant for outbound velocity, Table 4.2.

Return velocity is a measure of the peak velocity of yaw during a post-trial return movement. The results show that larger movements tend to contain a larger peak velocity. This observation agrees with that of the outbound velocity results. The results of the 3-way

ANOVA show a significant effect of target angle ($F_{(2, 78)} = 194.1$, $p < 0.001$). No other main or interaction effects were significant for return velocity, Table 4.2.

4.3.2   Saccade onset analysis

Saccade onset is often employed as an ecologically valid response for Posner style paradigms. To test the hypothesis that the proposed paradigm would elicit a delayed onset of saccade during invalid trials, all EOG onsets were submitted to a 3-way ANOVA. This analysis revealed a highly significant effect of cue validity ($F_{(1, 17)} = 81.9$, $p < 0.001$), representing a confirmation of the Posner cueing effect in saccade onset. There was also a significant main effect of target angle ($F_{(2, 34)} = 10.9$, $p < 0.001$) and a significant interaction effect of cue validity and target angle ($F_{(2, 34)} = 13.5$, $p < 0.001$) which is consistent with the onset of head movement results reported above. No other factors were significant in this analysis, Table 4.3.

Table 4-3

A summary of the 3-way repeated measure analysis of variance (ANOVA) results for EOG onset data. This table represents the group level data. Degrees of freedom (df), F- and p-values are reported for all tests. The 3 factors of interest in this analysis are cue validity (Valid), target side (Side) and target angle (Angle).

EOG Onset			
	df	**F**	**p**
Valid	(1,17)	81.9	<0.001
Side	(1,17)	0.6	0.46
Angle	(2,34)	10.9	<0.001
*Valid*Side*	(1, 17)	0.5	0.49
*Valid*Angle*	(2, 34)	13.5	<0.001
*Side*Angle*	(2, 34)	0.3	0.74
*Valid*Side*Angle*	(2, 34)	0.5	0.62

Changes in gaze are generated through a combination of eye, head, trunk and lower limb movements (Sklavos et al., 2010, Anastasopoulos et al., 2009, Bonnet et al., 2014). Furthermore, it has been observed that onset of saccades precede head movements in a well-characterized fashion (Scharli et al., 2013). To show this property of gaze under the

current paradigm, EOG was collected during testing for a subset of 18 participants. For both valid and invalid trials, it was observed that saccade onset preceded head movement onset for all target locations in a uniform fashion (Figure 4.4, a). This was verified in the ANOVA analysis. A statistically significant effect existed for cue validity ($F(1, 17 = 144.7$, $p < 0.001$)), representing the Posner effect which was observed in each modality independently. There was also a statistically significant effect of recording modality ($F(1, 17 = 32.5, p < 0.001$)), confirming that onset of eye movement occurs earlier than onset of head movement. The effect of target angle (($F(2, 34 = 11.9, p < 0.001$))) and interaction between target angle and cue validity ($F(2, 34 = 10.2, p < 0.001$)) mirror the results that were observed during the individual 3-way analysis. The effect of target angle could suggest that onset is faster when targets are closer to the central field of vision but further research is required to draw a definitive conclusion on this point. Finally, the interaction between cue validity and recording modality ($F(1, 17 = 5.3, p < 0.05$)) highlights that the Posner effect observed for saccade onsets is larger than that observed for onset of head movement, as may be observed from Figure 4.4. A full summary of this analysis is displayed in Table 4.4.

a HMD vs. EOG: Movement onset
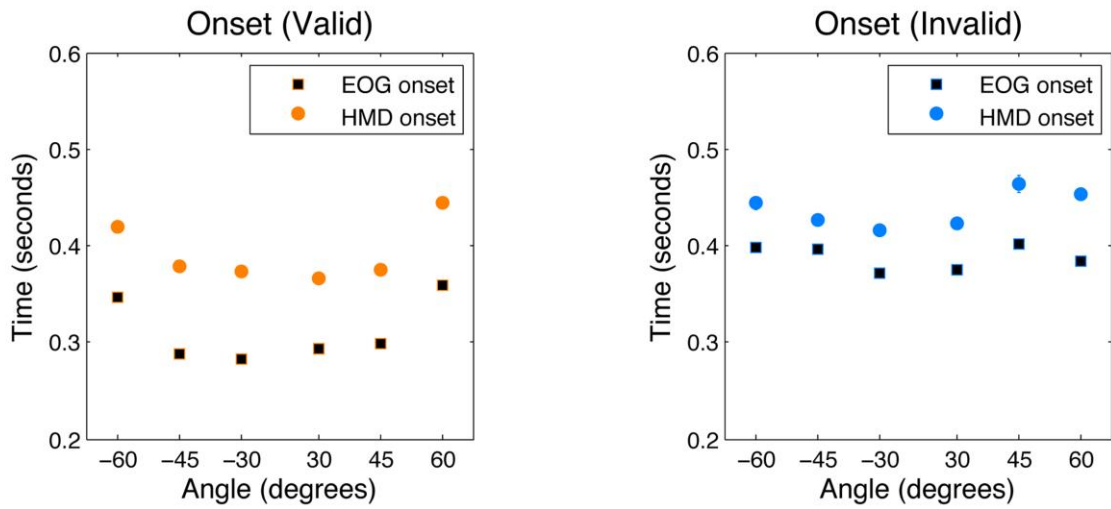
b Regression analysis
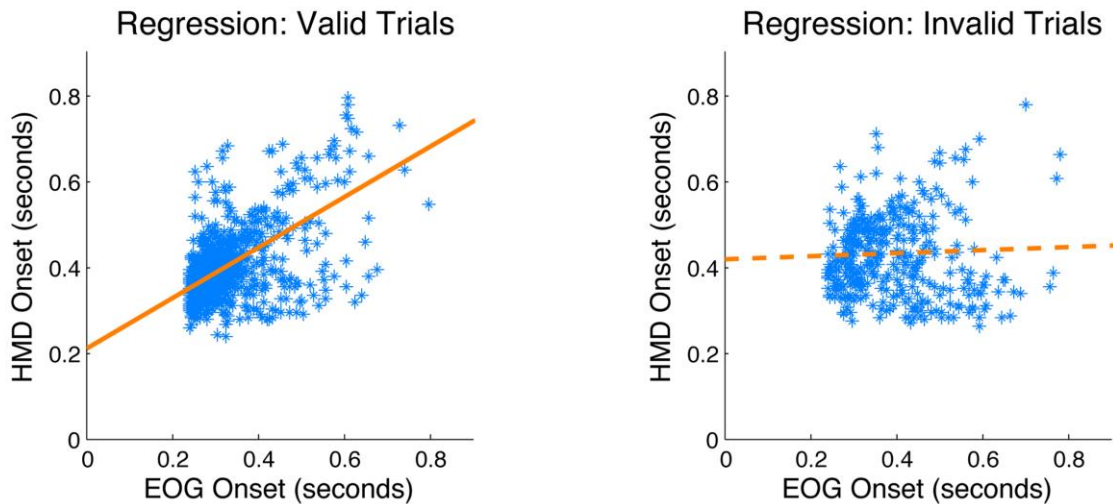
Figure 4-4

A plot of movement onsets for both head (solid) and eye (black centre) movements. The left plot represents valid trials (orange) and the right plot represents invalid trials (blue). These plots represent group mean data for all possible experimental conditions. Panel b contains a visualization of the group level regression analysis. The left plot represents the model created employing all valid trials while the right plot represents the model created employing all invalid trials. The orange line represents the regression equation, which is highly significant in both cases.

Table 4-4

A summary of the 4-way repeated measure analysis of variance (ANOVA) results for HMD vs EOG data depicted in Figure 4. This table represents the group level data. Degrees of freedom (df), F- and p-values are reported for all tests. The 4 factors of interest in this analysis are cue validity (Valid), recording modality (Modality), target side (Side) and target angle (Angle).

HMD & EOG Onset	df	F	p
Valid	(1, 17)	144.7	<0.001
Modality	(1, 17)	32.5	<0.001
Side	(1, 17)	3.1	0.01
Angle	(2, 34)	11.9	<0.001
*Valid*Modality*	(1, 17)	5.3	<0.05
*Valid*Side*	(1, 17)	0.1	0.89
*Modality*Side*	(1, 17)	0.2	0.63
*Valid*Modality*Side*	(1, 17)	0.7	0.39
*Valid*Angle*	(2, 34)	10.2	<0.001
*Modality*Angle*	(2, 34)	0.1	0.95
*Valid*Modality*Angle*	(2, 34)	0.3	0.77
*Side*Angle*	(2, 34)	0.4	0.67
*Valid*Side*Angle*	(2, 34)	1.8	0.19
*Modality*Side*Angle*	(2, 34)	1.2	0.33
*Valid*Modality*Side*Angle*	(2, 34)	0.2	0.81

To further probe the relationship between head movement onset and saccade onset, a linear regression model was created (Figure 4.4, b). The aim of this model was to demonstrate the strength of the relationship. In the case of valid trials, a significant regression equation was found ($F(1, 1301) = 761.8$, $p < 0.001$), with an adjusted R^2 value of 0.37. Participant's predicted onset of eye movement is equal to 0.067 + 0.626 (HMD Onset) seconds. The intercept value was significant in this model ($t = 7.3$, $p < 0.001$) as was the HMD coefficient ($t = 27.6$, $p < 0.001$). The model of invalid trials did not produce a significant regression equation ($F(1, 378) = .6$, $p = 0.45$). This is likely because there is a narrower range of values available for invalid trials, making it more difficult to observe a statistically significant relationship.

4.3.3 Single participant analysis

Single participant analysis was carried out to test the utility of the current protocol at a single participant level. The protocols and task described here may have applications across a wide range of movement disorders. In such cohorts, group level analysis is often less informative due to increased inter-participant variability and single participant analysis may therefore be more applicable. The aim of this analysis was to demonstrate that both the Posner effect and head movement/saccade onset relationship were reproducible a single participant level. As the Posner effect was only observed for targets at ±30° and ±45°, these angles were employed for the single participant analysis.

To test if the Posner effect was detectable at an individual level, trials from ±30° and ±45° were grouped for valid (N = 64) and invalid (N = 16) trials and then submitted to a 2-sample unpaired t-test for each of the 40 participants. A statistically significant difference ($p < 0.05$) was observed in 36 out of 40 participants (90% of participants). This result suggests that the Posner effect observed at group level is also highly reproducible at the single participant level.

To test the reproducibility of the saccade onset head movement onset relationship, the regression analysis was repeated at the single participant level. The results of this analysis reveal that this relationship is highly significant in 14 out of 18 participants ($p < 0.05$). R-values were also very consistent across participants (0.47 ± 0.32, mean ± SD). This analysis further highlights the uniformity with which saccade onsets lead head movement onsets during eccentric changes in gaze.

4.4 Results: Patient study

In a follow-on from the healthy control work, head movement data was collected from several cervical dystonia patients and healthy age matched controls. Given the results of

114

the regression analysis in the previous section, which indicated a strong relationship between eye and head movement onsets, and the additional difficulty involved in recording eye movements, it was decided that only head movements would be recorded for this study.

Given that the aim of this study was to compare covert attention abilities in cervical dystonia, the analysis focused on head movement onsets and employed the delay in onset during invalid trials (i.e. Posner effect) as a metric by which to compare the two groups. Only targets that were found to elicit a Posner effect in the initial study (30° and 45°) were considered here, targets at 60° have been excluded from this analysis. For each subject a single valid and invalid onset time was generated, these two values were then employed to calculate the Posner effect. This was taken as the mean value for left and right cues and for targets at 30° and 45°. These onset timings were then plotted as a univariate scatter plot shown in Figure 4.5. This data was submitted to a 2-way AVOVA analysis which examined variance related to cue type, valid and invalid, and group type, patient or control. This analysis revealed a significant effect of group ($F(1, 27) = 35.5$, $p < 0.001$) which highlights that patients have a slower movement onset when compared to age-matched controls. There was also a significant effect of cue type ($F(1, 27) = 98$, $p < 0.001$) which is consistent with the original research and confirms the presence of a Posner effect during invalid cues. Finally, a significant interaction between group and cue type was also observed ($F(1, 27) = 22.9$, $p < 0.001$) which would suggest that the Posner effect is larger in patients than in control subjects and may suggest an abnormality in covert attentional abilities in patients with cervical dystonia.
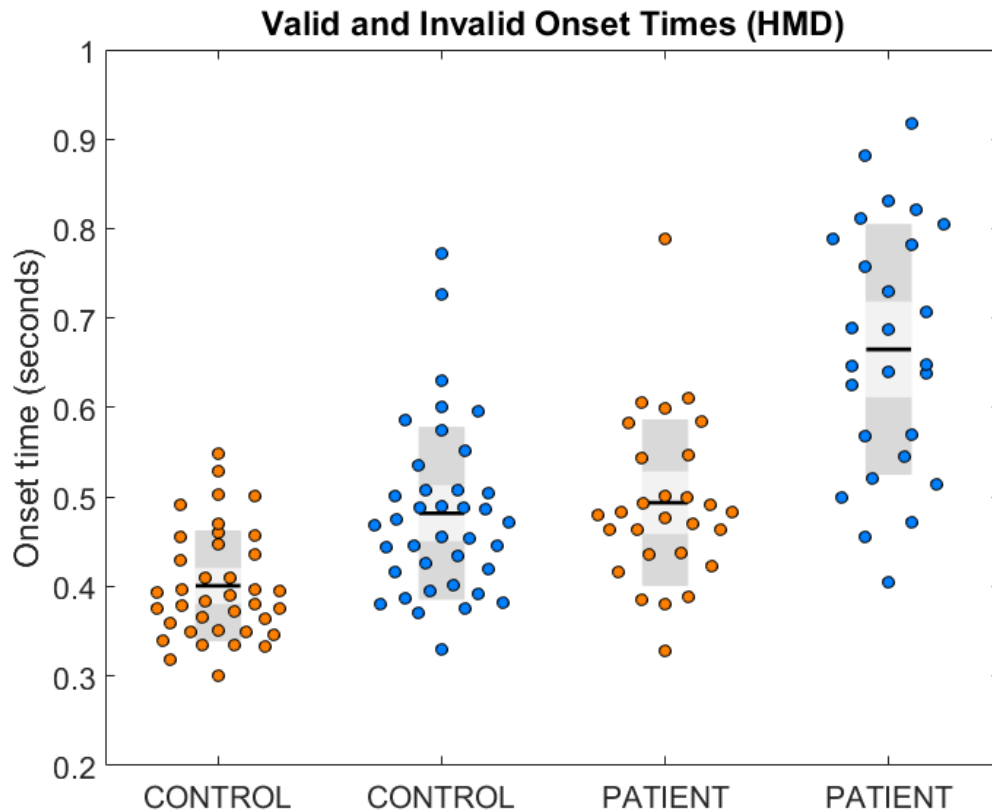
Figure 4-5

A univariate scatter plot of head movement onset timings for control and patient groups. Each point represents the subject average value for valid (orange) and invalid (blue) cue conditions for both the 30° and 45° targets. The group mean onset values are represented by the black horizontal line while the standard error and standard deviation are represented by the light and dark grey areas respectively. The data represented in this plot has been submitted to an ANOVA statistical analysis test.

To further examine the significant interaction between participant group and Posner effect a follow-on analysis was carried out. Posner effect was calculated for each participant using the valid and invalid onset timings displayed in Figure 4.5. The initial ANOVA analysis revealed that patient onsets were slower for both valid and invalid trials; to account for this, the Posner effect was calculated as a percentage increase in onset time between valid and invalid trials.

$$Normalised\ Posner\ Effect = \frac{RT_{invalid} - RT_{valid}}{RT_{valid}} * 100$$

Looking at a normalised increase rather than an absolute increase in time makes comparisons between groups more valid. Posner effect is plotted in Figure 4.6 for control subjects and patients.
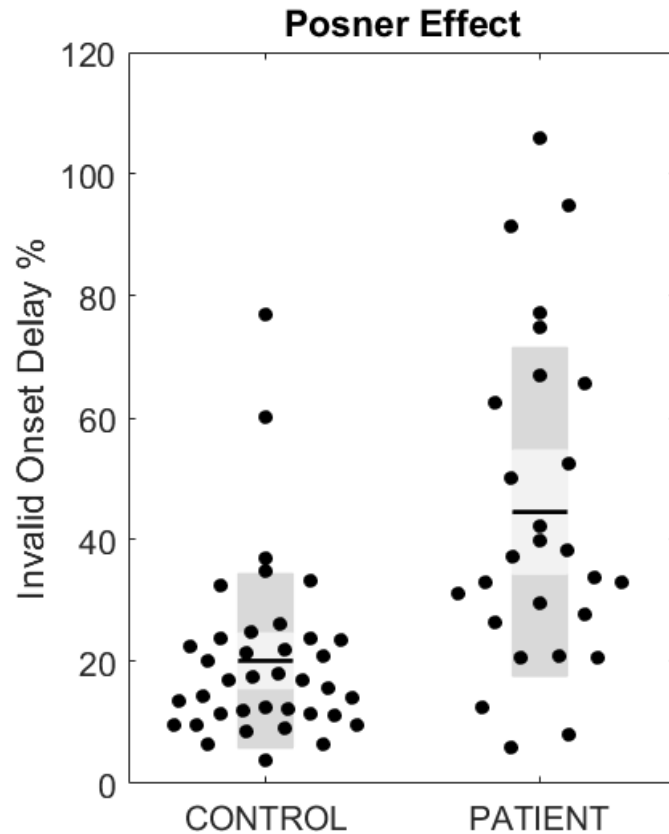
Figure 4-6

A univariate scatter plot of Posner effect for control and patient groups. Each point represents the % increase in onset time of a single participant during invalid trials. The group mean values are represented by the black horizontal line while the standard error and standard deviation are represented by the light and dark grey areas respectively. This data was also submitted to a 2-sample t-test which confirmed that patients have a significantly larger Posner effect than healthy controls.

Descriptive statistics reveal that movement onsets in healthy controls were 20.1% (81.1 ms) slower during invalid trials, while movement onsets in patients were 44.6% (171.3 ms) slower during invalid trials. The data displayed in Figure 4.6 was then submitted to a 2-sample t-test which confirmed that the % increase in onset timings during invalid trials is significantly larger in patients than in healthy age-matched controls ($p < 0.001$). While the

physical symptoms observed in cervical dystonia likely account for the slower onset times observed in the patient group, they do not fully explain why the Posner effect should be more than twice as large in patients. Given that the Posner effect has long be employed as a metric of covert attention, this result may be partially explained by covert attentional abnormalities, potentially arising from the same GABAergic deficit in the superficial layers of the superior colliculus that has been hypothesised to be the cause of abnormal temporal discrimination and cervical dystonia.

Cervical dystonia describes any form of dystonia which effects the cervical muscles of the neck. Given the complex anatomy of these cervical muscles, cervical dystonia can be sub-divided into several different categories which may be an important factor when considering the results presented above. The two most common manifestations of cervical dystonia present in the current cohort were right and left Torticollis. As the above calculation of Posner effect relied on mean onset values for left- and right-going movements it was important to clarify whether patients exhibit an imbalance of performance either toward or away from the effected side.

To address this concern two groups were generated from the whole patient group; these groups were made up of patients with right Torticollis (n = 11) and patients with left Torticollis (n = 10). Patients who fell outside these exact diagnoses were excluded from this analysis (n = 7). For each of these groups left- and right-going movements where plotted individually, as were valid and invalid trials. Figure 4.7. This data was then submitted to the 3-way ANOVA analysis which was designed to consider side of Torticollis, target side and cue validity.

The ANOVA analysis revealed a significant effect of cue validity ($F(1, 9) = 15.3$, $p < 0.005$), confirming the existence of the Posner effect as seen in previous analysis. No other

factors or interactions were significant in this analysis. Side did show a trending relationship (F(1, 9) = 3.9, p = 0.078) with onset which would suggest that all patients across both groups may have a preferential side, however, the fact that there was no interaction between side and torticollis shows that there is no imbalance of performance either toward or away from the effected side. These results suggest that side of Torticollis does not impact on onset of head movement during valid or invalid trials under the current paradigm. It is possible that an effect would be observed with greater numbers although the plots displayed in Figure 4.7 do not seem to suggest any trends in the current cohort. This analysis supports the hypothesis that the increased Posner effect is not just a result of manifestation of disorder and may in fact relate to an abnormality in the sub-cortical network for cover attention. If this were not the case, then we would expect to see a preferential side when splitting the group by effected side.

Table 4-5

A summary of the 3-way ANOVA results for the Torticollis segmented data depicted in Figure 5.7. Degrees of freedom (df), F- and p-values are reported for all tests. The 3 factors of interest in this analysis are cue effected side (Torticollis), cue validity (Valid), target side (Side) and target angle (Angle).

HMD & EOG Onset			
	Df	F	P
Torticollis	(1, 9)	0.63	0.448
Valid	(1, 9)	15.3	0.004
Side	(1, 9)	3.9	0.078
*Torticollis*Valid*	(2, 9)	2.8	0.128
*Torticollis*Side*	(1, 9)	2.2	0.175
*Valid*Side*	(1, 9)	1.1	0.317
*Tort*Valid*Side*	(1, 9)	0.1	0.73
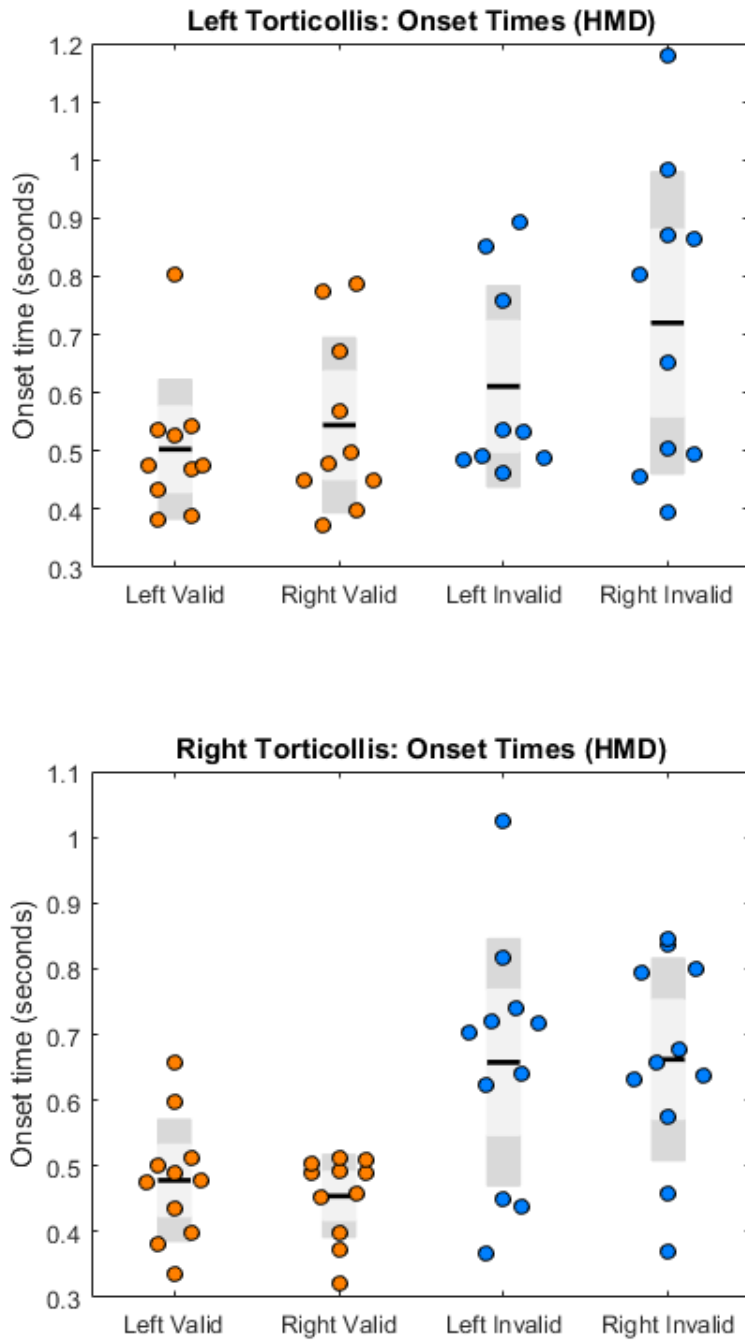
Figure 4-7

Univariate scatter plot showing onset timings for left and right and for valid and invalid trials separately. The upper figure contains patients with Torticollis on the left hand side while the lower plot contains patients with torticollis on the right. The group mean values are represented by the black horizontal line while the standard error and standard deviation are represented by the light and dark grey areas respectively. This data was submitted to a 3-way ANOVA, the results of which are reported above.

4.5 **Discussion**

In recent years, advances in sensing and display technologies have made virtual reality systems viable, and companies like Oculus VR have helped to make this technology widely available and affordable. These systems have the capacity to present immersive 3D stimuli while also tracking and recording movements of the user, making them suitable for research of human kinematics. In the current study, ecologically valid head and eye movements during a modified Posner cueing task were investigated using one such virtual reality system. The aim of this work was to show that these devices could collect robust data and have utility in the research of human movement and movement disorders.

4.5.1   Control study

Humans and other primates have evolved an elegant oculomotor system to better utilise images acquired by the retina. The oculomotor system is comprised of both low-level circuitry to rapidly reposition our line of site onto targets of interest, and high-level circuitry to implement flexible optimisation strategies. For example, dynamic orientation of visuospatial attention based on environmental cues enables us to react faster to salient stimulus appearing in our peripheral vision, as illustrated by the Posner cueing effect. The Posner spatial cueing effect (Posner, 1980) has been widely investigated using both manual button press (Feldmann-Wustefeld and Schubo, 2013, Rieth and Huber, 2013, Johnson et al., 2012) and automatic saccade (Dawel et al., 2015, Yokoyama et al., 2012, Chaminade and Okka, 2013) reaction times to help investigate the effects of covert orienting of attention in response to different cue conditions. In the current study, a modified Posner task was employed and reaction times of both saccade onset and head movement onset were investigated. Although saccade onsets are commonly employed in this context, this work, to our knowledge, represents the first time that onset of head movement has been investigated as the response for such a task in humans. Onset of head movement has been

used in a Posner style task for the investigation of attentional influence on sound-localization behaviour in barn owls (Johnen et al., 2001, Kettler and Wagner, 2014) and an effect of orientation of attention was observed.

Given that saccades are known to precede head movements during changes in gaze in a stereotyped manner (Bizzi et al., 1971, Hollands et al., 2004, Daye and Roberts, 2015, Scharli et al., 2013), it was hypothesised that the Posner effect should be present in onset of head movement in addition to onset of saccade. This relationship between onset of head movement and onset of saccade has been investigated in monkeys using neck electromyography (EMG) and eye tracking methods (Corneil et al., 2004). Given the considerable inertia of the head, it was unknown whether express saccades were accompanied by a parallel command to the head from the low level circuitry of the oculomotor system. Corneil et al. demonstrated that visual target presentation elicits time-locked, lateralised recruitment of neck muscles for both express and non-express saccades.

The results presented here indicate that the Posner effect is present in the onset of head movement data at both group level and at a single participant level (in 90% of participants). The effect was also observed in the EOG data for the subset of 18 participants, consistent with the existing literature (Dawel et al., 2015, Yokoyama et al., 2012, Langley et al., 2011). The analysis showed that the relationship between onset of head movement and onset of saccade activity is highly stereotyped at group level for both valid and invalid trials and at the single participant level for valid trials. The 4-way ANOVA analysis confirm that the Posner effect is larger for saccade onsets, however, no other interaction effects were observed in relation to recording modality, supporting the view that the head and eye movement onsets are highly related.

The presence of the Posner effect in saccade onset has been well documented in the literature (Dawel et al., 2015, Yokoyama et al., 2012, Chaminade and Okka, 2013), as has the relationship between saccade onset and head movement onset (Bizzi et al., 1971, Hollands et al., 2004, Daye and Roberts, 2015, Scharli et al., 2013); furthermore, this relationship has been demonstrated in the current study. Given these points, it is likely that the delay observed in onset of head movement during invalid trials is a novel representation of the classic Posner effect. Thus, head movement onset is a measure of the effect of covert orienting of attention and might be a useful alternative to button press responses and eye tracking methods.

While the subset of EOG recordings was useful in the current study, the results of the regression analysis presented here would suggest that little additional information is gained from the EOG data. This implies that future studies in control cohorts could rely on HMD data alone. It is possible that the relationship between head movement onset and saccade onset might be altered in some clinical settings, thus any novel research in such populations could benefit from collecting both eye and head movement data initially.

To further highlight the versatility of the HMD as a research tool, five additional movement parameters were extracted from the HMD data. The parameters investigated here included turning point, outbound and return movement durations and outbound and return maximum velocities. Each of these parameters was extracted from yaw data, although pitch, roll and positional data are also available from the system and could be informative for other tasks or populations. The results of this analysis were largely as expected; larger movements resulted in longer durations and higher maximum velocities, cue validity was a highly significant factor for outbound movements but was less so for self-initiated return movements. The results presented here show quantitative and qualitative similarity to those found using more traditional non-portable motion capture recording techniques (Hollands

et al., 2004, Anastasopoulos et al., 2009). On their own and for a healthy cohort, these parameters are not very informative, however, they could have utility for making comparisons between different clinical groups in future work. The same can be said about 60° targets included in the current paradigm, although these are not useful for investigating a Posner style question, the data collected during these trials may have utility for other research questions and its inclusion in the experiment makes this paradigm a more versatile research tool. Such movement parameters are easily extracted from the HMD data and in conjunction with novel paradigms, could be employed to answer specific and important research questions. The suitability of such parameters for research of abnormal movement in Parkinson's disease and dystonia has been demonstrated in studies that use motion capture technology to record whole body rotations during valid trials (Anastasopoulos et al., 2013, Anastasopoulos et al., 2011).

4.5.2   Patient study

In a follow-on analysis head turn data was collected from cervical dystonia patients and aged matched controls in an attempt to address the hypothesis that cervical dystonia may involve an abnormality of the sub-cortical circuit required to generate normal shifts in covert-attention. Although this paradigm does not have the power to pin-point the superior colliculus directly, it can show that some abnormality exists in the larger sub-cortical circuit and therefore contributes to the accumulating evidence that points toward superior colliculus involvement in the disorder. The analysis carried out for this patient study focused on onset data for cues located at 30° and 45° as the control study had demonstrated that this data was the most relevant data for a Posner effect. The statistical analysis revealed a significant effect of cue type, relating to the Posner effect, and a significant effect of group, highlighting that patients had a slower onset than controls. These results were expected and are uninformative about the current hypothesis. The more interesting result

was the interaction between group and cue type which revealed that patients present with a disproportionately large Posner effect when compared to age-matched controls. A follow-on analysis employing a within-subject normalization found that Posner effects were more than twice as large in patients. While the physical manifestation of cervical dystonia likely accounts for the slower onset times observed in the patient group, they do not fully explain why the Posner effect should be more than twice as large in patients. Given that the Posner effect has long be employed as a metric of covert attention, this result may be partially explained by covert attentional abnormalities, potentially arising from the same GABAergic deficit in the superficial layers of the superior colliculus that has been hypothesised to be the cause of abnormal temporal discrimination and cervical dystonia.

Data was recorded from patients with different forms of cervical dystonia, effecting different muscles of the neck. This may be an important factor when considering the results presented above and so a follow-on analysis was carried out. Right- and left-sided Torticollis are the most common forms of cervical dystonia and this was reflected in the current cohort. As the calculation of Posner effect relied on mean onset values for left- and right-going movements it was important to clarify whether patients exhibit an imbalance of performance either toward or away from the effected side. The results reported here suggest that side of Torticollis does not impact on onset of head movement during valid or invalid trials under the current paradigm, although numbers were comparatively small and so future work is still required in this area. The lack of an imbalance of performance supports the argument that the abnormal Posner effect is not purely caused my disorder. If disorder does have a significant impact on the Posner effect, then one would expect to see a larger Posner effect on the effected side. This was not the case in the current dataset and so the increased in Posner effect in the patient group may be related to some abnormality in the sub-cortical circuit involved in orientation of covert-attention.

4.6 **Conclusion**

Advances in commercial industries often lead to novel and important research tools. Here we posit that the advent of HMD virtual reality systems presents a cost effective and portable measurement solution for many branches of kinematic research. The results presented here demonstrate that the current protocol can be employed to investigate the effects of covert orienting of attention through an ecologically valid movement-based response. The current set of results also demonstrate how other movement parameters can be extracted from the HMD to answer a much wider set of research questions. Similar tasks could be created to measure the response of patients with movement disorders to novel interventions. It is also possible that the device could be employed as an intervention itself, when accompanied by patient-centred training or rehabilitation tasks. In this work, it has been demonstrated for the first time that the Posner cueing effect is present in onset of head movement as well as onset of saccade activity in a group of healthy adult humans. We have also shown the potential this approach to the study of movement disorders. Specifically, we have demonstrated that individuals with cervical dystonia display a larger than normal Posner effect. These studies were possible due to the unique ability of the HMD to simultaneously present a task, use the movements of the user as an ecologically valid input in real time, and output head position for later analysis.

5   Visuospatial learning and electrophysiological correlates

5.1 Introduction

There is a substantial body of work which suggests that AOIFD stems from a disorder of the basal ganglia loop and that the temporal discrimination threshold represents a method probing the functionality of this network, this idea is covered extensively in sections 2.4 - 2.6. One useful method for testing the validity of this statement is to look at other functions of the basal ganglia network and to test for abnormalities in AOIFD. This section details the development of a paradigm and accompanying objective measures of visuospatial learning, a task which involves the basal ganglia in a number of key ways.

Visuospatial memory is responsible for storing information about our environment and the spatial orientation of objects in that environment. Abnormal visuospatial processing has been observed in several clinical disorders including Autistic Spectrum Disorders (McGrath et al., 2012, McGrath et al., 2013), Parkinson's disease (Nantel et al., 2012, Leek et al., 2014) and Schizophrenia (White et al., 2011, Bourque et al., 2013). The task (as adapted from Stafford et al. (Stafford et al., 2012)) and novel analysis presented in the current study may have utility for probing the health of the basal ganglia network in AOIFD.

In a recent study Bednark et al. demonstrated a relationship between visuospatial learning and P3b amplitude (Bednark et al., 2013). Bednark investigated visuospatial learning by comparing behavioural movement times (MT) and electroencephalogram (EEG) components acquired during a target location task consisting of 30 repetitions (Bednark et al., 2013). In that study trials 1-15 were grouped together, as were trials 16-30. In this fashion Bednark et al. could show a relationship between P3b amplitude and MT across the first and second half of the task. The current study explores this relationship in greater detail by analysing behavioural and electrophysiological data at a consecutive trial level.

The P3b is a subcomponent of the P300 event related potential (ERP); it is a positive component usually peaking in the time window of 300-500 ms post stimulus. The P3b is most commonly observed in tasks that require an aspect of performance monitoring and where stimuli are relevant to task performance (Polich, 2007, Courchesne et al., 1975). It has been observed that the amplitude of the P3b is modulated by factors such as stimulus relevance, stimulus occurrence probability (Duncan-Johnson and Donchin, 1977), stimulus complexity (Isreal et al., 1980, Johnson, 1986) and inter stimulus intervals (Gonsalvez and Polich, 2002, Steiner et al., 2014, Croft et al., 2003, Steiner et al., 2013, Polich, 2003). While there have been several studies that suggest a link between the P3b component and various types of learning (Sailer et al., 2010, Bednark et al., 2013, Lindin et al., 2004, Batterink et al., 2015, Jongsma et al., 2006), it is a small subsection of these that explicitly link the P3b to visuospatial learning (Bednark et al., 2013).

Changes of alpha oscillations (8-12 Hz) have been strongly linked to the cognitive state of participants. Power in the alpha band over occipital regions is generally observed to decrease during tasks requiring greater effort and attentional loads (Bollimunta et al., 2008, Ergenoglu et al., 2004, Snyder and Foxe, 2010). Increases in alpha power have been associated with decreased attentional demand and with improvements in learning based tasks (Bays et al., 2015, Dockree et al., 2007). One interpretation of these characteristics is that increases in alpha power during repetitive tasks represent an aspect of automation of response from participants: As responses become automatic, less attention is required which in turn leads to increased alpha power (Jensen and Mazaheri, 2010, Bays et al., 2015). However, alpha power is also known to increase with time spent of repetitive tasks and is often accompanied by reduced performance (Foxe et al., 2012), reflecting a decrease in concentration by participants. This confound implies that for increased alpha power to represent an increase in automation, behavioural performance must also remain consistent.

This interpretation is only appropriate in tasks where habituation of response is possible, such as in the current paradigm.

This work confirms and extends the findings of Bednark and colleagues. In addition to investigating the P3b response, a novel analysis examines changes in alpha power during the learning process. P3b amplitudes and alpha power values were analysed at a consecutive trial level to study the dynamic time course of visuospatial learning across 30 consecutive trials. Correlation analysis was carried out to compare electrophysiological and behavioural metrics. Finally, correlation analysis was carried out at single participant level to test the reproducibility of the proposed electrophysiological metrics. It is hypothesized that the relationship between P3b amplitude and task performance is not an indication that P3b amplitude is reflecting visuospatial learning directly but may be driven by other well-documented properties of the P3b component.

5.2 **Methods and materials**

5.2.1 *Participants and ethics*

Eleven healthy adults participated in this study (25.3 ± 2.6 years, mean $\pm$ SD). All participants were right-handed as revealed by self-report and had normal or corrected to normal vision. Only male participants were included to account for gender imbalances in visuospatial processing (Roalf et al., 2006). In accordance with the declaration of Helsinki, all participants gave their written informed consent to the study, which was approved by the Faculty Ethics Committee of the Faculty of Health Sciences at Trinity College Dublin.

5.2.2 *The task*

The task used in the current study was adapted from previous work by Stafford et al. and Bednark et al. (Stafford et al., 2012, Bednark et al., 2013). Participants were seated in a comfortable chair, 70cm from a computer monitor in a dark and quiet room where they

were asked to complete a behavioural experiment. Participants were presented with a black

screen containing a white cursor (0.8° diameter, visual degrees), a grey cross hair and in

some conditions a grey annulus, as shown in Figure 5.1. Movement of the cursor within a

bounded, square search space (10.8° width) was controlled using a Kensington Orbit

Optical   Trackball.
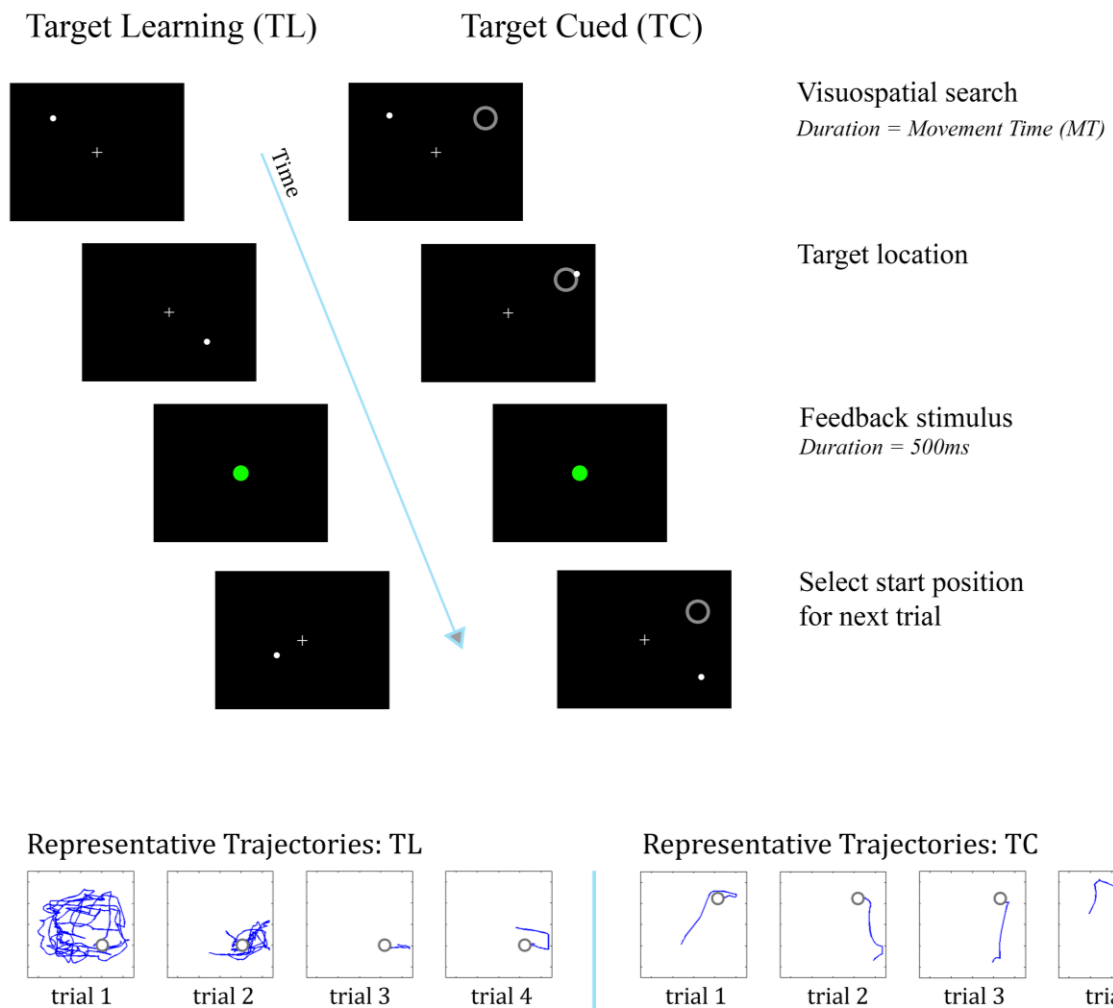
Figure 5-1

Sample frames from the Target Learning (TL) and Target Cued (TC) condition of the
visuospatial learning paradigm. The figure illustrates the progression from the start of a single
trial to the location of the target and finally the presentation of the 500 ms feedback stimulus.
Representative trajectories for each condition, for trials 1 to 4, are also displayed. The blue line
represents the trajectories of the cursor and the grey annulus represents the target location.

Prior to the experiment participants were informed that their aim was to move the cursor into a circular target location (3.2° diameter) in the fastest and most accurate manner possible. Participants completed a shortened practice session to help familiarize them with the paradigm. Providing detailed instructions and practice sessions to the participants represents a departure from the protocol of Bednark et al. but was introduced to eliminate unwanted learning effects in the opening blocks. The practice session consisted of 10 trials of each experimental condition with a single target location for each of the 10 trials. At the beginning of each trial the cursor appeared at a new random starting position inside the search space. To complete a single trial, participants were required to manoeuvre the cursor into the target location. When the cursor entered the target location a green circular stimulus (1.1° diameter) was presented at the centre of the search space for 500 ms, as shown in Figure 5.1. Each experimental block consisted of 30 trials. Within each block, the position of the target location remained consistent across all trials. At the beginning of each block a new target location was randomly generated. The target location could be generated at any point inside the search space providing it was never placed at the centre of the search space or directly adjacent to a bounding wall. This stipulation helped to reduce learning of target location in relation to visible landmarks and encourage visuospatial learning of the search space.

Participants completed this task under two conditions, Target Learning (TL) and Target Cued (TC). In the TL condition the position of the target location was hidden and participants were expected to learn the new location over the course of each block. In the TC condition the target location was highlighted by a grey annulus. The TC condition was designed as a control condition where visuospatial learning would not occur but a motor response would still be present. Participants completed 10 experimental blocks for each condition in alternating order.

5.2.3   Data acquisition

Continuous EEG data, sampled at 512 Hz, was collected from 64 scalp and 8 external active electrodes using a BioSemi high impedance recording system. Stimuli were generated and presented using Neurobehavioral Systems' Presentation software. Triggers were recorded at stimulus onset for offline EEG analysis. The international 10-20 electrode layout system was employed for recordings.

5.2.4   Data analysis

Movement time (MT) was defined as the time interval from the beginning of each trial to the point that the participant manoeuvred the cursor into the target location. Average MTs were calculated for all participants and group average MTs were calculated across participants to allow for comparison with group average ERP data.

EEG data were analysed using custom MATLAB R2013b scripts and EEGLAB (Delorme and Makeig, 2004). Data were first de-trended by removing the line of best fit from each channel to correct for signal drift. The data were then filtered using a 4th order band-pass Butterworth filter with a pass band of $0.1 - 40$ Hz. An external electrode on the nasion was employed to reject trials that contained eye blinks; any channel that contained a voltage greater than ± 80 µV was also rejected. Trials that consisted of more than 10% bad channels were excluded from further analysis. In trials where the number of bad channels was fewer than 10%, those bad channels were interpolated using four nearest "good" neighbours, as described in (Butler et al., 2011). Average reference was employed during analysis by re-referencing the data to the average of all channels (Michel et al., 2004, Nunez and Srinivasan, 2006); an 80 ms pre stimulus window was used as the baseline period. Average ERPs to feedback stimulus onset were calculated for a 600 ms window for each trial. Individual ERPs were calculated across all blocks for the TL and TC experimental conditions for each trial. Group average ERPs were calculated across all participants. P3b

133

amplitudes were calculated for each trial at group mean level by taking the mean value of the ERP waveform over the time interval 310-390 ms post-stimulus (Leue and Beauducel, 2015). This time window was selected to include the peak of the P3b component across all trials. This analysis was carried out over 9 central electrodes of interest (FC1, FC2, FCz, CP1, CP2, CPz, C1, C2, Cz) and the mean of these was taken as the P3b amplitude for a given trial.

Power in the alpha band was estimated using a 500 ms time window prior to target location and the presentation of the feedback stimulus. This time window was selected to provide electrophysiological data during participant response. Given that alpha oscillations are not stimulus locked it was necessary to calculate alpha power at a single trial level. To calculate the power in the $8 - 12$ Hz spectral band the Fourier Transform of the 500 ms window was calculated and the average power across the specified band was estimated. The alpha power of a single trial was calculated as the mean power in the $8 - 12$ Hz frequency band. Electrodes of interest (CP3, CP1, CPz, P5, P3, P1, Pz, P2, PO3, POz, O1, Oz) were used to calculate alpha power, where the topography showed alpha power to be most prominent. Group average mu alpha power was then calculated by generating the mean across blocks and participants.

5.2.5   Statistical analysis

MTs were submitted to a 2-way ANOVA to compare the mean differences between the TL and TC conditions. The independent variables used for this analysis were condition (level $= 2$, TL and TC) and trial (level $= 30$, trials 1 - 30); the dependent variable was MT. In follow up analysis, MTs from the TL and TC condition were submitted to a 1-way ANOVA to determine if significant differences existed due to trial number. The independent variable for this test was trial (level $= 30$, trials 1 - 30) and the dependent variable was MT. A Greenhouse-Geisser correction was applied to all analysis of variance carried out here. This

analysis was carried out to explore how the performance of participants varied over trials and across conditions. P3b amplitude data and alpha power data were also submitted to a 2-way ANOVA. This analysis was carried out to determine the significance of the observed changes across trials and condition in both data sets. Finally, these electrophysiological data sets were each submitted to a 1-way ANOVA to determine if significant differences existed due to trial number.

Due to the unique exploratory nature of trial 1 in the TL condition, it was hypothesised that results from this trial could strongly influence the ANOVA analysis. For this reason, all ANOVAs were carried out twice, with and without inclusion of trial 1.

Correlation analysis was carried out on P3b and MT data at the group mean level to explore the relationship between P3b amplitude and task performance in both the TL and TC experimental conditions across the 30 trials of the block. Alpha power was also compared against MT to determine the statistical relationship between these metrics. Finally, correlation analysis of alpha power and P3b amplitude data was carried out to determine if these distinct electrophysiological parameters were statistically related. Correlations were calculated using the grand average values to test for correlation over the 30 trials of the experimental block.

As with the ANOVA, all correlation tests were carried out twice, once with inclusion of trial 1 and once without. A significance level of 0.015 was selected to account for multiple comparisons of the MT variable (Bonferroni correction).

To test the reproducibility of the results at single participant level, single participant MT, P3b amplitude and alpha rhythm power averages were calculated and submitted to the same correlation analysis as outlined for the grand average data above. Single participant correlations were calculated using the average across blocks for all trials. All

reproducibility analysis was carried out with exclusion of trial 1. As with the group mean correlations, a significance level of 0.015 was selected to account for multiple comparisons.

5.3 **Results**

5.3.1 *Behavioural*

The behavioural measure of performance employed in this study was MT, the time taken for the participant to move the cursor into the target location in each trial. Figure 5.2(a) shows the group average MTs for both the TL and TC tasks. Figure 5.2(b) shows group average MTs with exclusion of trial 1. A steep increase in performance is observed over the first 5 trials of the TL task; MTs remain consistent over the remaining 25 trials. MTs remain consistent across the TL task with no obvious learning effect. A 2 (Condition: TL, TC) $\times$ 30 (trial: 1 to 30) repeated measures ANOVA was conducted on MTs and demonstrated a main effect of condition ($F(1, 10) = 75.7$, $p < 0.001$), a main effect of trial ($F(1.3, 12.9) = 51.8$, $p < 0.001$) and an interaction effect ($F(1.3, 13.1) = 49.8$, $p < 0.001$). This main effect of condition shows MTs are slower in the TL condition. Planned comparisons demonstrated significant differences between trials for the TL condition ($F(1.3, 12.9) = 51.2$, $p < 0.001$) but not for the TC condition ($F(3.7, 37.2) = 1.8$, $p = 0.15$). Exclusion of trial 1 from the MT ANOVA analysis did not alter the significance of the results; see Table 5.1. These results demonstrate that participants become progressively faster at the task in the TL condition over trials but not in the TC condition. A summary of repeated measures ANOVA and planned comparison analysis is displayed in Table 5.1.

a Movement Time (MT)

b Movement Time (MT): *excluding trial 1*
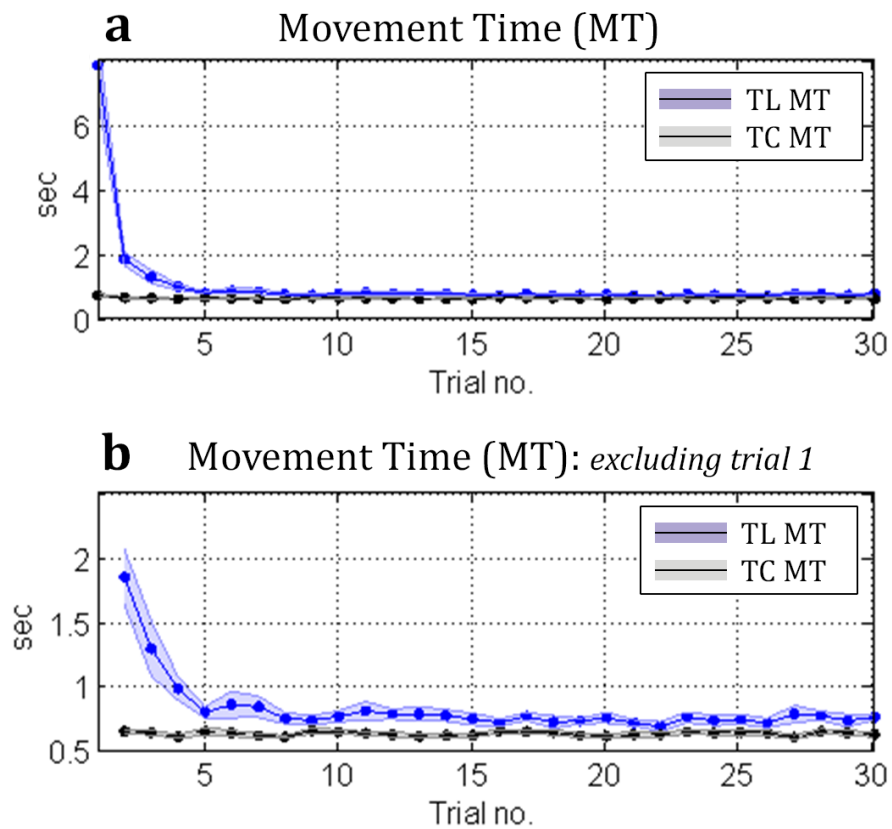
Figure 5-2

Panel A shows the group average movement times (MT) for the Target Learning (blue) and Target Cued (grey) conditions plotted against all trials, 1-30. Shaded areas represent the standard error across participants. Panel B illustrates the same MTs with exclusion of trial 1. Exclusion of trial 1 is incorporated to accommodate the unique exploratory nature of the first trial in the Target Learning condition.

Table 5-1

Summary of all repeated measures ANOVA and planned comparison analysis for movement times (MT), P3b amplitude and alpha power. F- and p- values are reported for all analysis carried out with inclusion of trial 1 and with exclusion of trial 1 (ex. 1). All main and interaction effects are reported, as are degrees of freedom (df). Greenhouse-Geisser corrected.

MT

		df	F	p	df	F ex. 1	p ex. 1
2-way ANOVA	*Condition*	1, 10	75.7	< 0.001	1, 10	34.1	< 0.001
	Trial	1.3, 12.9	51.8	< 0.001	2.4, 24.2	11.2	< 0.001
	*Cond.*Trial*	1.3, 13.1	49.8	< 0.001	2.5, 25.1	10.7	< 0.001
Planned Comp.							
(Trials) TC	*Trials*	3.7, 37.2	1.8	0.15	7.7, 76.6	1.3	0.117
(Trials) TL	*Trials*	1.3, 12.9	51.2	< 0.001	2.4, 23.5	11.4	< 0.001

P3b

		df	F	p	df	F ex. 1	p ex. 1
2-way ANOVA	*Condition*	1, 10	35.5	< 0.001	1, 10	31.6	< 0.001
	Trial	7.2, 72.1	6.1	< 0.001	7, 70.3	2.8	< 0.05
	*Cond.*Trial*	6.1, 61.2	7.7	< 0.001	5.7, 56.8	4	< 0.005
Planned Comp.							
(Trials) TC	*Trials*	5.9, 59.4	0.7	0.63	5.9, 59.4	0.7	0.85
(Trials) TL	*Trials*	6.4, 63.8	12.5	< 0.001	6.2, 62.1	5.9	< 0.001

Alpha Power

		df	F	p	df	F ex. 1	p ex. 1
2-way ANOVA	*Condition*	1, 10	5.1	< 0.05	1, 10	5.2	< 0.05
	Trial	4.7, 47.2	7.5	< 0.001	4.9, 48.9	6.2	< 0.001
	*Cond.*Trial*	5.5, 54.6	1.5	0.187	5.4, 53.9	1.5	0.187
Planned Comp.							
(Trials) TC	*Trials*	5.1, 51.3	4.3	< 0.05	5, 50	2.9	< 0.05
(Trials) TL	*Trials*	4.8, 47.8	5.6	< 0.001	4.9, 49.2	5.1	< 0.001

5.3.2 Electrophysiological

Figure 5.3(a) depicts the group average ERPs for the TL condition and Figure 5.3(b) shows the corresponding ERPs for the TC condition. There was no visible change in P3b amplitude after the 5th trial in either condition, therefore trials 6-30 are plotted as a mean curve with standard error displayed. The topographical distribution of the P3b component for both experimental conditions was calculated over an 80 ms window from 310-390 ms post stimulus onset. Group average topographical distributions for the first 5 trials of each condition are displayed, Figure 5.3(c). P3b amplitude was calculated for each of the consecutive 30 trials for the TL and TC condition, as described in the materials and methods section. These P3b amplitudes and corresponding standard errors were plotted for each condition to illustrate the observed change in P3b amplitude over the experimental block, as shown in Figure 5.3(d). The 2 (Condition: TL, TC) $\times$ 30 (trial: 1 to 30) repeated measures ANOVA on the P3b amplitudes showed a significant effect of condition ($F(1, 10) = 35.5$, $p < 0.001$), a significant effect of trial ($F(7.2, 72.1) = 6.1$, $p < 0.001$) and a significant interaction of condition by trial ($F(6.1, 61.2) = 7.7$, $p < 0.001$). This main effect of condition shows that P3b amplitude is larger in the TL condition. Planned within condition one-way repeated measures comparisons demonstrated significant differences between trials for the TL condition ($F(6.4, 63.8) = 12.5$, $p < 0.001$) but not for the TC condition ($F(5.9, 59.4) = 0.7$, $p = 0.63$). Exclusion of trial 1 from the P3b amplitude ANOVA analysis did not alter the significance of the results; see Table 5.1. This analysis demonstrates that P3b amplitude decreases over trials in the TL condition but remains consistently non-existent in the TC condition.
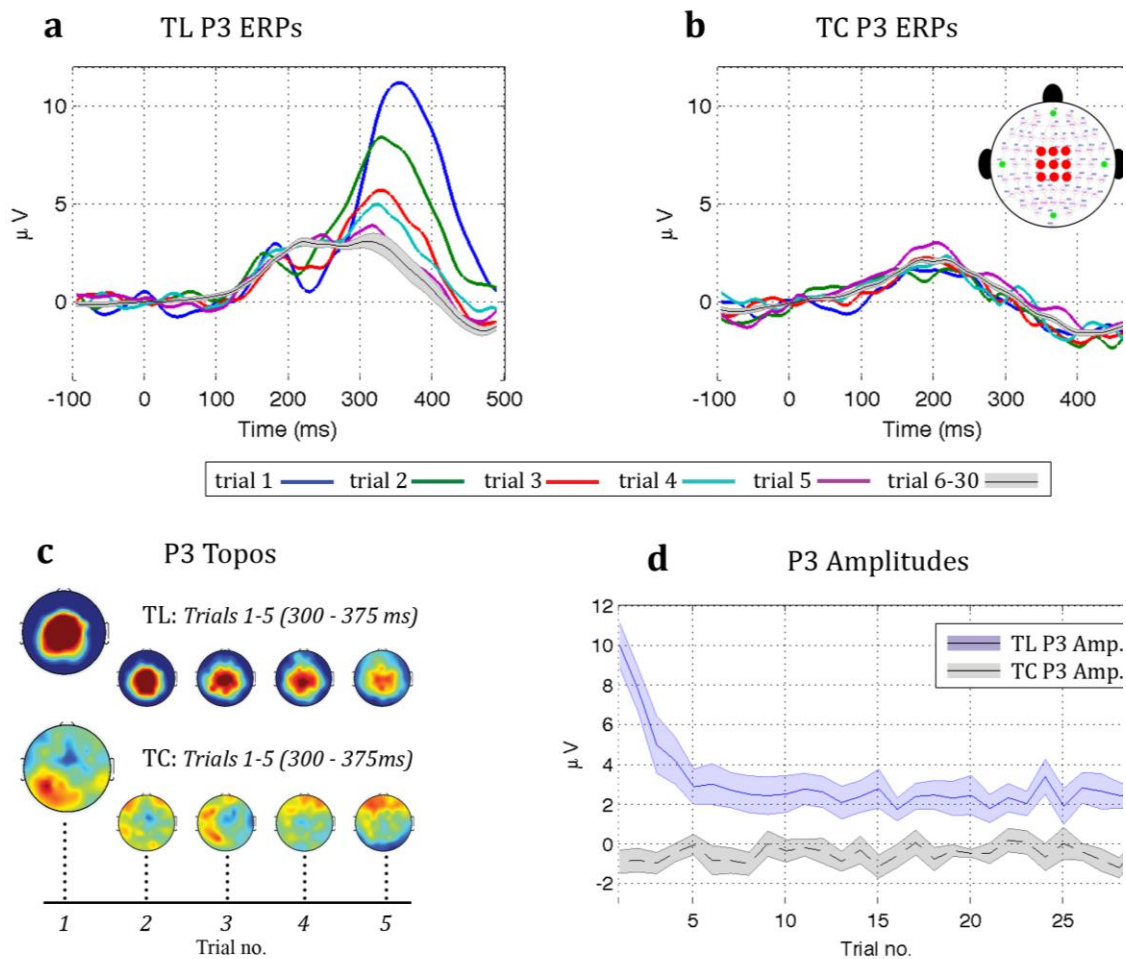
Figure 5-3

Panel A and B show the group average P3b responses for the Target Learning (TL) and Target Cued (TC) conditions respectively. In both cases, no change in amplitude was present after the 5th trial, for this reason the curves corresponding to trials 6-30 were plotted as a single mean with standard error indicated. Panel C contains a topographical distribution of the P3b component for the first 5 trials of the TL and TC conditions. This distribution was calculated over an 80 ms window from 310-390 ms post stimulus onset. Panel D illustrates the group average P3b amplitudes across all trials for the TL (blue) and TC (grey) conditions, shaded areas represent

In both the TL and TC conditions, an increasing trend in alpha power is observed over the course of the experimental block, as shown in Figure 5.4(a, b). A two (Condition: TL & TC) x 30 (trial: 1 to 30) repeated measures ANOVA revealed a significant effect of condition ($F_{(1, 10)} = 5.1$, $p < 0.05$), a significant effect of trial ($F_{(4.7, 47.2)} = 7.5$, $p < 0.001$) with no interaction effect ($F_{(5.5, 54.6)} = 1.5$, $p = 0.187$). This main effect of

condition represents that fact that alpha power seems to increase to its peak value at a faster rate in the TC condition, this is likely due to the lower attentional level required in this cued condition. Planned one-way ANOVA comparisons showed a significant effect of trial in both the TL condition ($F_{(5.1, 51.3)} = 4.3$, $p < 0.05$) and TC condition ($F_{(4.8, 47.8)} = 5.6$ $p < 0.001$). These results indicate that alpha power increases with trial number in both the TL and TC conditions. Exclusion of trial 1 from the alpha power ANOVA analysis did not alter the significance of these results; see Table 5.1. Correlation analysis of P3b amplitude and MT showed a significant relationship in the TL condition ($R = 0.85$, $p < 0.001$) with no significant relationship in the TC condition ($p = 0.828$). The correlation in the TL condition maintained with exclusion of trial 1 ($R = 0.95$, $p < 0.001$) while, again, no relationship was observed in the TC condition ($p = 0.14$). The positive correlation of P3b and MT in the TL task indicates that the amplitude of the P3b decreases with the reduction in MT. This relationship is not observed in the TC condition.
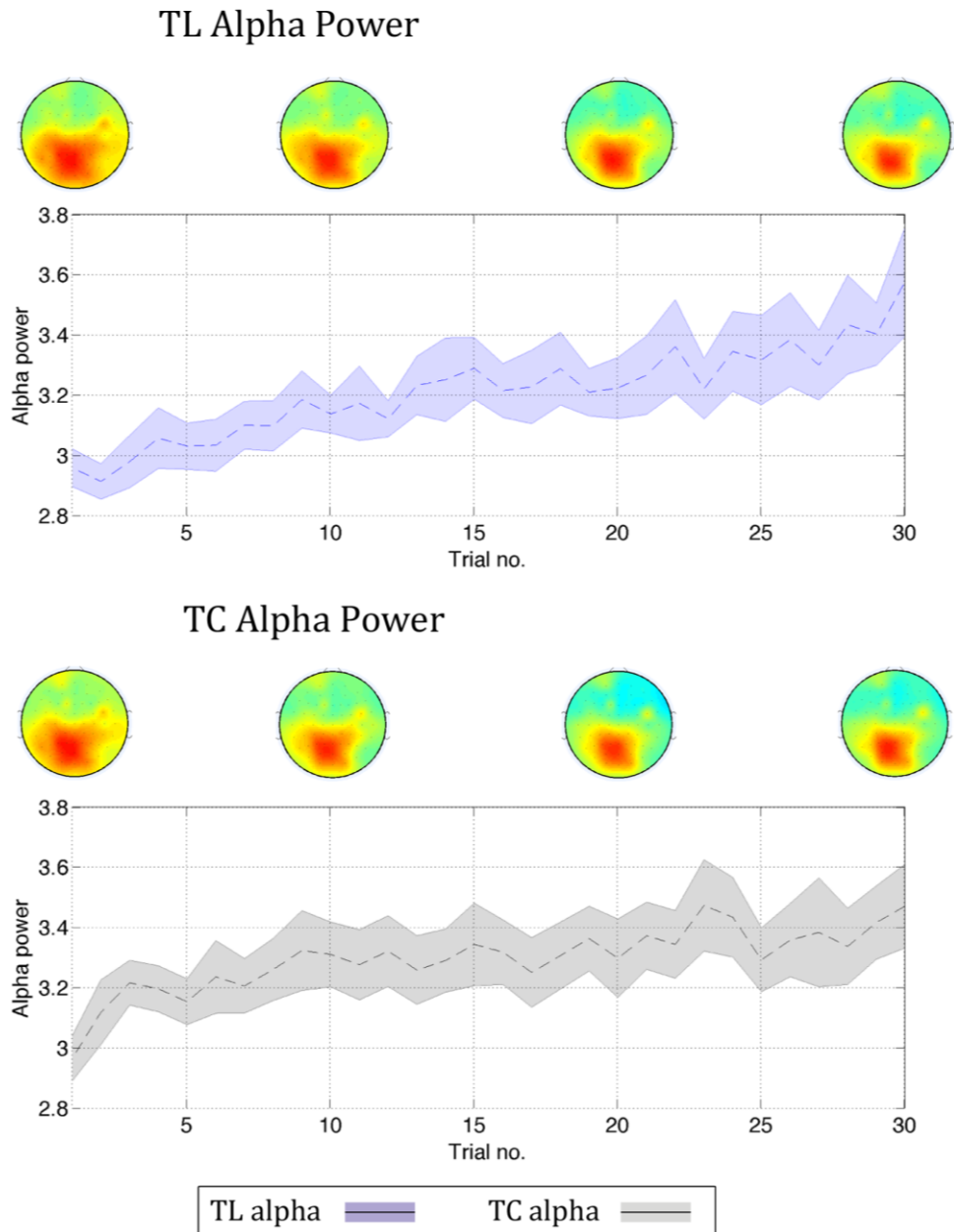
Figure 5-4

The figure contains alpha power plotted against trial number for the Target Learning (TL) and Target Cued (TC) experimental conditions, shaded areas represent standard error. A topographical plot of alpha power has been included for trials one, 10, 20 and 30. These plots highlight the increase in alpha power that occurs in both experimental conditions. The topographical plots also indicate that alpha power becomes more focal and left lateralised over
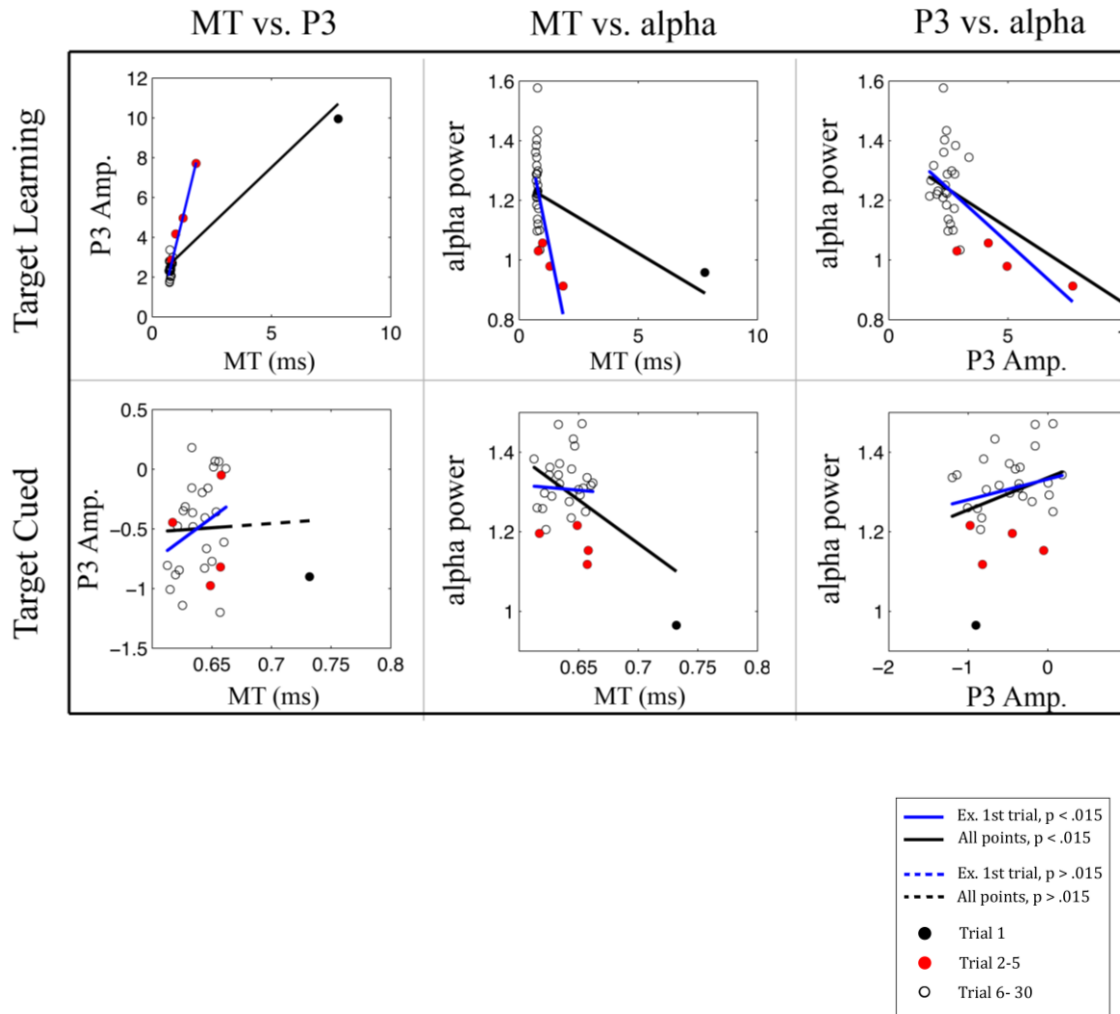
Figure 5-5

Scatter plots with line of best fit to illustrate all correlation analysis that was carried out at group mean level. Blue lines represent the fit with exclusion of data from trial 1; black lines illustrate the fit with all data points. Solid lines represent statistically significant correlations; dashed lines are used to indicate where no correlation was observed. The first trial on each plot is highlighted as a solid black point, trials 2-5 are indicated as a solid red point and all other trials are represented by a black annulus.

Alpha power was tested against MT to determine if it had any relationship with participant performance during the task. A relationship was observed between alpha power and MT for the TL experimental condition (R = -0.47, p < 0.015) while no significant relationship was seen in the TC condition (p = 0.14). Exclusion of the first trial did not alter the significance of the results; see Table 5.2. This negative correlation in the TL condition

indicates that alpha power increases with improvement in task performance as measured by decreasing MT.

To further probe the relationship between P3b amplitude and alpha power, a correlation analysis was carried out. At group mean level, the correlation analysis showed a significant relationship between these distinct electrophysiological parameters ($R = -0.67$, $p < 0.001$) in the TL experimental condition. No relationship was observed in the TC condition ($p = 0.15$). Exclusion of the first trial did not alter the significance of the results. A summary of these results is displayed in Table 5.2 and illustrated in Figure 5.5.

Table 5-2

A summary of correlation analysis results for Target Learning (TL) and Target Cued (TC) experimental conditions. Analysis was carried out for both experimental conditions with inclusion and exclusion of the first trial. Correlations between movement time (MT) and P3b amplitude, MT and alpha power and P3b amplitude and alpha power are included. F- and p-values are reported. (* $p < 0.015$, ** $p < 0.005$, *** $p < 0.001$).

	TL	TC	TL ex. 1st trial	TC ex. 1st trial
MT vs. P3b	$R = 0.85$	$R = 0.04$	$R = 0.95$	$R = 0.29$
	$p < .001$ ***	$p = 0.828$	$p < .001$ ***	$p = 0.14$
MT vs. alpha	$R = -0.47$	$R = -0.45$	$R = -0.63$	$R = 0.015$
	$p < .015$ *	$p = 0.14$	$p < .001$ ***	$p = 0.937$
P3b vs. alpha	$R = -0.64$	$R = 0.27$	$R = -0.6$	$R = 0.197$
	$p < .001$ ***	$p = 0.15$	$p < .001$ ***	$p = 0.305$

To test the reproducibility of P3b amplitude and alpha power, correlations were calculated at single participant level. The corresponding p-values are summarized in Figure 5.6 and Table 5.3. A significant relationship was observed between MT and P3b amplitude in 8 of the 11 participants in the TL condition, the remaining participants showed no relationship between MT and P3b amplitude. In the TC condition, no significant relationship was observed between MT and P3b amplitude. This result shows that the relationship between P3b amplitude and MT is highly reproducible at single participant level. A significant

144

relationship between MT and alpha power was observed in 6 participants in the TL condition. In the TC condition, there was only one significant relationship across participants. Finally, the reproducibility of the relationship between P3b amplitude and alpha power was tested. It was observed in the TL condition that this result was significant in 2 participants only. In the TC condition one significant relationship was observed. This result would suggest that the relationship between P3b and alpha is not highly reproducible at the single participant level.
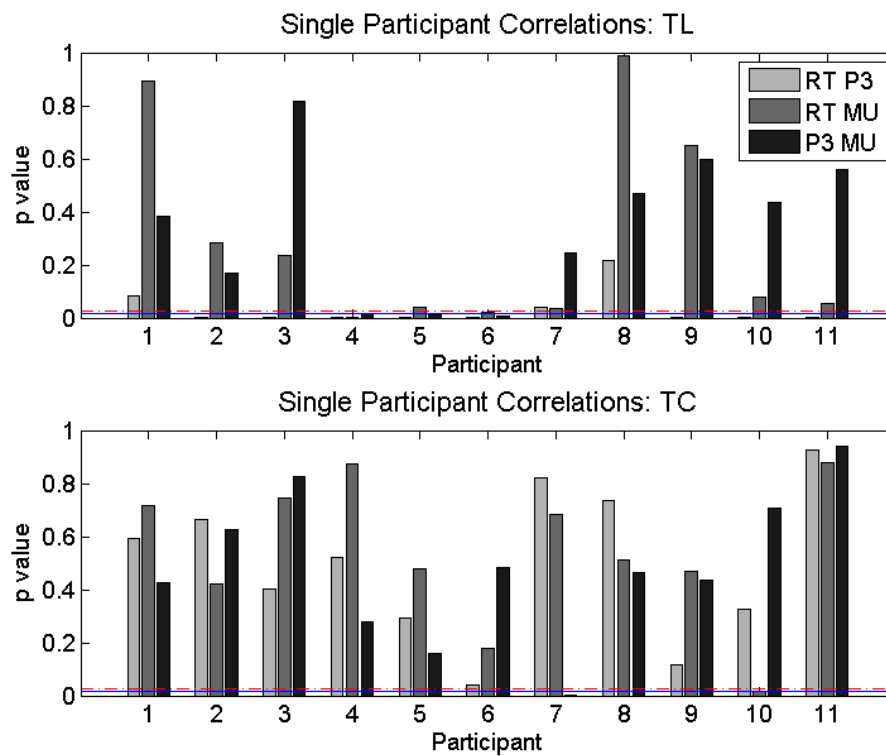
Figure 5-6

This figure shows the individual p-values that were calculated between P3 amplitude and movement time (MT), alpha power and MT and between P3 amplitude and alpha power. The solid blue line represents the significant threshold (p>0.015) while the dashed red line represents the trending threshold (p > 0.025).

Table 5-3

A summary of the single participant reproducibility analysis for Target Learning (TL) and Target Cued (TC) conditions. Significance has been defined as a p-value less than 0.015. Correlations between movement time (MT) and P3b amplitude, MT and alpha power and P3b amplitude and alpha power are reported. These results indicate a high level of reproducibility of P3b amplitude and alpha power analysis presented in the current study.

	Significant	Non-significant
TL: MT vs. P3b	8	3
TL: MT vs. alpha	6	5
TL: P3b vs. alpha	2	9
TC: MT vs. P3b	0	11
TC: MT vs. alpha	1	10
TC: P3b vs. alpha	1	10

5.4 Discussion

The work covered in this chapter was an investigated of electrophysiological and behavioural measures collected during visuospatial learning in a motor search task. Given the results presented above and the existing literature, it is hypothesised that the observed changes in task performance, as measured by movement time (MT), are influenced though a combination of visuospatial learning and automation of response. Furthermore, it is suggested that the observed changes in P3b amplitude primarily reflect a decreasing MT, rather than visuospatial learning directly. In this section the result and implications of this work will be discussed in addition to the application of this paradigm as a tool for investigating the basal ganglia loop in dystonia.

5.4.1 Movement times

MT was employed as a behavioural metric of task performance as is common place in visuospatial learning tasks (Stafford et al., 2012, Bednark et al., 2013, Thirkettle et al., 2013). Results show a significant decrease in MT across the first 5 trials in the TL condition,

no such change is visible in the TC. This decrease in MT represents a robust metric of visuospatial learning for the given task. In the TL condition MTs decrease to a low plateau, although they remain slower than that of the TC condition. It is hypothesized that the observed change in MT in the TL condition primarily represents the process of visuospatial learning, however, there may also be a secondary effect on performance due to automation of response. It is possible that the use of more sensitive metrics would allow these effects to be distinguished and this is an area which should be investigated during any future works.

5.4.2 P3b interpretation

Bednark et al. demonstrated that both MT and the amplitude of the P3b component decreased between the first and second half of this 30 trial experiment (Bednark et al., 2013). In the current study P3b amplitude was analysed at consecutive trial level across all 30 trials. This novel analytic approach facilitated a deeper investigation into the relationship between visuospatial learning and P3b amplitude. The current set of results reveal a strong relationship between P3b amplitude and MT in the TL condition, which is highly consistent with the results presented by Bednark and colleagues, however, examining these amplitudes at the consecutive trial level has facilitated a novel interpretation of this effect. An important property of the P3b component is that its amplitude is modulated by inter-stimulus intervals (ISI) (Gonsalvez and Polich, 2002, Steiner et al., 2014, Croft et al., 2003, Steiner et al., 2013, Polich, 2003). Given that MT directly equates to ISI in this task, it is possible that the observed decrease in P3b amplitude is an effect of the decreasing MT (and ISI). If the change in P3b amplitude is an effect of ISI, then this change could only be considered a secondary effect of visuospatial learning rather than a direct measure. Bednark et al. addressed this concern through inclusion of a third condition in which cursor movement did not elicit a stimulus but ISI was matched to the TL condition, i.e. movement $\neq$ outcome. In this condition, no relationship was observed between P3b amplitude and MT.

This result could suggest that the change in P3b is not a factor of ISI, however, it could also result from lowered participant engagement during a task where one's responses are meaningless and stimulus relevance has therefore been removed.

P3b amplitude is also modulated by stimulus relevance for a wide range of visual and auditory tasks (Sawaki and Katayama, 2006, Briggs and Martin, 2009). This property of the P3b may also have a role in the observed correlation. It is plausible that stimulus relevance is higher during the early stages of learning and decreases as the target location is learned and feedback is no longer required. This decrease in stimulus relevance during visuospatial learning could explain why a decrease in P3b amplitude is observed over the early trials of the TL condition. This mechanism would also explain why the TC condition failed to elicit a P3b: As the participant always knows the target location, the feedback stimulus is not relevant to task completion and would therefore not be expected to produce a P3b response.

Whether the change in P3b amplitude in the TL condition is a factor of ISI, decreasing stimulus relevance or a combination of the two, it has utility as an electrophysiological metric of task performance rather than a direct measure of visuospatial learning. While it is possible that the P3b component is reflecting visuospatial learning independently of ISI in the current task, the strength of the correlation observed here and the extensive literature on this point (Gonsalvez and Polich, 2002, Steiner et al., 2014, Croft et al., 2003, Steiner et al., 2013, Polich, 2003) reduce the plausibility of this hypothesis. This therefore implies that the P3b will not be a useful metric for assessing basal ganglia functional abnormalities in AOIFD.

5.4.3   Alpha power and learning

The current set of results show that in both the TL and TC condition of this task a significant increase in alpha power is observed across trials. Increases in alpha power during repetitive visual tasks can be explained by two distinct mechanisms. 1) Some studies suggest that increases in alpha power reflect a level in automation during repetitive tasks where it is possible for the participant to learn the required response (Jensen and Mazaheri, 2010, Bays et al., 2015). In such studies, increases in alpha power have been observed to correlate with improvements in performance. 2) On the other hand, when habituation of response is not possible, alpha power has been observed to increase with time-on-task and has been seen to correlate with reduced performance (Foxe et al., 2012). In both cases, it seems that alpha power tends to increase as attention levels decrease. As habituation of response is possible in the current paradigm and performance is not observed to decrease with increases is alpha, it is plausible that the increase observed here represents a level of automation of response and a reduced attention load over the experimental block. Alpha power has also been observed to undergo event related desynchronization in the time window of 400 – 700 ms post stimulus presentation (Wright et al., 2015, Makin et al., 2014, Klimesch et al., 2007). Given than the 500 ms pre-stimulus time window employed in the current study will overlap with this 400 – 700 ms time window from the previous trial in some cases, it is possible that the observed increases in alpha power could be impacted by a reduced level of event related desynchronization.

The fact that this result is present in both experimental conditions would suggest that this automation occurs in both the TL and TC condition. For this hypothesis to be accurate, differences observed between the TL and TC conditions for MT and P3b amplitude data must be explained by a process other than automation of response. This agrees with the previous hypothesis that those changes were a result of improved task performance, which

we suggested are primarily driven by visuospatial learning with automation of response as a smaller secondary factor. One limitation to this theory is that no correlation is observed between alpha power and MT in the TC condition, as would be expected under the given hypothesis. This may be explained by a lack of sensitivity of the performance metric MT.

This interpretation of decreasing alpha power gives alpha power utility as an independent measure of the automation that occurs during visuospatial and motor learning tasks. This metric may therefore be useful for assessing visuospatial learning in AOIFD. If visuospatial learning is negatively impacted by this basal ganglia disorder one may expect that this increase of alpha power would not occur. It is likely that MTs would still decrease, potentially at a slower rate, as participants would employ compensatory mechanisms to complete the task, however, true automation may not occur and therefor the increase in alpha power may be absent or reduced. This is an important question and one which needs to be addressed with future research.

5.4.4   *Electrophysiological and behavioural correlation analysis*

The correlation analysis for the TL condition revealed a significant relationship between alpha power and MT and between P3b amplitude and MT. No such relationship was observed in the TC condition. These results support the view that MT reflects an overall measurement of performance, which is affected by changes in visuospatial learning and automation of response. Furthermore, the results of the correlation analysis reveal that this change in alpha power is strongly related to the observed change in P3b amplitude in the TL condition at the group mean level. Given the hypothesis that the changes in P3b are driven by changes in MT, this correlation likely reflects the alpha-MT correlation rather than a separate relationship between P3b and alpha power. The results of the single participant correlation analysis reveal that the relationships between P3b amplitude and MT and alpha power and MT are both highly reproducible. The relationship between P3b and

alpha was not robust at this level, supporting the view that the correlation at group level was not meaningful. These results support the group average correlations and suggest that the current paradigm and proposed metrics have utility for research at a single participant level.

5.4.5 *Implications for basal ganglia function in AOIFD and future work*

The primary aim of this study was to develop a task which would allow basal ganglia function to be assessed in AOIFD to help further the hypothesis that AOIFD and abnormal temporal discrimination are caused by a disorder of the superior colliculus, a vital short latency input to this basal ganglia loop. This task was selected for a number of reasons. Visually responsive neurons in the intermediate and deep layers of the superior colliculus have direct dopaminergic projections to the ventral midbrain and are thought to play an important role in the visual reinforcement aspect of action-outcome learning (Dommett et al., 2005). For a participant to be efficient in the current task they must be aware of their cursor position at the exact time of target location. This point has been highlighted in studies which show that if timing of feedback stimulus is delayed, learning of target location is negatively affected. It is plausible that abnormally poor temporal discrimination abilities will have a similar effect in AOIFD and will therefore result in slower learning rates which should correlate with TDT abilities. There is also a deal of accumulating evidence that the basal ganglia is involved in the action selection process which is vital for being successful in the current task (Redgrave et al., 2011) (Schultz, 1998). This function of the basal ganglia offers a second mechanism by which a patient's abilities in the current task may be negatively affected.

By looking at MT in conjunction with P3b and alpha power at the consecutive trial level in a group of AOIFD patients, first degree relatives with and without abnormal temporal discrimination abilities and age matched controls researches will be able to answer many

key questions about visuospatial learning abilities in AOIFD. The first question would be whether visuospatial learning is slower in patients and first degree relatives with abnormal temporal discrimination than in healthy controls and relatives with normal temporal discrimination. If this is the case it would further the argument for TDT as a robust mediational endophenotype of AOIFD while also helping to validate the hypothesis that AOIFD is a disorder of the basal ganglia network. Given the conclusion drawn here that P3b is primarily reflecting ISI it is hypothesised that this will be maintained throughout all groups such that a strong correlation is maintained between MT and P3b amplitudes. Given the hypothesis that changes in alpha power reflect an aspect of automation of response under the current paradigm it is likely that this electrophysiological measure could be most informative in such a study. If visuospatial learning is indeed affected in patients and relatives with abnormal temporal discrimination it is likely this would be reflected by this proposed automation of response metric. If it was observed that alpha power did not increase over the block or increased at a significantly reduced rate it would imply that automation of response was not occurring in the same way that has been observed in controls.

5.5   Conclusion

The task presented here has many qualities that make it suitable for the study of visuospatial learning; it is repeatable without a learning effect, it provides an objective measure of performance, it is intuitive and engaging for participants and it is scalable in difficulty (Stafford et al., 2012). These qualities make it suitable for deployment in movement disorders studies such as Parkinson's disease or dystonia where participants have varying levels of motor control. The novel analysis presented here highlights how P3b amplitudes and alpha power can be assessed at a consecutive trial level and demonstrates the versatility of such tasks in visuospatial learning research.

In the current study, it has been demonstrated that performance in this visuospatial learning task, as measured by movement time, is highly correlated with both alpha power and P3b amplitude at a consecutive trial level. It is hypothesised here that the relationship between MT and P3b amplitude is driven by factors such as ISI and stimulus novelty rather than being a direct reflection of visuospatial learning. The hypothesis that alpha power could reflect an increasing level of automation in the given task is supported by the correlation between alpha power and MT in the TL condition but is hindered by the lack of correlation in the TC condition. It is possible that the use of a more sensitive behavioural measure would allow for more definitive conclusions on this point but further research is required to fully address this question. The analysis carried out here has shown that the data collected in this paradigm is robust enough to be analysed at a consecutive trial level. This novel analytic approach has allowed for a deeper understanding of the relationships between MT, P3b amplitudes and alpha power and has informed the hypotheses presented in the current work. Another important implication of this work is that the analysis presented by Bednark et al. (Bednark et al., 2013) could likely be carried out with less data, allowing for shorter recording sessions in clinical populations. This work has also demonstrated that this analysis is highly reproducible at a single participant level. This gives the current paradigm further utility in clinical populations where inter-participant variability may be inflated, and group mean analysis may not be appropriate.

6 Discussion

Dystonia is amongst the most common movement disorders and yet today we know comparatively little about it. Although we have developed several successful treatment strategies including physical therapies, deep brain stimulation and botulinum toxin injections, the underlying neuronal mechanisms and genetics remain a mystery. The studies carried here out here will help to address some of the unanswered questions surrounding the neurology involved in AOIFD and perhaps more importantly will endow future researchers with the tools and knowledge to answer many more.

A robust mediational endophenotype is an extremely useful tool for carrying out investigative research on disorders with poorly understood genetics and low penetrance levels such as AOIFD. Without such a marker, research would be restricted to control-patient comparisons and would be limited by additional confounds related to the manifestation of a movement disorder rather than being sensitive to those subtle changes in behaviour and response which can be informative of disorder mechanism. This is especially true for techniques such as fMRI, EEG, EOG and kinematics where unwanted movements can introduce noise and undermine many of the basic assumptions that modern statistical analysis techniques are built upon. Temporal discrimination, which describes our ability to detect asynchronicity between distinct effects in time, is widely accepted to represent a true mediational endophenotype of AOIFD and has facilitated much of the work carried out during this thesis and over the past decade of AOIFD research. The introduction of a mediational endophenotype allows for the comparison of uneffaced relatives with and without the endophenotype. This acts as a proxy for comparing two groups with and without a genetic abnormality, while also avoiding confounds introduced by abnormal movements in one of the groups.

A recent publication examining the existing literature surrounding AOIFD and abnormal temporal discrimination proposed a hypothesis that would adequately explain much of the

existing evidence (Hutchinson et al., 2013). This hypothesis states that abnormal temporal discrimination and cervical dystonia are caused by a disorder of the midbrain network for covert attentional orienting caused by reduced gamma-aminobutyric acid inhibition, resulting from undetermined genetic mutations. Such disinhibition is manifested in at least two ways: (1) subclinically, by abnormal temporal discrimination due to prolonged duration firing of the visual sensory neurons in the superficial laminae of the superior colliculus. (2) Clinically by AOIFD due to disinhibited burst activity of the cephalomotor neurons of the intermediate and deep laminae of the superior colliculus. It was the primary aim of the studies in this thesis to address this hypothesis by employing a combination of existing and novel neurological engineering techniques.

Attempting to address such a hypothesis in man is complicated by the size and the location of the superior colliculus. The superior colliculus is very small and located on the anterior section of the brain stem, adjacent to the internal carotid artery. This depth rules out direct investigation using EEG, and even MEG, which is generally capable or targeting deeper brain areas than EEG, would struggle given the small size and therefore small neuronal population of the superior colliculus. Unlike EEG and MEG, fMRI is not limited to cortical regions and with a voxel size of 2-3mm for a 3T scanner it is generally considered to have excellent spatial resolution. Saying this, a voxel size of 3 mm is still comparatively large given the superior colliculus is only about 6-7 mm in diameter. This relatively low spatial resolution certainly limits the ability of any current 3T fMRI studies from distinguishing between the superficial and deeper layers of the superior colliculus which would be required to fully address the current hypothesis. Cardiovascular noise which is introduced by the internal carotid artery also represents a significant problem when looking at the BOLD signal arising from the superior colliculus and adds a significant limitation to any fMRI work in this area.

These problems have shaped the content and the approach adopted in the studies proposed in this thesis and each experimental section can be thought of as a proposed solution which taken together aims to provide a significant level of evidence supporting the stated hypothesis. In the first section, fMRI was employed to investigate superior colliculus activation directly. This study involved overcoming some of the key problems which have been outlined here. The following studies investigated superior colliculus function by looking at behavioural outputs rather than attempting to image the structures directly. The first of these studies investigates head movements, eye movements and covert attention in a novel iteration of the classic Posner Paradigm. The final study involved the development of a visuospatial learning task in which both behavioural and electrophysiological objective measures were employed to track the process of visuospatial learning and automation of movement. The process of error detection is critical to visuospatial learning and known to involve the basal ganglia loop, in addition the task outlined here employed a feedback system which would be highly dependent on healthy superior colliculus function.

6.1   Looming responses in the superior colliculus

This study addressed several key research questions, as outlined in Chapter 2, by looking at BOLD signal responses of the superior colliculus to looming, receding and random visual stimulus. This study focused on first-degree relatives of cervical dystonia patients with normal and abnormal temporal discrimination. fMRI recordings were gathered from 36 relatives, 18 with normal temporal discrimination and 18 with abnormal temporal discrimination. These groups were age and gender matched to reduce unwanted variance in the BOLD signal.

It was initially unclear if a group level GLM analysis would be able to show superior colliculus activation given the relatively low resolution (compared to the size of the

superior colliculus) of the 3T scanner being employed for this study. To test this, the data from all subjects was initially grouped so an exploratory analysis of superior colliculus responses under the current paradigm could be carried out with the maximum possible statistical power. This analysis approach was very successful and showed activation in response to looming stimulus and several other contrasts including combinations of looming and receding stimulus. In addition, the contrast of looming vs. random stimulus produced a statistically significant activation of the bi-lateral superior colliculus. These results confirmed the applicability of the proposed paradigm for further analysis at the segmented group level.

The groups were then divided into normal and abnormal relatives and a similar GLM analysis was carried out. The results of this analysis showed significant and striking differences in superior colliculus responses between the two groups. Most notably, it was observed that responses in the abnormal relative groups were diminished when compared to the normal relative group for looming visual stimulus.

A DCM analysis was then employed to test the hypothesis that the putaminal abnormalities observed in abnormal relatives may be linked to the functional superior colliculus abnormalities that have been observed in the current study. A model of the covert attention circuit was developed and employed to test if inhibitory self-connections of the superior colliculus were related to abnormal temporal discrimination. This analysis supported the hypothesis that these putaminal and temporal discrimination abnormalities may be related to a GABAergic deficit in the superior colliculus. This is an area that should be investigated in more detail in future research.

This study has answered several important research questions and has generated others, these include:

- Further investigations of neural connectivity between the superior colliculus and the putamen. More complex DCM analysis could be carried out in healthy control subjects and in these normal/abnormal relative groups. Such studies could explore more complex circuitry and investigate the involvement of SNpc and the thalamus in the current paradigm.

- Other connectivity analysis could also be explored for the current dataset; these may include an investigation of structural connectivity using diffusion tensor imaging or other forms of effective connectivity analysis such as theoretical graph analysis.

- This investigation has been unable test if the proposed GABAergic abnormality is a global or local phenomenon. Future imaging studies, specifically magnetic resonance spectroscopy, should be able to confirm or dismiss the hypothesis of a GABAergic abnormality in AOIFD and be informative about the location(s) of such an abnormality.

- It is highly likely that data collected in the current study is effected by cardiovascular noise, especially near the internal carotid artery, as is the case for the superior colliculus. Future imaging studies would benefit from the inclusion of pulse oximetry during all scans. This would allow researchers to include hearth rate as a nuisance regressors and explain irrelevant variance in the BOLD signal. This addition would help to increase the statistical power of both the GLM and DCM analysis.

- The analysis presented in the current study has been hypothesis driven and has focused on activation of the superior colliculus and putamen. The current dataset may contain other key findings, further exploratory analysis of this dataset should be carried out to investigate other cortical, sub-cortical and connectivity abnormalities related to AOIFD and abnormal temporal discrimination.

6.2   Head kinematics, eye movements and orientation of attention

This study explored a novel method for investigating superior colliculus function in patients with AOIFD by examining some well-established behavioural outputs of the neural circuitry involved in orientation of covert attention. Two studies were carried out and the results of both have been detailed in Chapter 4. In the first study, the paradigm and proposed metrics were validated in several healthy control subjects. These studies highlighted the most relevant aspects of the paradigm and a more streamlined method was then employed for collecting data from AOIFD patients and aged matched controls. A custom micro-controller circuit enabled the head turn program to interface directly with a Bio-Semi electrophysiological recording system, this allowed for synchronous recording of EOG data which facilitated the head-eye onset validation work that was carried out here.

During the healthy control pilot study, several kinematic and eye-movement parameters were extracted from the data. Most of these parameters were extracted to show the versatility of the system and were not very informative given the healthy cohort. Of particular interest was the onset data for head and eye movements. First, the onset of eye movement confirmed the presence of a Posner effect under this novel iteration of the task. This was an important validation for the paradigm and enabled further analysis for head kinematic data. The presence of a Posner effect was then observed for the first time in onset of head movement.

A patient study was then carried out to compare healthy control subjects and cervical dystonia patients under the streamlined head turn paradigm. The fact that cervical dystonia is a movement disorder effecting the muscles of the neck introduced a significant limitation and reduces the salience of the intergroup comparisons. An inter-subject normalized Posner effect was calculated for each subject and analysis revealed that this effect was more than twice as large in patients as in healthy controls. It is difficult to determine if this result is

driven solely by the symptoms associated with cervical dystonia although a segmentation analysis looking at effected side in patients supports the idea that the increased Posner effect is not fully explained by manifestation of disorder.

Further research questions and work arising from the study described in Chapter 4:

- An investigation of Posner effect size in normal and abnormal relatives would be highly informative for the current hypothesis and should be carried out as the next logical progression of the work presented here.

- Previous work has shown age and sex related changes in temporal discrimination abilities in patients and in relatives with abnormal temporal discrimination. If similar changes are observed for Posner effect size it would support the argument that both abnormalities are caused by similar neural mechanisms.

- The patient data presented here was collected from patients who receive botulinum toxin injections as a treatment for cervical dystonia. A study investigating the effects of this treatment on Posner effect size would help to determine the role of symptom manifestation in the current results. Such a study would require recording from each patient in both the "ON" and "OFF" state of medication.

- Since the conception of the current paradigm, novel HMD devices have been developed with the added functionality of retinal eye tracking. Such a device would represent a significant upgrade over the EOG eye tracking used here, it would provide absolute eye position and pupilometry data and should be considered for future research.

- The generation of fast saccades are known to originate in the superior colliculus. It can be difficult to reliable generate fast saccades in an experimental context. It is possible that the immersive nature of the HMD may be of benefit in this regard. It is currently unclear if the new generation of HMD devices can record fast saccadic activity but this

area of research should be of interest to the current hypothesis regarding a GABAergic deficit in the superior colliculus and should be investigated further.

- The incorporation of EMG recordings in future studies would provide additional information about preparatory movement events which movement-based recordings cannot detect. The use of surface electrodes would provide limited information given the complex anatomy of the neck and so the use of needle electrodes should be considered.

6.3 Visuospatial learning and electrophysiological correlates

The study carried out in Chapter 5 was based on the same principal as the head turn experiment, that is, to investigate the function of the sub-cortical covert attention network by looking as a task known involve this circuit. The study detailed in Chapter 5 has focused on the development of a visuospatial learning paradigm and behavioural and electrophysiological metrics that should be sensitive to abnormalities in action acquisition that would arise from a GABAergic abnormality in the superior colliculus.

The paradigm employed in this study was adapted from Bednark et al. and the findings and analysis carried out in this section represent a significant extension of the original work. One of the primary aims of this study was to determine if the relationship between P3b amplitude and movement time observed by Bednark was relevant to visuospatial learning and thus determine if it would have utility as a metric in future AOIFD research. By investigating this relationship in greater detail at a single trial level it was possible to show that the correlation was most likely being driven by other aspects of the P3b component and was not providing additional information.

The role of alpha power during visuospatial learning was then investigated as an alternative electrophysiological parameter. Given the literature surrounding alpha power it was

expected that this frequency analysis may be informative about the role of automation of response during a motor-based visuospatial learning task. It was observed that alpha power increased at a consistent rate over the course of the block and the argument has been made that this slow increase may represent the automation process that occurs in visuospatial learning. These results suggest that additional and informative information can be gained from the inclusion of EEG in future visuospatial learning studies in an AOIFD cohort.

Further research questions and studies arising from the study described in Chapter 5:

- This study was carried out in a young control population for validation and testing purposes. The next research step would be to collect data from first degree relatives of AOIFD patients with and without abnormal temporal discrimination.

- If abnormal temporal discrimination is related to an abnormality of the covert attention circuit, then it is likely that these abnormal relatives will have reduced visuospatial learning abilities. Such an abnormality may not be detected by the movement time metric but it would likely be reflected by the alpha power analysis which has been outlined here.

- It is possible that other behavioural metrics could be employed to measure automation of response. For example, looking at repeatability and reliability of movement may provide researchers with such a tool. This could then be compared against alpha power and may be able to confirm the utility of alpha as a metric of automation of response.

- If abnormalities do exist in abnormal relatives, then it will be important to test for the same sex and age related changes that have been observed in temporal discrimination. Given that the same recommendation was made for the head turn work it may be prudent to carry out these studies in tandem.

- EEG is limited to cortical responses and so its usefulness for the current paradigm is also limited. It may be informative to carry out a simplified version of the current

paradigm in an fMRI based study. This would allow researchers to pinpoint sub cortical abnormalities under the current task.

6.4   Limitations of current study

There is no ideal neuroimaging method for investigating neural function. Methods like EEG, MEG and fMRI can provide us with information about population level events and more invasive methods like electrocorticography can observe the firing of single neurons. Attempting to understand the mechanisms involved in disorders like AOIFD will certainly require collaboration of many of these imperfect methods for the formation and elimination of different hypothesises. Section 6.4.1 will detail some of the practical limitations that have impacted the studies presented in this thesis.

6.4.1   Looming responses in the superior colliculus

- **Poor temporal and spatial resolution of fMRI.** fMRI is generally considered to have excellent spatial resolution and poor temporal resolution, however, given the largest diameter of the superior colliculus is 6-7 mm and the minimum voxel size available for the current study was 3 mm, both spatial and temporal resolution represent significant limitations for the current work. As the technology of fMRI advances the spatial resolution will continue to improve, the current generation of 9T scanners are proofing to be very capable for imaging the superior colliculus (Loureiro et al., 2017). However, the poor temporal resolution of the BOLD signal is a manifestation of human physiology and will always limit the questions that fMRI based analysis can answer.

- **Movement in scanner.** The time taken for a scanner to acquire 1 full scan coupled with the slow response of the BOLD signal means that any subject movement will result in a "blurring" of data, this is akin to the effects of long exposure times in photography. By estimating movement and including this in our models we can explain the variance

related to this unwanted movement, however, the effectiveness of this method will be reduced with movement size and frequency. This limitation may make the inclusion of AOIFD patients infeasible in future studies.

- **Stimulus presentation.** Due to the magnetic nature of fMRI, visual stimulus is presented via a mirror to a projected image outside the scanner. It can be difficult to ensure that all subjects experience a similar stimulus as misalignment of the mirror or differences in face size/shape may affect the image arriving at the retina. It is likely that a more immersive presentation method, such as the HMD device employed in Chapter 5, would improve BOLD responses, although this is not currently possible with available technology.

- **Lack of pulse oximetry.** It is difficult to determine the effects of cardiovascular noise in the current dataset but the literature would suggest the inclusion of pulse oximetry for superior colliculus fMRI work is recommended. Any variance in the BOLD signal arising from such noise is currently unaccounted for in the analysis presented in Chapter 4 and this may have a negatively impacted the observed results.

- **Loom recede results.** The literature surrounding the loom paradigm suggests that a functional difference should have been observed in the loom recede contrast, at least in the normal relative group. This was not observed in the current set of analysis; this may be related to any combination of the limitations that have been outlined above.

- **Significance in group level GLM.** During group level GLM analysis a significance level of $p = 0.001$ uncorrected was selected. This excludes a family wise error correction, the inclusion of which is generally considered best practise. Again, this may be related to any combination of the limitations relating to fMRI technology or the lack of heartrate data in the current study.

- **Model complexity in DCM.** The model that was developed and tested in the current DCM work is a significant simplification of the covert attention circuit that was examined in Chapter 2. This is an essential step for all DCM analysis as overly complex models would run into over-fitting issues and could take weeks to estimate. This simplification, while necessary, also reduce our ability to draw precise conclusions from our analysis. While the results reported here seem to support the current hypothesis, it is unlikely that a DCM approach could ever confirm such a hypothesis with a high degree of certainty.

6.4.2   Head kinematics, eye movements and orientation of attention

- **Use of EOG.** EOG was selected for eye-tracking because it could be used in conjunction with the HMD and no retinal eye-tracking products for in-HMD recording were available at the time. EOG has very good temporal resolution and so it was sufficient for detection of saccade onset. Drawbacks include its inability to record pupil size and absolute position, it is also subject to electrical noise and requires pre-processing and artefact detection.

- **Use of a proxy: covert attention.** The patient control study carried out here employed covert attention as a measure for the function of the covert attention circuit of interest. While an abnormality in this circuit would likely result in abnormal Posner cueing effect, it is not the only possible cause of such an abnormality. The results presented in this chapter do not contradict the current hypothesis but neither do they explicitly link AOIFD to the proposed covert circuit. The use of fMRI in future work may help to avoid this limitation.

- **Patient control comparison.** The most important result arising from this study, for the current hypothesis, is that the Posner effect was disproportionately large in patients compared to control subjects. While the evidence presented in this study supports the

argument that this is not an entirely an effect of disordered movement, it cannot state this conclusively. Further research must be carried out in normal and abnormal relatives to address this limitation.

- **Lack of EMG.** Movements of the head are generated by the activity of several neck muscles and the contribution of different muscles cannot easily be determined from gross head movements alone. Also, preparatory muscle activations, which are especially relevant during in-valid cues, are not observed in head movement data. The timing of such preparatory activity could be extremely informative for the current hypothesis given that they can arise from the superior colliculus.

- **Testing in the "OFF" state.** All patient recordings were collected prior to botulinum toxin injection and so data was collected in the "OFF" state of medication. It is beneficial that this factor was consistent across patients, however, this timing maximised the effect of disorder on the observed results. It has been proposed that future work should investigate the effects of botulinum toxin injection on Posner effect by testing patients at various stages of their medication cycle.

- **Lacking an objective measure of AOIFD severity.** One method that could be employed to show that the increased Posner effect is not a factor of disorder would be to test for a correlation between disorder severity and effect size. If a correlation existed, it would suggest that the increased effect was a factor of disorder manifestation rather than abnormal processing in the covert attention circuit. Unfortunately, an objective measure of disorder severity was not available for the current dataset.

6.4.3 *Visuospatial learning and electrophysiological correlates*

- **EEG is limited to cortical responses.** The current hypothesis is defined around an abnormality of a deep brain circuit which cannot be directly targeted using EEG. However, the brain is an extremely complex self-organising network and so

167

abnormalities in one area will likely result in abnormalities elsewhere. EEG was employed to detect cortical abnormalities arising from abnormal superior colliculus function. This limitation of EEG is still a significant limitation for applications in AOIFD research.

- **Alpha power as a measure of automation of response requires validation.** The evidence presented in this study supports the argument that increasing alpha power is reflecting automation of movement during the current paradigm and, therefore, this metric would likely reflect any abnormalities in superior colliculus function. However, given that there is no gold standard measurement for automation of motion under the current paradigm it is impossible to definitively conclude that the increase in alpha power is reflecting automation. It has been suggested that future research should explore additional behavioural metrics of automation which may help to address this limitation.

- **Use of a proxy – visuospatial learning.** This study employs metrics recorded during a visuospatial learning study as a proxy for testing the function of the covert attention circuit. As with the head turn work, any abnormalities that are observed in a patient or abnormal relative cohort will help to support the current hypothesis regarding a GABAergic abnormality in the superior colliculus. Unfortunately, abnormities in visuospatial learning could also arise from other neural mechanisms and so this test is not conclusive. The hope is that, taken together with other evidence, this test can help to advance our understanding of the neural mechanisms that cause AOIFD.

6.5   Conclusion

The primary objective of this thesis was to address the hypothesis that AOIFD and abnormal temporal discrimination are caused by a disorder of the midbrain network for covert orientation of attention, stemming from reduced GABA inhibition in the superficial

layers of the superior colliculus. It is unlikely that any single study or current method could fully address such a hypothesis and so it will likely be an accumulation of evidence, arising from a variety of research methods, which will ultimately validate or reject this hypothesis. This thesis presented three such studies. BOLD signals, arising from the superior colliculus of AOIFD relatives, support the hypothesis by highlighting an important link between superior colliculus functional activity and temporal discrimination. A disproportionately large Posner effect in patients with cervical dystonia would suggest an abnormality in covert attention processes, also supporting the current hypothesis. And finally, a novel paradigm and objective metrics of visuospatial learning will allow future researchers to test for additional abnormalities that may help to link AOIFD to a disordered midbrain network for covert attentional orienting.

References

ANASTASOPOULOS, D., ZIAVRA, N., HOLLANDS, M. & BRONSTEIN, A. 2009. Gaze displacement and inter-segmental coordination during large whole body voluntary rotations. *Exp Brain Res,* 193**,** 323-36.

ANASTASOPOULOS, D., ZIAVRA, N., PEARCE, R. & BRONSTEIN, A. M. 2013. Trunk bradykinesia and foveation delays during whole-body turns in spasmodic torticollis. *J Neurol,* 260**,** 2057-65.

ANASTASOPOULOS, D., ZIAVRA, N., SAVVIDOU, E., BAIN, P. & BRONSTEIN, A. M. 2011. Altered eye-to-foot coordination in standing parkinsonian patients during large gaze and whole-body reorientations. *Mov Disord,* 26**,** 2201-11.

ARTIEDA, J., PASTOR, M. A., LACRUZ, F. & OBESO, J. A. 1992. Temporal discrimination is abnormal in Parkinson's disease. *Brain,* 115 Pt 1**,** 199-210.

BATTERINK, L. J., REBER, P. J., NEVILLE, H. J. & PALLER, K. A. 2015. Implicit and explicit contributions to statistical learning. *J Mem Lang,* 83**,** 62-78.

BAYS, B. C., VISSCHER, K. M., LE DANTEC, C. C. & SEITZ, A. R. 2015. Alpha-band EEG activity in perceptual learning. *J Vis,* 15**,** 7.

BEDNARK, J. G., REYNOLDS, J. N., STAFFORD, T., REDGRAVE, P. & FRANZ, E. A. 2013. Creating a movement heuristic for voluntary action: electrophysiological correlates of movement-outcome learning. *Cortex,* 49**,** 771-80.

BILLINGTON, J., WILKIE, R. M., FIELD, D. T. & WANN, J. P. 2011. Neural processing of imminent collision in humans. *Proc Biol Sci,* 278**,** 1476-81.

BIZZI, E., KALIL, R. E. & TAGLIASCO, V. 1971. Eye-head coordination in monkeys: evidence for centrally patterned organization. *Science,* 173**,** 452-4.

BLACK, K. J., ONGUR, D. & PERLMUTTER, J. S. 1998. Putamen volume in idiopathic focal dystonia. *Neurology,* 51**,** 819-24.

BOLLIMUNTA, A., CHEN, Y., SCHROEDER, C. E. & DING, M. 2008. Neuronal mechanisms of cortical alpha oscillations in awake-behaving macaques. *J Neurosci,* 28**,** 9976-88.

BONNET, C. T., MORIO, C., SZAFFARCZYK, S. & ROUGIER, P. R. 2014. Postural mechanisms to control body displacements in the performance of lateral gaze shifts. *J Mot Behav,* 46, 397-405.

BOURQUE, J., LAKIS, N., CHAMPAGNE, J., STIP, E., LALONDE, P., LIPP, O. & MENDREK, A. 2013. Clozapine and visuospatial processing in treatment-resistant schizophrenia. *Cogn Neuropsychiatry,* 18, 615-30.

BRADLEY, D., WHELAN, R., KIMMICH, O., O'RIORDAN, S., MULROONEY, N., BRADY, P., WALSH, R., REILLY, R. B., HUTCHINSON, S., MOLLOY, F. & HUTCHINSON, M. 2012. Temporal discrimination thresholds in adult-onset primary torsion dystonia: an analysis by task type and by dystonia phenotype. *J Neurol,* 259, 77-82.

BRADLEY, D., WHELAN, R., WALSH, R., O'DWYER, J., REILLY, R., HUTCHINSON, S., MOLLOY, F. & HUTCHINSON, M. 2010. Comparing endophenotypes in adult-onset primary torsion dystonia. *Mov Disord,* 25, 84-90.

BRADLEY, D., WHELAN, R., WALSH, R., REILLY, R. B., HUTCHINSON, S., MOLLOY, F. & HUTCHINSON, M. 2009. Temporal discrimination threshold: VBM evidence for an endophenotype in adult onset primary torsion dystonia. *Brain,* 132, 2327-35.

BREMEN, P., VAN DER WILLIGEN, R. F., VAN WANROOIJ, M. M., SCHALING, D. F., MARTENS, M. B., VAN GROOTEL, T. J. & VAN OPSTAL, A. J. 2010. Applying double-magnetic induction to measure head-unrestrained gaze shifts: calibration and validation in monkey. *Biol Cybern,* 103, 415-32.

BRIGGS, K. E. & MARTIN, F. H. 2009. Affective picture processing and motivational relevance: arousal and valence effects on ERPs in an oddball task. *Int J Psychophysiol,* 72, 299-306.

BURBAUD, P., BONNET, B., GUEHL, D., LAGUENY, A. & BIOULAC, B. 1998. Movement disorders induced by gamma-aminobutyric agonist and antagonist injections into the internal globus pallidus and substantia nigra pars reticulata of the monkey. *Brain Res,* 780, 102-7.

BUTLER, A. G., DUFFEY, P. O., HAWTHORNE, M. R. & BARNES, M. P. 2004. An epidemiologic survey of dystonia within the entire population of northeast England over the past nine years. *Adv Neurol,* 94, 95-9.

BUTLER, J. S., MOLHOLM, S., FIEBELKORN, I. C., MERCIER, M. R., SCHWARTZ, T. H. & FOXE, J. J. 2011. Common or redundant neural circuits for duration processing across audition and touch. *J Neurosci,* 31, 3400-6.

BUTLER, J. S., MOLLOY, A., WILLIAMS, L., KIMMICH, O., QUINLIVAN, B., O'RIORDAN, S., HUTCHINSON, M. & REILLY, R. B. 2015. Non-parametric bootstrapping method for measuring the temporal discrimination threshold for movement disorders. *J Neural Eng,* 12, 046026.

CHAMINADE, T. & OKKA, M. M. 2013. Comparing the effect of humanoid and human face for the spatial orientation of attention. *Front Neurorobot,* 7, 12.

CHAN, J., BRIN, M. F. & FAHN, S. 1991. Idiopathic cervical dystonia: clinical characteristics. *Mov Disord,* 6, 119-26.

CHEN, L. L., LEE, D., FUKUSHIMA, K. & FUKUSHIMA, J. 2012. Submovement composition of head movement. *PLoS One,* 7, e47565.

COIZET, V., OVERTON, P. G. & REDGRAVE, P. 2007. Collateralization of the tectonigral projection with other major output pathways of superior colliculus in the rat. *J Comp Neurol,* 500, 1034-49.

COLLEWIJN, H. 1977. Eye- and head movements in freely moving rabbits. *J Physiol,* 266, 471-98.

CORNEIL, B. D. & MUNOZ, D. P. 2014. Overt responses during covert orienting. *Neuron,* 82, 1230-43.

CORNEIL, B. D., OLIVIER, E. & MUNOZ, D. P. 2004. Visual responses on neck muscles reveal selective gating that prevents express saccades. *Neuron,* 42, 831-41.

COURCHESNE, E., HILLYARD, S. A. & GALAMBOS, R. 1975. Stimulus novelty, task relevance and the visual evoked potential in man. *Electroencephalogr Clin Neurophysiol,* 39, 131-43.

CROFT, R. J., GONSALVEZ, C. J., GABRIEL, C. & BARRY, R. J. 2003. Target-to-target interval versus probability effects on P300 in one- and two-tone tasks. *Psychophysiology,* 40, 322-8.

DAUNIZEAU, J., DAVID, O. & STEPHAN, K. E. 2011. Dynamic causal modelling: a critical review of the biophysical and statistical foundations. *Neuroimage,* 58, 312-22.

DAWEL, A., PALERMO, R., O'KEARNEY, R., IRONS, J. & MCKONE, E. 2015. Fearful faces drive gaze-cueing and threat bias effects in children on the lookout for danger. *Dev Sci,* 18, 219-31.

DAYE, P. M. & ROBERTS, D. C. 2015. Vestibulo-ocular reflex suppression during head-fixed saccades reveals gaze feedback control. 35, 1192-8.

DELORME, A. & MAKEIG, S. 2004. EEGLAB: an open source toolbox for analysis of single-trial EEG dynamics including independent component analysis. *J Neurosci Methods,* 134, 9-21.

DOCKREE, P. M., KELLY, S. P., FOXE, J. J., REILLY, R. B. & ROBERTSON, I. H. 2007. Optimal sustained attention is linked to the spectral content of background EEG activity: greater ongoing tonic alpha (approximately 10 Hz) power supports successful phasic goal activation. *Eur J Neurosci,* 25, 900-7.

DOMMETT, E., COIZET, V., BLAHA, C. D., MARTINDALE, J., LEFEBVRE, V., WALTON, N., MAYHEW, J. E., OVERTON, P. G. & REDGRAVE, P. 2005. How visual stimuli activate dopaminergic neurons at short latency. *Science,* 307, 1476-9.

DRAGANSKI, B., SCHNEIDER, S. A., FIORIO, M., KLOPPEL, S., GAMBARIN, M., TINAZZI, M., ASHBURNER, J., BHATIA, K. P. & FRACKOWIAK, R. S. 2009. Genotype-phenotype interactions in primary dystonias revealed by differential changes in brain structure. *Neuroimage,* 47, 1141-7.

DUBINSKY, R. M., GRAY, C. S. & KOLLER, W. C. 1993. Essential tremor and dystonia. *Neurology,* 43, 2382-4.

DUJARDIN, K., BOURRIEZ, J. L. & GUIEU, J. D. 1995. Event-related desynchronization (ERD) patterns during memory processes: effects of aging and task difficulty. *Electroencephalogr Clin Neurophysiol,* 96, 169-82.

DUNCAN-JOHNSON, C. C. & DONCHIN, E. 1977. On quantifying surprise: the variation of event-related potentials with subjective probability. *Psychophysiology,* 14, 456-67.

DYBDAL, D., FORCELLI, P. A., DUBACH, M., OPPEDISANO, M., HOLMES, A., MALKOVA, L. & GALE, K. 2013. Topography of dyskinesias and torticollis evoked by inhibition of substantia nigra pars reticulata. *Mov Disord,* 28, 460-8.

ENDO, T., YANAGAWA, Y., OBATA, K. & ISA, T. 2005. Nicotinic acetylcholine receptor subtypes involved in facilitation of GABAergic inhibition in mouse superficial superior colliculus. *J Neurophysiol,* 94, 3893-902.

ERGENOGLU, T., DEMIRALP, T., BAYRAKTAROGLU, Z., ERGEN, M., BEYDAGI, H. & URESIN, Y. 2004. Alpha rhythm of the EEG modulates visual detection performance in humans. *Brain Res Cogn Brain Res,* 20, 376-83.

ETGEN, T., MUHLAU, M., GASER, C. & SANDER, D. 2006. Bilateral grey-matter increase in the putamen in primary blepharospasm. *J Neurol Neurosurg Psychiatry,* 77, 1017-20.

ETHIER, A. A., MUCKLE, G., JACOBSON, S. W., AYOTTE, P., JACOBSON, J. L. & SAINT-AMOUR, D. 2015. Assessing new dimensions of attentional functions in children prenatally exposed to environmental contaminants using an adapted Posner paradigm. *Neurotoxicol Teratol,* 51, 27-34.

FAHN, S. 1984. The varied clinical expressions of dystonia. *Neurol Clin,* 2, 541-54.

FAHN, S. 1988. Concept and classification of dystonia. *Adv Neurol,* 50, 1-8.

FAHN, S., BRESSMAN, S. B. & MARSDEN, C. D. 1998. Classification of dystonia. *Adv Neurol,* 78, 1-10.

FAN, J., GU, X., GUISE, K. G., LIU, X., FOSSELLA, J., WANG, H. & POSNER, M. I. 2009. Testing the behavioral interaction and integration of attentional networks. *Brain Cogn,* 70, 209-20.

FELDMANN-WUSTEFELD, T. & SCHUBO, A. 2013. Textures shape the attentional focus: evidence from exogenous and endogenous cueing. *Atten Percept Psychophys,* 75, 1644-66.

FELSEN, G. & MAINEN, Z. F. 2012. Midbrain contributions to sensorimotor decision making. *J Neurophysiol,* 108, 135-47.

FIORIO, M., GAMBARIN, M., VALENTE, E. M., LIBERINI, P., LOI, M., COSSU, G., MORETTO, G., BHATIA, K. P., DEFAZIO, G., AGLIOTI, S. M., FIASCHI, A. & TINAZZI, M. 2007. Defective temporal processing of sensory stimuli in DYT1 mutation carriers: a new endophenotype of dystonia? *Brain,* 130, 134-42.

FOXE, J. J., MORIE, K. P., LAUD, P. J., ROWSON, M. J., DE BRUIN, E. A. & KELLY, S. P. 2012. Assessing the effects of caffeine and theanine on the maintenance of vigilance during a sustained attention task. *Neuropharmacology,* 62, 2320-7.

FREEDMAN, E. G. & SPARKS, D. L. 1997. Activity of cells in the deeper layers of the superior colliculus of the rhesus monkey: evidence for a gaze displacement command. *J Neurophysiol,* 78, 1669-90.

FRIMA, N., NASIR, J. & GRUNEWALD, R. A. 2008. Abnormal vibration-induced illusion of movement in idiopathic focal dystonia: an endophenotypic marker? *Mov Disord,* 23, 373-7.

FRISTON, K. J. 2011. Functional and effective connectivity: a review. *Brain Connect,* 1, 13-36.

FRISTON, K. J., HARRISON, L. & PENNY, W. 2003. Dynamic causal modelling. *Neuroimage,* 19, 1273-302.

FRISTON, K. J., STEPHAN, K. M. & FRACKOWIAK, R. S. 1997. Transient phase-locking and dynamic correlations: Are they the same thing? *Hum Brain Mapp,* 5, 48-57.

GERSTEIN, G. L. & PERKEL, D. H. 1969. Simultaneously recorded trains of action potentials: analysis and functional interpretation. *Science,* 164, 828-30.

GONSALVEZ, C. L. & POLICH, J. 2002. P300 amplitude is determined by target-to-target interval. *Psychophysiology,* 39, 388-96.

GRANERT, O., PELLER, M., JABUSCH, H. C., ALTENMULLER, E. & SIEBNER, H. R. 2011. Sensorimotor skills and focal dystonia are linked to putaminal grey-matter volume in pianists. *J Neurol Neurosurg Psychiatry,* 82, 1225-31.

GUNDERSEN, H. J. 1992. Stereology: the fast lane between neuroanatomy and brain function--or still only a tightrope? *Acta Neurol Scand Suppl,* 137, 8-13.

HARRISON, L., PENNY, W. D. & FRISTON, K. 2003. Multivariate autoregressive modeling of fMRI time series. *Neuroimage,* 19, 1477-91.

HENTSCHEL, F., DRESSLER, D., ABELE, M. & PAUS, S. 2017. Impaired heart rate variability in cervical dystonia is associated to depression. 124, 245-251.

HOLLANDS, M. A., ZIAVRA, N. V. & BRONSTEIN, A. M. 2004. A new paradigm to investigate the roles of head and eye movements in the coordination of whole-body movements. *Exp Brain Res,* 154, 261-6.

HOLLINGWORTH, A., MATSUKURA, M. & LUCK, S. J. 2013. Visual working memory modulates low-level saccade target selection: evidence from rapidly generated saccades in the global effect paradigm. *J Vis,* 13, 4.

HOLMES, A. L., FORCELLI, P. A., DESJARDIN, J. T., DECKER, A. L., TEFERRA, M., WEST, E. A., MALKOVA, L. & GALE, K. 2012. Superior colliculus mediates cervical dystonia evoked by inhibition of the substantia nigra pars reticulata. *J Neurosci,* 32, 13326-32.

HUANG, Y. F., TAN, E. G., SOON, C. S. & HSIEH, P. J. 2014. Unconscious cues bias first saccades in a free-saccade task. *Conscious Cogn,* 29, 48-55.

HUTCHINSON, M., ISA, T., MOLLOY, A., KIMMICH, O., WILLIAMS, L., MOLLOY, F., MOORE, H., HEALY, D. G., LYNCH, T., WALSH, C., BUTLER, J., REILLY, R. B., WALSH, R. & O'RIORDAN, S. 2014. Cervical dystonia: a disorder of the midbrain network for covert attentional orienting. *Front Neurol,* 5, 54.

HUTCHINSON, M., KIMMICH, O., MOLLOY, A., WHELAN, R., MOLLOY, F., LYNCH, T., HEALY, D. G., WALSH, C., EDWARDS, M. J., OZELIUS, L., REILLY, R. B. & O'RIORDAN, S. 2013. The endophenotype and the phenotype: temporal discrimination and adult-onset dystonia. *Mov Disord,* 28, 1766-74.

ISREAL, J. B., CHESNEY, G. L., WICKENS, C. D. & DONCHIN, E. 1980. P300 and tracking difficulty: evidence for multiple resources in dual-task performance. *Psychophysiology,* 17, 259-73.

JANKOVIC, J., LEDER, S., WARNER, D. & SCHWARTZ, K. 1991. Cervical dystonia: clinical findings and associated movement disorders. *Neurology,* 41, 1088-91.

JANSEN, B. H., ZOURIDAKIS, G. & BRANDT, M. E. 1993. A neurophysiologically-based mathematical model of flash visual evoked potentials. *Biol Cybern,* 68, 275-83.

JENSEN, O. & MAZAHERI, A. 2010. Shaping functional architecture by oscillatory alpha activity: gating by inhibition. *Front Hum Neurosci,* 4, 186.

JOHANNESSON, O. I., ASGEIRSSON, A. G. & KRISTJANSSON, A. 2012. Saccade performance in the nasal and temporal hemifields. *Exp Brain Res,* 219, 107-20.

JOHNEN, A., WAGNER, H. & GAESE, B. H. 2001. Spatial attention modulates sound localization in barn owls. *J Neurophysiol,* 85, 1009-12.

JOHNSON, K. N., CONTURE, E. G. & WALDEN, T. A. 2012. Efficacy of attention regulation in preschool-age children who stutter: a preliminary investigation. *J Commun Disord,* 45, 263-78.

JOHNSON, R., JR. 1986. A triarchic model of P300 amplitude. *Psychophysiology,* 23, 367-84.

JONGSMA, M. L., EICHELE, T., VAN RIJN, C. M., COENEN, A. M., HUGDAHL, K., NORDBY, H. & QUIROGA, R. Q. 2006. Tracking pattern learning with single-trial event-related potentials. *Clin Neurophysiol,* 117, 1957-73.

JOST, W. H. & TATU, L. 2015. Selection of Muscles for Botulinum Toxin Injections in Cervical Dystonia. *Movement Disorders Clinical Practice,* 2, 224-226.

KANEDA, K. & ISA, T. 2013. GABAergic mechanisms for shaping transient visual responses in the mouse superior colliculus. *Neuroscience,* 235, 129-40.

KETTLER, L. & WAGNER, H. 2014. Influence of double stimulation on sound-localization behavior in barn owls. *J Comp Physiol A Neuroethol Sens Neural Behav Physiol,* 200, 1033-44.

KIMMICH, O., BRADLEY, D., WHELAN, R., MULROONEY, N., REILLY, R. B., HUTCHINSON, S., O'RIORDAN, S. & HUTCHINSON, M. 2011. Sporadic adult onset primary torsion dystonia is a genetic disorder by the temporal discrimination test. *Brain,* 134, 2656-63.

KIMMICH, O., MOLLOY, A., WHELAN, R., WILLIAMS, L., BRADLEY, D., BALSTERS, J., MOLLOY, F., LYNCH, T., HEALY, D. G., WALSH, C., O'RIORDAN, S., REILLY, R. B. & HUTCHINSON, M. 2014. Temporal discrimination, a cervical dystonia endophenotype: Penetrance and functional correlates. *Mov Disord*.

KLIMESCH, W., SAUSENG, P. & HANSLMAYR, S. 2007. EEG alpha oscillations: the inhibition-timing hypothesis. *Brain Res Rev,* 53, 63-88.

LACRUZ, F., ARTIEDA, J., PASTOR, M. A. & OBESO, J. A. 1991. The anatomical basis of somaesthetic temporal discrimination in humans. *J Neurol Neurosurg Psychiatry,* 54, 1077-81.

LANGLEY, L. K., FRIESEN, C. K., SAVILLE, A. L. & CIERNIA, A. T. 2011. Timing of reflexive visuospatial orienting in young, young-old, and old-old adults. *Atten Percept Psychophys,* 73, 1546-61.

LEE, M. S., KIM, H. S. & LYOO, C. H. 2005. "Off" gait freezing and temporal discrimination threshold in patients with Parkinson disease. *Neurology,* 64, 670-4.

LEEK, E. C., KERAI, J. H., JOHNSTON, S. J., HINDLE, J. V. & BRACEWELL, R. M. 2014. Impaired visuospatial transformation but intact sequence processing in Parkinson disease. *Cogn Behav Neurol,* 27, 130-8.

LESTIENNE, F. G. & THULLIER, F. 1998. Performance of visually triggered wrist movements task in monkey: an application of information theory to evaluate deficits following unilateral substantia nigra pars reticulata lesion. *Neurosci Lett,* 251, 177-80.

LETTIERI, C., RINALDO, S., DEVIGILI, G., PISA, F., MUCCHIUT, M., BELGRADO, E., MONDANI, M., D'AURIA, S., IUS, T., SKRAP, M. & ELEOPRA, R. 2015. Clinical outcome of deep brain stimulation for dystonia: constant-current or constant-voltage stimulation? A non-randomized study. *Eur J Neurol,* 22, 919-26.

LEUBE, B., KESSLER, K. R., GOECKE, T., AUBURGER, G. & BENECKE, R. 1997. Frequency of familial inheritance among 488 index patients with idiopathic focal dystonia and clinical variability in a large family. *Mov Disord,* 12**,** 1000-6.

LEUE, A. & BEAUDUCEL, A. 2015. Effects of injustice sensitivity and sex on the P3 amplitude during deception. *Biol Psychol,* 109**,** 29-36.

LINDIN, M., ZURRON, M. & DIAZ, F. 2004. Changes in P300 amplitude during an active standard auditory oddball task. *Biol Psychol,* 66**,** 153-67.

LOPEZ, S. G., FUSTER, J. I., REYES, M. M., COLLAZO, T. M., QUINONES, R. M., BERAZAIN, A. R., RODRIGUEZ, M. A., DIAS DE VILLARVILLA, T., BOBES, M. A. & VALDES-SOSA, M. 2011. Attentional network task in schizophrenic patients and theirs unaffected first degree relatives: a potential endofenotype. *Actas Esp Psiquiatr,* 39**,** 32-44.

LOUREIRO, J. R., HAGBERG, G. E., ETHOFER, T., ERB, M., BAUSE, J., EHSES, P., SCHEFFLER, K. & HIMMELBACH, M. 2017. Depth-dependence of visual signals in the human superior colliculus at 9.4 T. *Hum Brain Mapp,* 38**,** 574-587.

LYOO, C. H., LEE, S. Y., SONG, T. J. & LEE, M. S. 2007. Abnormal temporal discrimination threshold in patients with multiple system atrophy. *Mov Disord,* 22**,** 556-9.

MAKIN, A. D., RAMPONE, G., WRIGHT, A., MARTINOVIC, J. & BERTAMINI, M. 2014. Visual symmetry in objects and gaps. *J Vis,* 14**,** 12.

MARSDEN, C. D. 1976. Dystonia: the spectrum of the disease. *Res Publ Assoc Res Nerv Ment Dis,* 55**,** 351-67.

MATSUMOTO, N., MINAMIMOTO, T., GRAYBIEL, A. M. & KIMURA, M. 2001. Neurons in the thalamic CM-Pf complex supply striatal neurons with information about behaviorally significant sensory events. *J Neurophysiol,* 85**,** 960-76.

MCGRATH, J., JOHNSON, K., ECKER, C., O'HANLON, E., GILL, M., GALLAGHER, L. & GARAVAN, H. 2012. Atypical visuospatial processing in autism: insights from functional connectivity analysis. *Autism Res,* 5**,** 314-30.

MCGRATH, J., JOHNSON, K., O'HANLON, E., GARAVAN, H., LEEMANS, A. & GALLAGHER, L. 2013. Abnormal functional connectivity during visuospatial processing is associated with disrupted organisation of white matter in autism. *Front Hum Neurosci,* 7**,** 434.

MCINTOSH, A. R. 2000. Towards a network theory of cognition. *Neural Netw,* 13**,** 861-70.

MICHEL, C. M., MURRAY, M. M., LANTZ, G., GONZALEZ, S., SPINELLI, L. & GRAVE DE PERALTA, R. 2004. EEG source imaging. *Clin Neurophysiol,* 115**,** 2195-222.

MINK, J. W. 2003. The Basal Ganglia and involuntary movements: impaired inhibition of competing motor patterns. *Arch Neurol,* 60**,** 1365-8.

MOLLOY, A., KIMMICH, O., WILLIAMS, L., BUTLER, J. S., BYRNE, N., MOLLOY, F., MOORE, H., HEALY, D. G., LYNCH, T., EDWARDS, M. J., WALSH, C., REILLY, R. B., O'RIORDAN, S. & HUTCHINSON, M. 2014a. An evaluation of the role of environmental factors in the disease penetrance of cervical dystonia. *J Neurol Neurosurg Psychiatry*.

MOLLOY, A., KIMMICH, O., WILLIAMS, L., QUINLIVAN, B., DABACAN, A., FANNING, A., BUTLER, J. S., O'RIORDAN, S., REILLY, R. B. & HUTCHINSON, M. 2014b. A headset method for measuring the visual temporal discrimination threshold in cervical dystonia. *Tremor Other Hyperkinet Mov (N Y),* 4**,** 249.

MOLLOY, F. M., CARR, T. D., ZEUNER, K. E., DAMBROSIA, J. M. & HALLETT, M. 2003. Abnormalities of spatial discrimination in focal and generalized dystonia. *Brain,* 126**,** 2175-82.

NANTEL, J., MCDONALD, J. C., TAN, S. & BRONTE-STEWART, H. 2012. Deficits in visuospatial processing contribute to quantitative measures of freezing of gait in Parkinson's disease. *Neuroscience,* 221**,** 151-6.

NUNEZ, P. L. & SRINIVASAN, R. 2006. *Electric fields of the brain: the neurophysics of EEG*, Oxford university press.

O'DWYER, J. P., O'RIORDAN, S., SAUNDERS-PULLMAN, R., BRESSMAN, S. B., MOLLOY, F., LYNCH, T. & HUTCHINSON, M. 2005. Sensory abnormalities in unaffected relatives in familial adult-onset dystonia. *Neurology,* 65, 938-40.

OPPENHEIM, H. 1911. Über eine eigenartige Krampfkrankheit des kindlichen und jugendlichen Alters (Dysbasia lordotica progressiva, Dystonia musculorum deformans). *Neurologische Centralblatt,* 30, 1090-107.

PAL, P. K., SAMII, A., SCHULZER, M., MAK, E. & TSUI, J. K. 2000. Head tremor in cervical dystonia. *Can J Neurol Sci,* 27, 137-42.

PASSINGHAM, R. E., STEPHAN, K. E. & KOTTER, R. 2002. The anatomical basis of functional localization in the cortex. *Nat Rev Neurosci,* 3, 606-16.

PASTOR, M. A., DAY, B. L., MACALUSO, E., FRISTON, K. J. & FRACKOWIAK, R. S. 2004. The functional neuroanatomy of temporal discrimination. *J Neurosci,* 24, 2585-91.

POLICH, J. 2003. *Theoretical overview of P3a and P3b,* Detection of Change: Event-Related Potential and fMRI Findings, Kluwer Academic Press.

POLICH, J. 2007. Updating P300: an integrative theory of P3a and P3b. *Clin Neurophysiol,* 118, 2128-48.

POSNER, M. I. 1980. Orienting of attention. *Q J Exp Psychol,* 32, 3-25.

REDGRAVE, P., COIZET, V., COMOLI, E., MCHAFFIE, J. G., LERICHE, M., VAUTRELLE, N., HAYES, L. M. & OVERTON, P. 2010. Interactions between the Midbrain Superior Colliculus and the Basal Ganglia. *Front Neuroanat,* 4.

REDGRAVE, P., VAUTRELLE, N. & REYNOLDS, J. N. 2011. Functional properties of the basal ganglia's re-entrant loop architecture: selection and reinforcement. *Neuroscience,* 198, 138-51.

REUTER, B., MOLLERS, D., BENDER, J., SCHWEHN, A., ZIEMEK, J., GALLINAT, J. & KATHMANN, N. 2011. Volitional saccades and attentional mechanisms in schizophrenia patients and healthy control subjects. *Psychophysiology,* 48, 1333-9.

RIETH, C. A. & HUBER, D. E. 2013. Implicit learning of spatiotemporal contingencies in spatial cueing. *J Exp Psychol Hum Percept Perform,* 39, 1165-80.

ROALF, D., LOWERY, N. & TURETSKY, B. I. 2006. Behavioral and physiological findings of gender differences in global-local visual processing. *Brain Cogn,* 60, 32-42.

SAILER, U., FISCHMEISTER, F. P. & BAUER, H. 2010. Effects of learning on feedback-related brain potentials in a decision-making task. *Brain Res,* 1342, 85-93.

SAWAKI, R. & KATAYAMA, J. 2006. Stimulus context determines whether non-target stimuli are processed as task-relevant or distractor information. *Clin Neurophysiol,* 117, 2532-9.

SCHARLI, A. M., VAN DE LANGENBERG, R., MURER, K. & MULLER, R. M. 2013. Postural control and head stability during natural gaze behaviour in 6- to 12-year-old children. *Exp Brain Res,* 227, 523-34.

SCHULTZ, W. 1998. Predictive reward signal of dopamine neurons. *J Neurophysiol,* 80, 1-27.

SHAIKH, A. G., WONG, A., ZEE, D. S. & JINNAH, H. A. 2015a. Why are voluntary head movements in cervical dystonia slow? *Parkinsonism Relat Disord,* 21, 561-6.

SHAIKH, A. G., WONG, A. L., ZEE, D. S. & JINNAH, H. A. 2013. Keeping your head on target. *J Neurosci,* 33, 11281-95.

SHAIKH, A. G., ZEE, D. S. & JINNAH, H. A. 2015b. Oscillatory head movements in cervical dystonia: Dystonia, tremor, or both? *Mov Disord,* 30, 834-42.

SKLAVOS, S., ANASTASOPOULOS, D. & BRONSTEIN, A. 2010. Kinematic redundancy and variance of eye, head and trunk displacements during large horizontal gaze reorientations in standing humans. *Exp Brain Res,* 202, 879-90.

SNYDER, A. C. & FOXE, J. J. 2010. Anticipatory attentional suppression of visual features indexed by oscillatory alpha-band power increases: a high-density electrical mapping study. *J Neurosci,* 30, 4024-32.

STAFFORD, T., THIRKETTLE, M., WALTON, T., VAUTRELLE, N., HETHERINGTON, L., PORT, M., GURNEY, K. & REDGRAVE, P. 2012. A novel task for the investigation of action acquisition. *PLoS One,* 7, e37749.

STEINER, G. Z., BARRY, R. J. & GONSALVEZ, C. J. 2013. Can working memory predict target-to-target interval effects in the P300? *Int J Psychophysiol,* 89, 399-408.

STEINER, G. Z., BARRY, R. J. & GONSALVEZ, C. J. 2014. Stimulus-to-matching-stimulus interval influences N1, P2, and P3b in an equiprobable Go/NoGo task. *Int J Psychophysiol,* 94, 59-68.

STOJANOVIC, M., CVETKOVIC, D. & KOSTIC, V. S. 1995. A genetic study of idiopathic focal dystonias. *J Neurol,* 242, 508-11.

SURMEIER, D. J. & GRAYBIEL, A. M. 2012. A feud that wasn't: acetylcholine evokes dopamine release in the striatum. *Neuron,* 75, 1-3.

SYLVESTER, R., JOSEPHS, O., DRIVER, J. & REES, G. 2007. Visual FMRI responses in human superior colliculus show a temporal-nasal asymmetry that is absent in lateral geniculate and visual cortex. *J Neurophysiol,* 97, 1495-502.

TARSY, D. & SIMON, D. K. 2006. Dystonia. *N Engl J Med,* 355, 818-29.

THIRKETTLE, M., WALTON, T., SHAH, A., GURNEY, K., REDGRAVE, P. & STAFFORD, T. 2013. The path to learning: action acquisition is impaired when visual reinforcement signals must first access cortex. *Behav Brain Res,* 243, 267-72.

THORN, C. A. & GRAYBIEL, A. M. 2010. Pausing to regroup: thalamic gating of cortico-basal ganglia networks. *Neuron,* 67, 175-8.

THRELFELL, S., LALIC, T., PLATT, N. J., JENNINGS, K. A., DEISSEROTH, K. & CRAGG, S. J. 2012. Striatal dopamine release is triggered by synchronized activity in cholinergic interneurons. *Neuron,* 75, 58-64.

TRUONG, D. D. & JOST, W. H. 2006. Botulinum toxin: clinical use. *Parkinsonism Relat Disord,* 12, 331-55.

TSUI, J. K., EISEN, A., MAK, E., CARRUTHERS, J., SCOTT, A. & CALNE, D. B. 1985. A pilot study on the use of botulinum toxin in spasmodic torticollis. *Can J Neurol Sci,* 12, 314-6.

VOLKMANN, J., WOLTERS, A., KUPSCH, A., MULLER, J., KUHN, A. A., SCHNEIDER, G. H., POEWE, W., HERING, S., EISNER, W., MULLER, J. U., DEUSCHL, G., PINSKER, M. O., SKOGSEID, I. M., ROESTE, G. K., KRAUSE, M., TRONNIER, V., SCHNITZLER, A., VOGES, J., NIKKHAH, G., VESPER, J., CLASSEN, J., NAUMANN, M. & BENECKE, R. 2012. Pallidal deep brain stimulation in patients with primary generalised or segmental dystonia: 5-year follow-up of a randomised trial. *Lancet Neurol,* 11, 1029-38.

VOLLE, M. & GUITTON, D. 1993. Human gaze shifts in which head and eyes are not initially aligned. *Exp Brain Res,* 94, 463-70.

WADDY, H. M., FLETCHER, N. A., HARDING, A. E. & MARSDEN, C. D. 1991. A genetic study of idiopathic focal dystonias. *Ann Neurol,* 29, 320-4.

WANG, C. H., LIANG, W. K., TSENG, P., MUGGLETON, N. G., JUAN, C. H. & TSAI, C. L. 2015. The relationship between aerobic fitness and neural oscillations during visuo-spatial attention in young adults. *Exp Brain Res,* 233, 1069-78.

WATANABE, M., MATSUO, Y., ZHA, L., MACASKILL, M. R. & KOBAYASHI, Y. 2014. Fixational saccades alter the gap effect. *Eur J Neurosci,* 39, 2098-106.

WHITE, T., HONGWANISHKUL, D. & SCHMIDT, M. 2011. Increased anterior cingulate and temporal lobe activity during visuospatial working memory in children and adolescents with schizophrenia. *Schizophr Res,* 125, 118-28.

WILLIAMS, L. J., BUTLER, J. S., MOLLOY, A., MCGOVERN, E., BEISER, I., KIMMICH, O., QUINLIVAN, B., O'RIORDAN, S., HUTCHINSON, M. & REILLY, R. B. 2015. Young Women do it Better: Sexual Dimorphism in Temporal Discrimination. *Front Neurol,* 6, 160.

WRIGHT, D., MAKIN, A. D. & BERTAMINI, M. 2015. Right-lateralized alpha desynchronization during regularity discrimination: hemispheric specialization or directed spatial attention? *Psychophysiology,* 52**,** 638-47.

YOKOYAMA, T., NOGUCHI, Y. & KITA, S. 2012. Attentional shifts by gaze direction in voluntary orienting: evidence from a microsaccade study. *Exp Brain Res,* 223**,** 291-300.